Fault Detection and Diagnosis of Industrial Heat Pumps of GEA B.V.

M. Hofstad

Technische Universiteit Delft

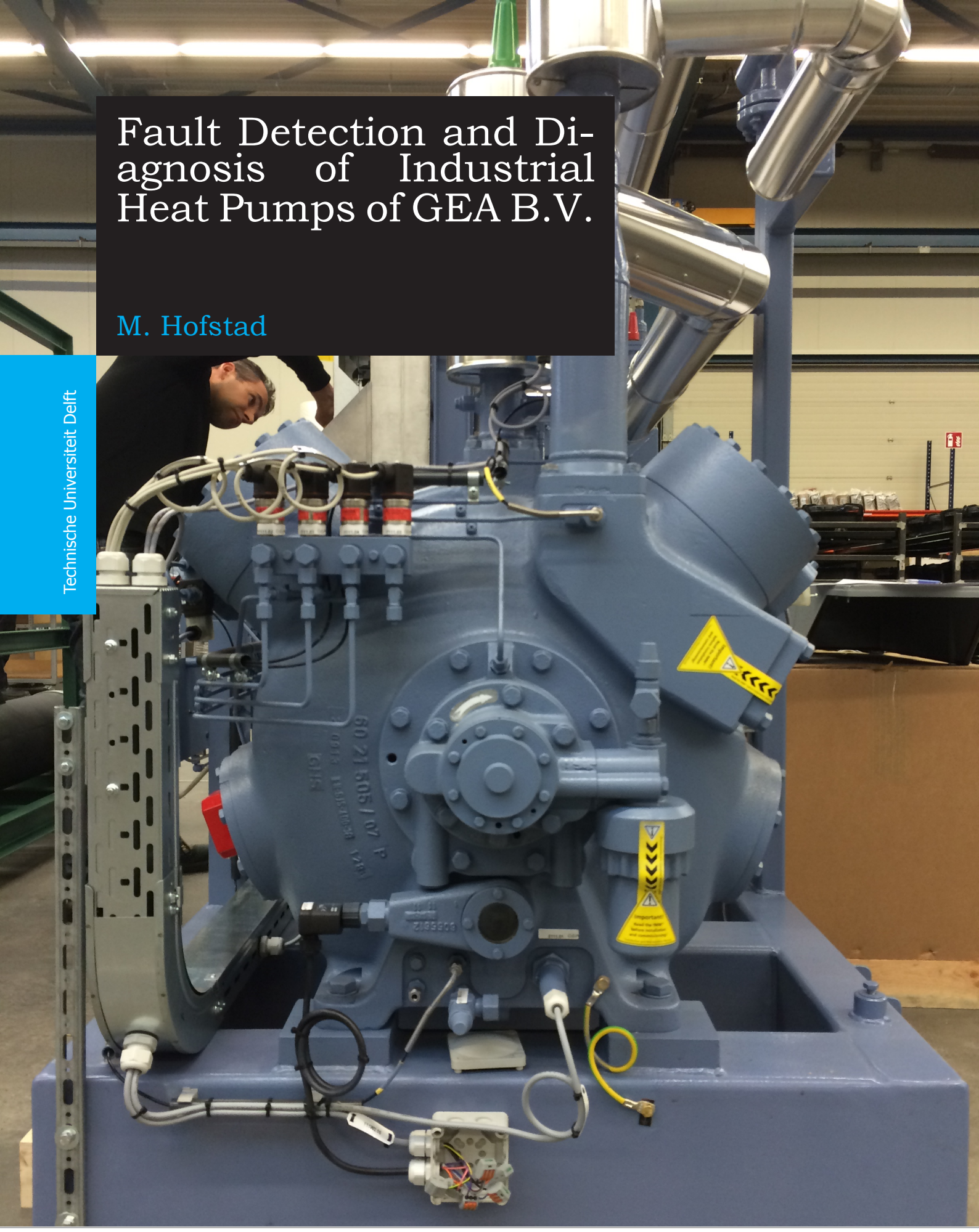

TU Delft Delft University of Technology

GEA engineering for a better world

Challenge the future

Fault Detection and Diagnosis of Industrial Heat Pumps of GEA B.V.

by

M. Hofstad
4631285

in partial fulfillment of the requirements for the degree of

Master of Science
in Mechanical Engineering

at the Delft University of Technology,
to be defended publicly on Friday November 2, 2018 at 13:30 PM.

Supervisor:	Dr. ir. C.A. Infante Ferreira,	TU Delft
Thesis committee:	Prof. dr. ir. T. J. H. Vlugt,	TU Delft
	Dr. R. Ferrari,	TU Delft
	Ir. J. H. Gerritsen,	GEA Group

This thesis is confidential and cannot be made public until November 3, 2023.

An electronic version of this thesis is available at http://repository.tudelft.nl/.

TU Delft Delft University of Technology

Abstract

Heat pumps represent an effective technology to convert electrical energy to thermal energy through the expansion and compression of a refrigerant. Heat pumps are becoming increasingly more efficient which decreases energy consumption. However as heat pumps are getting increasingly more efficient, complexity is also increasing which leads to failures.

GEA is one of Europe's largest providers of industrial heat pumps, delivering a variety of different industrial heat pumps for food production, breweries, waste heat recovery, and thermal power plants. As industrial heat pump systems are becoming increasingly complex, so is the task of detecting faults in the systems. Whenever a heat pump breaks down it is challenging to see what the reason for the failure is without visual inspection. A typical service engineer will have data from over 20 sensors, each with over two and a half million measurement intervals, to inspect and look for the cause of failure. Visual inspection of the heat pump systems can only be done by experienced engineers who knows exactly what to look for and where to look for it.

As heat pumps have been developing so has the sensor technology and computational resources available in modern computers. Over the last decades the price of sensors has decreased rapidly while the capability and reliability of sensors has improved. The computational power of modern computers has increased significantly while the price for these resources has decreased.

Several other industries have, with the development in sensor technology and computational power, investigated the possibilities of implementing Fault Detection & Diagnosis (FDD) programs to automatically analyze sensor data in order to detect failures and diagnose the failure cause. FDD programs were previously limited to critical processes, for example power plants, aerospace, or national defence. They were expensive programs due to the sensor requirements, the computational resource requirements and the development costs. However, as the price of sensors and computational resources has been decreasing, FDD is becoming increasingly more popular for less critical equipment. For the past two decades FDD programs have been developed for different Heating, Ventilation, Air-Conditioning and Refrigeration (HVAC&R) equipment with a special focus to refrigeration (Katipamula and Brambley, 2005a).

This project aims to develop a FDD program for GEAs industrial heat pump systems. Following a literature study it was concluded that thus far, FDD programs have not been utilized for heat pump systems of this complexity. It was seen that most FDD programs use a quantitative, qualitative or process history based approach to detect faults. Quantitative FDD programs aim to design a digital twin of the system at hand based on physical relations, and compare measured values to defined values for faulty or fault-free operation. Qualitative FDD programs aim to mimick the behaviour of system experts and base decisions on previously seen failures and cases. Process history based FDD programs aim to learn how systems should ideally behave through an abundance of operational data, and compare systems to sampled data (Venkatasubramanian et al., 2002b).

The FDD program for GEA uses a qualitative approaches for all faults where expert knowledge is available. For faults not seen before, a process history based approach classifies operation as faulty or fault-free. The complexity of the faults and the system do not allow for a quantitative FDD program. A predefined list of in total 23 faults was agreed upon, the FDD program further aims to detect all 23 failures and diagnose the failure cause.

The project is meant as a proof of concept for GEA. By proving that an off-line FDD program is possible, GEA can ultimately implement the algorithms used in this off-line FDD program in to the control system of the heat pumps to increase the reliability of their heat pumps and detect faults as they are occurring.

Acknowledgements

First, I would like to thank my supervisors, Dr. ir. C.A. Infante Ferreira and Ir. J. Gerritsen for their continuous supervision and everlasting patience. Having two supervisors with different interests and approaches to the project helped me stay critical throughout the process. I especially want to thank Dr. ir. C.A. Infante Ferreira for supervising me the last 14 months through my internship and graduation teaching me to become more of a critical thinker.

I want to thank GEA for all their help from all different departments, the continuous interest and help from GEA was a motivation throughout the process. I further want to thank Ir, W. Kanters, Ir. H. Vermeer and Ir. M. van Mierlo for their assistance in understanding the possible heat pump failures and the GEA compressor software.

I want to thank all the friends I have made during my time in Delft for all the support I have received. For their help in keeping my focused when needed and for also helping me unwind and relax when needed. Thanks to my family for their continuous support over the two last years. Special thanks to my closest family and friends in Norway for all their help, phone calls and all the visits.

Finally, I would like to thank TU Delft, the Energy and Process Department, GEA, all the teachers, staff and fellow students for making this journey what it was.

M. Hofstad
Delft, October 2018

Contents

Nomenclature

A	Coefficient of a linear curve	
a	Coefficient of an exponential curve	
B	Coefficient of a linear curve	
b	Coefficient of an exponential curve	
C	Constant to calculate motor power	rpm^{-1}
c	Coefficient of an exponential curve	
$Capacity$	Running capacity of the heat pump compressor	%
d	Estimating coefficient	
F	Counter counting time steps with fault symptom	
h	Enthalpy	kJ/kg
i	Time step	
I_{motor}	Current drawn from the motor driving the compressor	A
j	Time step counter	
K	Counter counting time steps of total operation	
LL	Liquid level	%
M	Matrix containing measured variables for FDD	
$\dot{m}$	Mass flow	kg/s
$N_{cylinders}$	Number of cylinders in compressor	
N_k	Total amount of capacity steps during startup of a compressor	
N_{RPM}	Rotational speed of the motor driving the compressor	rpm
P	Power	kW
p	Pressure	bar
$\dot{Q}$	Rate of heat transfer	kW
r	Time step counter	
T	Temperature	K
t	Time	s
V_{grid}	Voltage available in the grid	V
x	Variable used as x-value for fault detection by linear regression	
y	Variable used as y-value for fault detection by linear regression	
z	Output variable	

Abbreviations

ANN	Artificial Neural Networks
BBN	Bayesian Belief Network
COP	Coefficient of Performance
FDD	Fault Detection and Diagnosis
GUI	Graphical User Interface
HEX	Heat Exchanger
HVAC&R	Heating, Ventilation, Air-Conditioning and Refrigeration
IDE	Integrated Development Environments
PCA	Principle Component Analysis
PLS	Partial Least Squares
SRM	Sensitivity Ratio Method
VBA	Visual Basic for Applications

Greek

Δ	Difference	
σ	Standard deviation	
τ	Torque in shaft connecting motor to compressor	Nm

Subscripts

air	Air
$ambient$	Ambient
ch	Chiller
$comp$	Compressor
$cond$	Condenser
$conv$	Convergence
$design$	Design value for system
dis	Discharge of compressor
e	Electrical motor power
$evap$	Evaporator
exp	Exponential prediction
$fric$	Friction
frq	Frequency Converter
HP	Heat pump system
i	Time step
in	Entering value

$Initial$	Initial
k	Counter counting amount of capacity steps of compressor
$leak$	Leakage
lin	Linear
$losses$	Losses
$measured$	Measured power consumed from the grid
NO	Non-operating
oil	Oil
out	Exiting value
PR	Predicted by the compressor prediction tool
$PR - measured$	Predicted value from compressor prediction tool minus measured value
r	Refrigerant
ra	Return air to evaporating coil
reg	Value estimated by a regression model
RP	Refrigeration plant
$sampled$	Sampled
sat	Saturated value
sc	Subcooling
sh	Superheating
$shaft$	Shaft coupling the electric motor to the compressor
$shutdown$	Compressor shutdown
$start$	Start of steady state operation period
suc	Suction of compressor
$system$	Heat pump system value
$total$	Total
$uncertainty$	Uncertainties present in predictions
vap	Vaporization
$water$	Water
wb	Wet-bulb

1

Introduction

Heat pumps are an effective technology that efficiently drives the transfer of heat. Industrial heat pumps are becoming increasingly popular because several industries have large heating requirements at relatively low temperatures, which can be achieved by heat pumps in an efficient way. Heat pumps use the heat available in stable heat sources at relatively low temperatures. This heat source evaporates a refrigerant with a low boiling point in an evaporator. The now gaseous refrigerant is compressed in a compressor driven by an electric motor which increases the temperature and pressure and adds energy to the refrigerant. After the refrigerant is compressed it goes through a Heat Exchanger (HEX) called the condenser. Afterwards, it transfers its latent and sensible heat to a secondary fluid which exploits this heat at a higher temperature than the heat source. The refrigerant then goes through a thermal expansion valve where the pressure is decreased, before the refrigerant again enters a HEX where it is evaporated, taking heat from the stable heat source. This process is illustrated in Fig. 1.1. Industrial

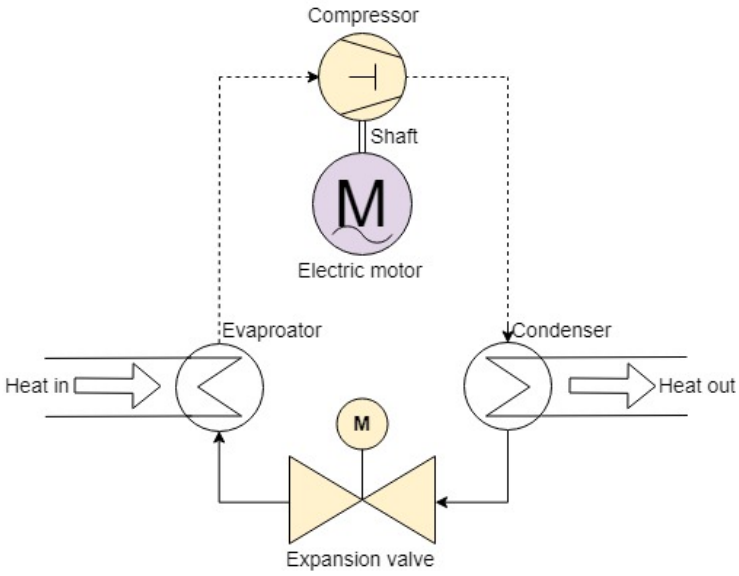

Figure 1.1: Simplified schematic of a standard heat pump setup. This illustrates the scope of the heat pumps considered for this project. The refrigerant loop, the incoming and outgoing flow of the heat source and heat sink, and to some extent the electric motor driving the compressor and the shaft coupling them.

heat pumps are relatively complex systems, thus whenever a fault is imposed on an industrial heat pump it is time demanding and costly to repair it. Faults may require shutdown for several days, and expert engineers analyzing the heat pump to diagnose faults. Sensors in heat pump systems are as of today mostly used for limit checking to ensure safe operation through control systems. Heat pumps are monitored and shut down if certain values exceed the design specification, but the reason for the values reaching beyond defined limits cannot be diagnosed properly. For example a control system

can detect that the discharge pressure in the compressor of a heat pump is too high, and shut down the heat pump, but the control system is not able to diagnose why the pressure was too high.

Fault Detection and Diagnosis (FDD) programs aim to automate the detection and more so the diagnosis of faults in different systems through data analysis programs. FDD programs connect the sensor data being logged to the actual physical fault. However, as of today FDD methods are mostly applied to critical and costly equipment to increase safety and decrease the costs associated with not operating (underachieving equipment). But with the decreasing cost of sensors and the decreasing cost of computational resources it is becoming increasingly more viable to perform FDD for less critical and costly equipment.

1.1. Project Description and Problem Boundary

The aim of this project is to design a FDD program for GEAs industrial heat pumps to lessen the time and effort required to perform maintenance. Fig. 1.1 shows the boundary of the heat pump systems considered. The refrigerant loop is considered as a whole, while the flow of the heat sink and source is only considered by an input and output. Lastly, the electric motor driving the compressor and the shaft coupling the two are considered to some extent, however the analysis is limited by the variables measured.

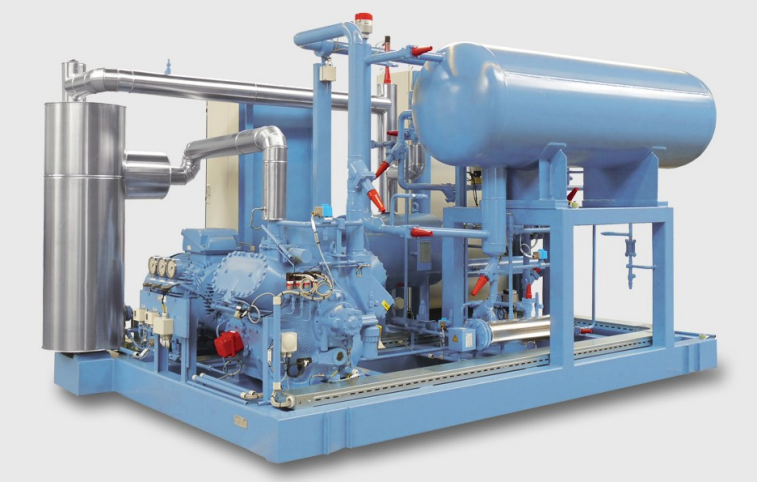

Figure 1.2: One of GEAs industrial heat pumps, functioning as a water cooled heat pump.

1.1.1. Heat Pump Systems Considered

The industrial heat pumps from GEA are mostly used in production plants and food processing plants. The heat pumps are usually a part of a larger more complex production scheme where cooling and heating are required. Due to this the heat source and the heat sink of the heat pump system is usually connected or coming from another process. GEA also produces refrigeration plants to provide cooling for processes, they can use their heat pumps as an add-on technology to their own refrigeration plants. By doing that, GEA can deliver a system that can support heating at temperatures up to 120 °C and cooling at temperatures down to -20 °C. The heat pump will use the heat from the refrigeration plant as a heat source, making the heat pump dependent on the operation of the refrigeration plant.

Three different types of heat pump systems are considered for this project. A heat pump as an add-on to refrigeration plants with an open and a closed configuration of the HEX between the heat pump and the refrigeration plant, and a water cooled heat pump. These heat pumps are all powered by two different piston compressors. Fig. 1.2 is an example of a water cooled heat pump. The add-on heat pump systems apply heat from the refrigeration plant in an evaporator, where one side has a refrigerant evaporating (the heat pump side) and the other side has a refrigerant condensing (refrigeration plant side). Furthermore the evaporator could either be an open or closed HEX for the add-on heat pump where an open configuration is illustrated in Fig. 1.3. The closed configuration keeps the two

streams separated as later illustrated in Fig. 5.7. For the scope of this project it was decided to focus on the heat pump systems and not look into the refrigeration plant.

Typical applications of GEAs industrial heat pumps are breweries, dairy plants, food processing and

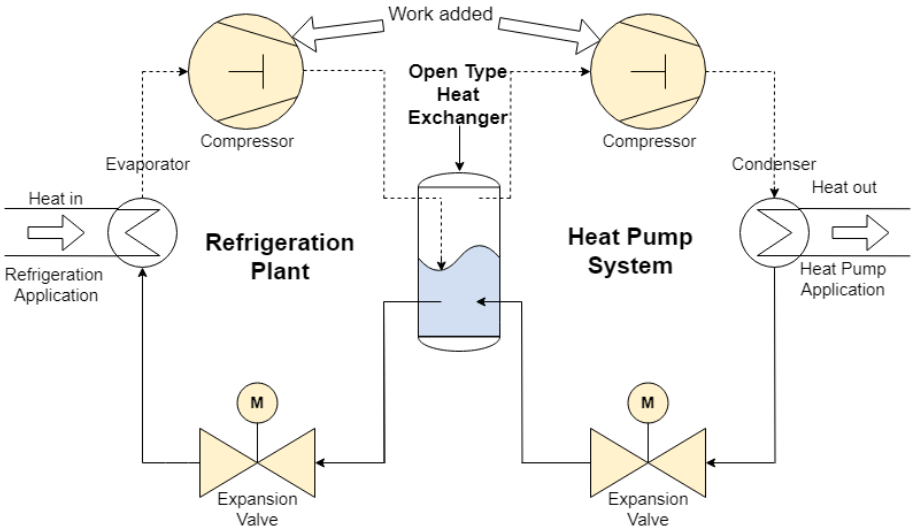

Figure 1.3: Simplified schematic of a heat pump functioning as an add-on to a refrigeration plant, with an open type HEX mixing the refrigerant from the refrigeration plant and the heat pump system.

waste heat recovery. An example of the add-on heat pump is Snow World in Zoetermeer in the Netherlands. Here GEA has a refrigeration plant creating the necessary conditions for an indoor skiing hill, while using the heat from the refrigeration plant to provide hot water for showers and cleaning.

Measured Variables

There are in total 23 variables that have to be measured to detect all the faults later introduced in section 4, 5, and 6.

The electric motor has a frequency converter between the motor and the electricity grid that converts the grid frequency of the current and the voltage to that of the electric motor. This frequency converter also measures certain values. The motor current is measured as an input to the motor in the frequency converter. The rotational speed of the motor is measured as the requested rotational speed from the control system of the motor, i.e. not the actual rotational speed. The torque measured is the theoretical torque of the shaft based on the current consumed by the motor. The motor power is measured in the frequency converter as the power going into the motor not considering its efficiency or the friction losses in the shaft connecting the motor to the compressor.

All pressures and temperatures are measured through temperature and pressure transmitters and sensors in the heat pump system. The pressure measurements are accurate without any time delay. The measured temperatures are prone to the thermal mass of the system and the sensor. For the temperature sensor to pick up on changing temperatures, the sensor needs to reach the same temperature as the fluid volume surrounding it. Temperatures are not uniformly distributed, thus the temperature experienced by the sensor might not be the same as in the rest of the system due to the heat transfer abilities of the medium. The issues with the thermal mass of the fluid volume result in an observed time delay in the temperature measurements. The measured temperature will often be the temperature experienced in the heat pump system several seconds earlier. However, the pressures are uniformly distributed and the sensor picks up on changes as they occur.

1.1.2. Prediction Tools

GEA has developed models that can predict the performance parameters of the compressor based on regression models from process history data in a compressor tool. The models are derived from

laboratory measurements of different heat pumps and compressors. The prediction tools can be used to compare measured data to predicted data of different measured variables in the heat pump. The models deviate from the measured data due to the general fit of the regression models, and due to noise and sensor uncertainty. The models are based on a black-box approach, which will be further discussed in section 2.

The prediction tool requires the design characteristics of the compressor and the running conditions of it. The outputs from the model include among other values the power lost to friction in the shaft, the refrigerant mass flow, the required power to drive the shaft, the delivered condenser heat, and the oil crankcase temperature.

1.1.3. Objective of FDD Program

The heat pump systems of interest are relatively complex systems which are prone to a number of different failure modes. Some failure modes are almost impossible to detect upon visual inspection. An example of a heat pump plant from GEA is shown in Fig. 1.4. Some faults can be present in the heat pump system without the heat pump operator noticing a different behaviour. The complexity of the systems do not allow for manually analyzing the performance data, as the data files logged from operation record over 20 variables usually every second of operation. At the instance a heat pump operator notices unusual behaviour, the fault could have been propagating over the past month. Hence the heat pump operator would have to analyze data containing approximately 20 variables for almost 3 million time steps to look for irregularities. If none of the known and defined faults are apparent in the heat pump system, there could still be a previously unknown failure present in the heat pump system.

The objective of this master thesis is to design a FDD program which can automatically detect and

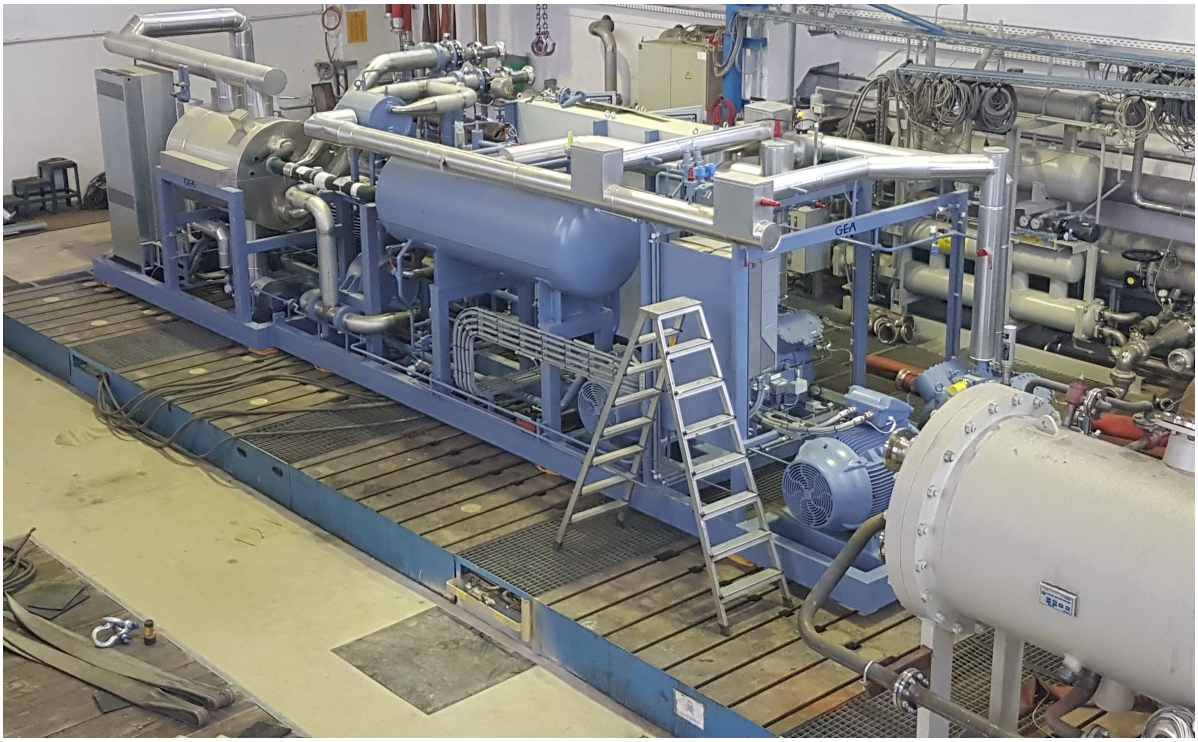

Figure 1.4: An industrial heat pump system delivered by GEA used as a water cooled heat pump planned to be operated for waste heat recovery of heat from the London underground.

diagnose faults in GEAs industrial heat pumps based on the data measured by sensors in the heat pump. It is intended that the FDD program will analyze the data from heat pump systems and compare it to a database of known fault trends, and draw conclusions based on the similarity between the database trends and the recorded data. The specific requirements of the FDD program imposed by GEA can be seen in the following subsection where the problem and the problem boundaries are

defined.

Most faults previously seen in the heat pump occur on a system level, i.e. inside the refrigerant loop of the heat pump. A list of 23 faults was agreed upon as the scope of this project, these were the 23 most commonly occurring faults, where the fault symptom was well known. A detailed description of the faults, the data available from those faults, the fault symptoms, the fault recognition algorithm, and the results of the FDD program for the individual fault will follow in section 4, 5, and 6.

1.2. Desired FDD characteristics

FDD programs are usually evaluated on the ten different parameters in Table 1.1 (Venkatasubramanian et al., 2002b). FDD programs can be constructed in multiple ways, thus it is vital for clarity to have a set of parameters that the program can be evaluated against. Each parameter in Table 1.1 is rated with ”+”, ”++” or ”0” to define how important it is for GEAs FDD program. ”++” means it is absolutely demanded of the program. ”+” symbolizes that it would be a nice asset to the program, but it is not demanded. ”0” symbolizes it is not relevant for GEAs FDD program.

Table 1.1: Common factors to evaluate FDD programs on. The column furthest to the right shows how important each factor is for GEA.

Quick detection and diagnosis	The FDD program should be able to quickly detect and diagnose faults before any serious damage is imposed	+
Isolability	The FDD program should be able to tell different faults apart and isolate the imposed fault	+
Robustness	The FDD program should be able to block out noise and uncertainties from measurements, so that it does not give false alarms or misses faults.	0
Novelty identifiability	The FDD program should be able to classify faulty and fault-free operation, and when faulty it should be able to classify if it is a known fault or not.	+
Classification error estimate	The FDD program needs to be designed so that the operator is confident in its findings.	0
Adaptability	The FDD program should be able to adapt to physical system changes and to different systems without needing much re-programing.	++
Explanation facility	The FDD program should provide an explanation on how the fault developed and propagated into its current state.	++
Modeling requirements	The FDD program should not require too much modeling efforts if a quick deployment is desired.	0
Storage and computational requirements	The FDD program should not require a large computational effort as it will make it slower and more costly, but models which are less computationally demanding often require a higher storage capacity.	0
Multiple fault identifiability	The FDD program should be able to diagnose multiple faults occurring at the same time, which might prove difficult due to their interacting nature	0

Regarding the first point in Table 1.1, ”*Quick detection and diagnosis*”, it is only denoted with a single ”+” as it is not important at this point for GEA. However it is worth noting that GEAs ultimate goal is to have a FDD program integrated in the control system of the heat pump that can analyze the system on-line and detect faults as they occur, this will be further explained in subsection 2.2. For the scope of this thesis however, the constructed FDD program will analyze previous data explicitly.

The ”*Adaptability*” is especially important as this FDD program is meant for three different heat pump systems that can all be fitted with two different compressors. They are all industrial systems with different applications, thus within these three types no systems are alike. The ”*Explanation facility*” is meant to provide the heat pump operator with an explanation on how the fault developed and what the cause was rendering it more important than other factors.

1.2.1. Requirements of the measurements

For the FDD program to detect all the defined failures in the heat pump system it is dependent on having accurate measurements of 23 variables. The faults occurring during the compressor or heat pump startup, require a measurement interval of 1 second as indicated by Table 1.2, as the failure trend is apparent for a few seconds only. It is important to have a clear picture of which variables are needed for the detection of each fault. Table 1.2 shows which variables are needed for particular

faults. Table 1.2 also indicates the required measurement interval for each fault and it is assumed that the FDD analysis tool will follow this measurement interval. In the same table it is indicated for which heat pump system and which compressor type the fault is occurring. The different compressor types will be further explained in section 3 and section 4.

Table 1.2: All variables needed for a complete FDD program to detect the faults outlined in section 4, 5, and 6. The "Y" marks that the certain fault requires the certain variable, the faults are labeled by their respective subsection. The required time step interval for Fault 4.7 will be further discussed in subsection 4.7, it is due to variations in the rotational speed of the motor. The period of occurrence marks when the fault can be detected where 'SU', 'SD', 'SS' and 'O' stands for startup, shutdown, standstill and operation of the heat pump compressor respectively.

Variable/Fault	4.1	4.2	4.3	4.4	4.5	4.6	4.7	5.1	5.2	5.3	5.4	5.5	5.6	5.7	5.8	5.9	5.10	5.11	6.1	6.2	6.3	6.4	6.5
Compressor Prediction Tool Dependent			Y	Y	Y					Y			Y	Y	Y	Y							
Compressor type	All	All	5HP	All	All	All	All	All	All	All	All	5HP	All	All	All	All	All	All	All	All	All	All	5HP
Heat pump system	All	All	All	All	All	All	All	All	Open type add-on	Add-on	All	All	All	All	All	All	All	All	All	All	All	All	All
Required measurement interval [s]	1	1	10	30	1	1	0.02*	1	30	1	1	5	1	1	30	30	1	1	1	1	30	60	1
Period of occurrence*	SU and SD	SU	O	O	SU and O	SD	O	SU and SS	O	O	O	SS	O	SU and O	O	O	SU	O	SD	SU	O	SS	SU and O
I_{motor}	Y	Y	Y	Y	Y	Y	Y	Y	Y	Y	Y	Y	Y	Y	Y	Y	Y	Y	Y	Y	Y	Y	Y
$Capacity$	Y	Y			Y			Y	Y														
N_{RPM}			Y				Y			Y	Y				Y	Y							
Δp_{oil}			Y									Y											Y
$T_{PR,dis}$				Y										Y									
T_{dis}				Y	Y			Y	Y	Y	Y		Y	Y	Y	Y		Y	Y		Y		Y
$T_{dis,sat}$								Y	Y	Y			Y					Y					
p_{dis}	Y				Y					Y	Y		Y		Y	Y	Y		Y				
$p_{dis,system}$																		Y	Y				
P_e			Y		Y					Y			Y		Y	Y							
$P_{PR,e}$			Y		Y										Y	Y							
T_{suc}						Y		Y					Y		Y	Y							
$T_{suc,sat}$						Y		Y		Y			Y										
p_{suc}	Y				Y					Y	Y				Y	Y	Y		Y	Y	Y		
$p_{suc,system}$										Y											Y		
$T_{water,cond,in}$													Y				Y						
$T_{water,cond,out}$									Y				Y										
$T_{ambient}$								Y															
LL_{evap}																					Y	Y	
$T_{cond,out}$										Y			Y					Y					
$T_{evap,RP,in}$										Y													
$T_{evap,RP,out}$										Y													
τ_{shaft}							Y			Y													

It it apparent from Table 1.2 that the motor current, I_{motor} and T_{dis} are the variables needed in most faults. However, I_{motor} is mostly used to verify whether or not the compressor is operating, thus it has low requirements for accuracy. T_{dis} is used to predict the startup time until the system reaches steady state which will be discussed in further detail in subsection 3.3.1.

Sensor accuracy

The frequency converter logs the motor current, motor power, and the shaft torque before applying a filter to the measured data. The accuracy of the sensors measuring the variables are not considered in detail. Some variables are taken as what the control system requests from the heat pump system (N_{RPM} and $Capacity$), while others are measured. Some measured variables work as an input to the prediction tool predicting the heat pump system performance. Enthalpies are calculated based on measured variables in the heat pump system, and thus depend on the sensor accuracy.

Due to this complexity it is further assumed that all sensors are accurate and the sensor measurement uncertainty is negligible in comparison to the measured values.

1.2.2. Multiple fault identifiability and Isolability

The intertwining nature of different faults and how they are connected and depend on each other is illustrated by Fig. 1.5. It also shows the different symptoms of the faults later mentioned in section 4, 5, and 6, and how some symptoms can lead to detection of several faults. As several faults share failure symptoms it is important for the detection of these faults that they have several symptoms to isolate the them.

As is mentioned later for the individual faults, not all faults can be isolated, however as seen in Table 1.1 this is not the most important metric for GEAs FDD program.

In Fig. 1.5 the discharge temperature, T_{dis}, can affect many faults. For the calculations of the condenser heat, $\dot{Q}_{cond}$, the enthalpy at the discharge is required, discussed later in section 3. From

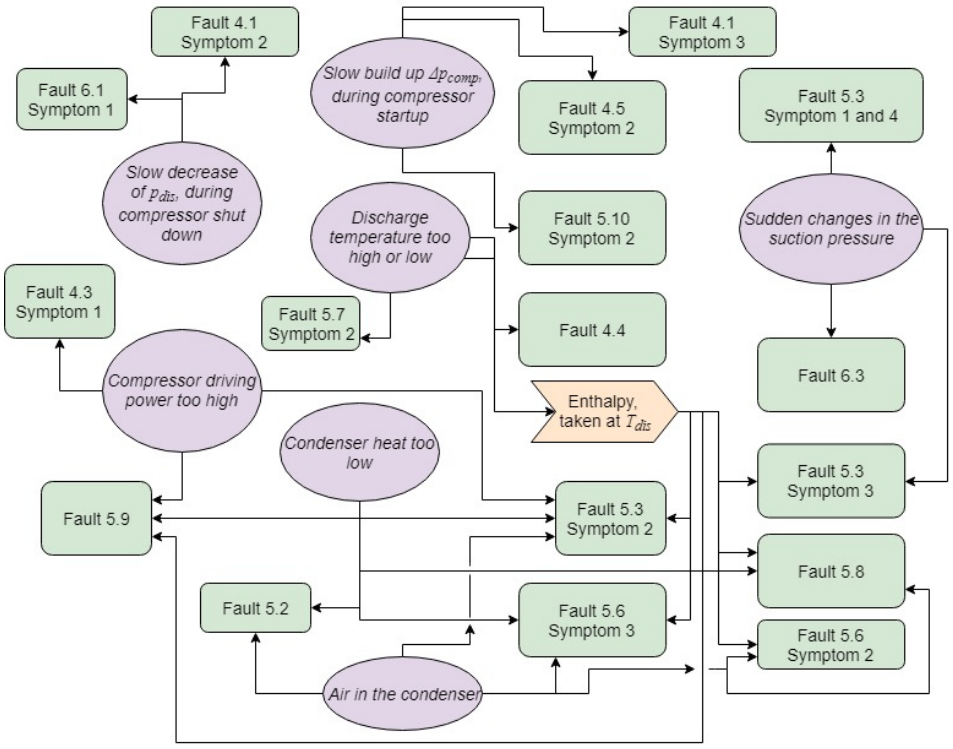

Figure 1.5: Schematic showing the relation between some specific fault symptoms (purple boxes) and how they are detectable for several faults (green boxes).

$\dot{Q}_{cond}$, all mass flows can be derived, making several faults indirectly dependent on the accuracy of T_{dis}.

1.3. Approach

The project is approached in several steps. The steps required to solve the described problem are outlined in this subsection of the report.

1.3.1. Step 1 - Literature Study

The literature study can be further divided into three different steps.

- In section 1 the problem definition, an overview of the problem, and the boundary of the problem which this thesis sets out to solve is given.
- Existing literature is examined in order to establish the different approaches for FDD program creation. An overview is provided outlining all relevant types of FDD methods which have previously been applied in similar industries. This will follow in section 2.
- The literature study lastly outlines the different available options for the programming language in which the FDD will be constructed. This will follow in subsection 2.3.

1.3.2. Step 2 - Fault Discovery

Once a clear overview of the FDD methods is established, the next step is to outline the most typical faults observed in the heat pumps under investigation. Data or knowledge about the typical faults occurring is gathered. In total 23 faults were defined as the scope of the FDD program, they are outlined in section 4, 5, and 6.

1.3.3. Step 3 - Choice of Appropriate Approach

The third step once all the faults are known is to choose the appropriate FDD approach from the literature study which is the most suitable to the defined faults to design the FDD program. This

includes both an evaluation of which programming option to use and a choice of the FDD method(s) for the individual fault. Thus this is the combination of step 1 and step 2. The FDD approach for the individual faults are explained through flowcharts in section 4, 5, and 6.

1.3.4. Step 4 & 5 - Development and Validation of Model

Once the methodology for the FDD program is decided along with the software in which the FDD program will be constructed, the FDD program itself can then be developed. This will be the most demanding step in terms of time and effort and will be divided into a set of smaller steps. The program will be constructed in an iterative manner based on the available fault data, thus the validation and model construction will overlap each other. Each fault will be classified based on data available from said fault and the design will be based on the data available from the fault.

2

Methods of FDD

FDD programs aim to construct a model of the system at hand which is compared to the monitored data from the system. By comparing the estimated data to the measured data, a fault can be detected when certain parameters are outside their expected range for given operating conditions. As seen in the previous section the compressor has a model already developed by GEA; this could help to further simplify the FDD program design and increase its accuracy given that the model is accurate.

The modeling and the comparison can be done in numerous different ways. FDD is generally seen to have three different approaches to diagnose faults; quantitative, qualitative and process history based. These three methods overlap in several ways, what generally separates them is how each fault diagnosis is generated. Although the construction of the models could be similar in many ways or overlap each other the generation of the fault diagnostic can generally be classified in three different methods as seen below (Katipamula and Brambley, 2005a).

Quantitative models are based on a physical model of the system and they are depending on having analytical redundancy or hardware redundancy. Quantitative models are limited by the sensor availability (the hardware redundancy) and the computational power available (the analytical redundancy). Analytical redundancy is explained as overly complicated models that can calculate all states of the system and connect all sensors mathematically, while hardware redundancy is explained as having a redundant amount of actual sensors to guarantee no faulty measurements.

Physical models compute the expected values for components in the heat pump based on known physical relations and laws. These calculated values are furthermore compared to the monitored values, mostly by investigating the residuals in some manner i.e. the Sensitivity Ratio Method (SRM) or Bayesian Belief Network (BBN). These models tend to be very specific for each setup, and to make it interchangeable requires an analytical redundancy. Only quantitative models can model the behavior during dynamical operation i.e. start-up and shut-down and they are able to classify faulty operation without sampling data from faulty operation. Quantitative models are time-demanding to develop and they require a hardware redundancy, hence for larger systems they are often limited to simple linear relationships to decrease the computational effort and unsuitable for on-line models (Venkatasubramanian et al., 2002b). It has been seen that quantitative models are especially suitable for situations with a lack of logged data (Katipamula and Brambley, 2005a). In (Gordon and Ng, 1995) an universal model for all existing chiller models at the time was designed, hence quantitative models should be able to overcome the adaptability issue.

Qualitative models use a knowledge basis to draw conclusions about a system, they are well suited for data rich environments. It requires a high level of a priori knowledge about the system at hand, however it does not require any physical or analytical knowledge about the system. It is developed from extensive experience with each component of the system and typical fault symptoms. By creating a large tree or map of if-then-else rules the program runs through the tree for every data-point and sees if the operation can be labeled faulty or fault-free, the program aims to mimic the behavior of

an expert of the system. The expert experience is typically revolved around seeing what the measured sensor values have represented earlier, thus if a new fault is introduced, the system will often not detect it. Some models map or group the parameters so that the trajectory or the propagation of each parameter from fault-free operation to the faulty values is apparent, which makes predictive maintenance possible as well (Venkatasubramanian et al., 2002a). Qualitative models score well on the explanation facility factor; the propagation from fault-free operation to faulty.

Process history based relies on an extensive amount of logged data. A program is constructed based on previous data from faulty and fault-free operation, models are less demanding to develop for all types of systems, but might not be as accurate. The process history based approach is not able to diagnose multiple faults occurring at the same time or new faults. Process history based models extract and present data from the system as a priori knowledge, in a process called feature extrapolation. Feature extrapolation can be achieved in two manners; qualitative (black-box models) or quantitative (gray-box models). The process history based approach is a way of machine learning where a program is trained based on data from previous operation, both fault-free and faulty. Often programs are trying to detect the dependencies between the measured variables, combine these variables to make less variables. The process history based approach is the most applied in industry, mainly due to low requirements of priori knowledge and modeling effort (Venkatasubramanian et al., 2002c).

These are the three different approaches to generate fault diagnostics. When comparing the models with the measured data there are several different methods as well, dependent on availability of data etc. They all produce residuals in the case of a fault between expected values and measured values. How to evaluate those residuals and connect them to certain faults can be done in several ways as well as it is seen below.

2.1. Description of existing FDD technologies and an overview

Below is a classification of different and popularly used FDD methods from several applications. It is not in any way a full overview of all techniques, but rather the more popular methods. In Fig. 2.1 below the classification of the relevant methods is presented.

Quantitative

- Sensitivity Ratio Method (SRM) uses measurements and predictions of temperatures or other parameters to construct ratios which are uniquely sensitive to individual faults. A residual between estimated values and measured values for a parameter insensitive to a certain fault is divided by a residual sensitive to the same fault to create a ratio, furthermore this ratio is evaluated with a threshold. (Chen and Braun, 2000).

- Bayesian Belief Network (BBN) is a way of mapping all available sensors and expected faults with certain probabilities. A BBN investigates which sensors are activated and then subsequently it gives a probability for each preprogrammed fault in the system. BBN allows for a robust consideration of all uncertainties available in sensors and other parameters. For complicated systems with several possible faults it can however be quite an extensive network where complex probability models must be applied (Mehranbod et al., 2005).

Qualitative

- Bond graphs are domain independent graphical representations of physical systems based on energy exchange between different components through directional power connections. FDD is achieved through generation of adaptive thresholds which are robust when experiencing parametric uncertainties (Jha et al., 2017, Broenink, 1999).

- Physics-based models enable conclusions about a process without exact expressions governing the process and precise numerical inputs through a detailed algorithm (Katipamula and Brambley, 2005a, Venkatasubramanian et al., 2002a).

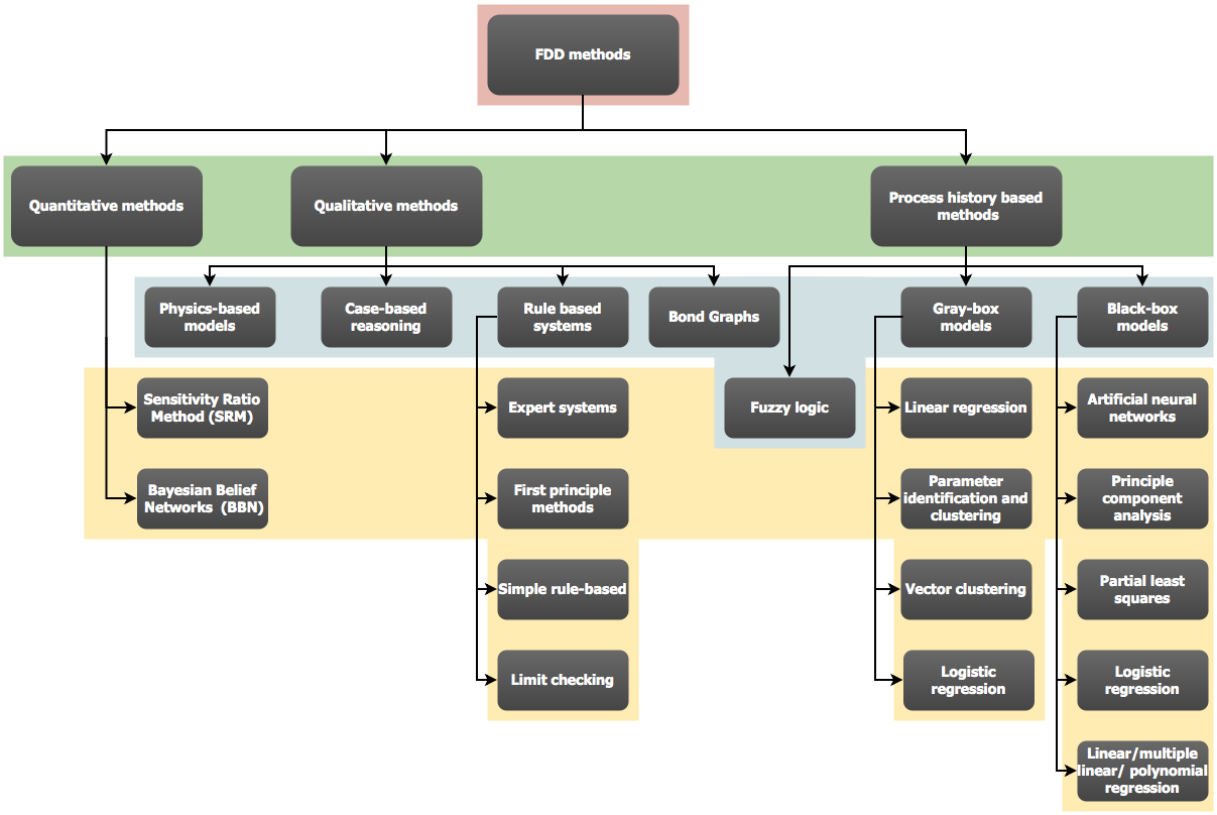

Figure 2.1: Classification scheme for FDD methods relevant for GEAs industrial heat pumps.

- Case-based reasoning utilizes the gained knowledge from previously experienced concrete problem situations. A case is a problem description accompanied by a solution to the problem, thus problems encountered are diagnosed by navigating through a database of old cases (Dexter and Pakanen, 2001).
- Rule-based systems aim to mimic the behavior of human experts on the system, by using a priori knowledge to derive a set of if-then-else rules and an inference mechanism that searches through the rule-space to draw conclusions (Katipamula and Brambley, 2005a). Faults are detected by observing deviations in the residuals between measured and predicted variables (Schein and Bushby, 2005, Delgoshaei et al., 2017).
  - Expert systems mimic the cognitive behavior of a human expert in a knowledge bank and an inference engine that searches through the knowledge bank to derive conclusions from given facts in a particular domain (Schagen et al., 2016).
  - First principle methods navigate through a threshold decision tree structure derived from physical relations in a knowledge base to conclude on the operational mode based on the measured data (Katipamula and Brambley, 2005a).
  - Simple Rule-Based methods evaluate raw data, and find combinations of parameters that are insensitive to operating conditions and sensitive only to one fault which reduces the required computational effort (Chen and Braun, 2000).
  - Limit checking defines simple thresholds independently of operating conditions for relevant variables to define an operating range (Vecchio, 2014). GEAs heat pumps already have this in built in to ensure safe operation.

Process history based

- Gray-Box models use a combination of physical known relations to the process with coefficients estimated from process history data (Katipamula and Brambley, 2005a).

- Linear regression of process history data from equipment manufacturers, laboratory tests or field monitoring of operations estimate the coefficients necessary to construct the relations between the process components (Katipamula and Brambley, 2005a). A typical gray-box regression example is given in (Gordon and Ng, 2001) and repeated below in Equation 2.1, it is used to estimate a chiller COP, based on three input parameters; $T_{evap,water,in}$,$T_{cond,water,in}$ and $\dot{Q}_{ch}$.

$$\left(\frac{1}{COP+1}\right)\frac{T_{evap,water,in}}{T_{cond,water,in}} - 1 = d_1\frac{T_{evap,water,in}}{T_{cond,water,in}} + d_2\frac{T_{cond,water,in} - T_{evap,water,in}}{T_{cond,water,in}\dot{Q}_{ch}} + d_3\frac{(1/COP+1)\dot{Q}_{ch}}{T_{cond,water,in}} \tag{2.1}$$

  The variables d_1, d_2 and d_3 all have a physical meaning and in this case they represent the irreversible entropy losses, the rate of heat loss ($\dot{Q}_{leak}$) and the total HEX thermal resistance respectively.

- Multiple linear regression is the standard technique for modeling linear relationships between two or more independent input variables and one dependent response variable. It includes techniques like ordinary least squares and quantile regression (Frank et al., 2016).
- Parameter Identification and Clustering finds a relation between all measured parameters that influence each other in a system through a least squares approach in a square matrix. Dependent on which matrix value is deviating and in which range the value is found a fault can be diagnosed if present (Zogg et al., 2005).
- Vector Clustering is similar to parameter clustering, except it maps the trajectory a parameter undergoes when going from a fault free mode to a faulty mode with a vector, thus providing an explanation (Zogg et al., 2005).

- Black-Box models deviate from gray-box models in how the input/output relations are estimated. For black-box modeling these model parameters have no physical meaning, they are purely based on empirical process history data in a statistical or non-statistical (pattern recognition) manner (Li and Braun, 2002, Katipamula and Brambley, 2005a).

  - Artificial Neural Networks (ANN) are a non-statistical method that performs well when interpolating data, but not when extrapolating data. Input received is weighted and combined based on previously seen process history data in a hidden layer, and combinations of weighted inputs can give outputs which correspond to faults (Rebouças and Leite, 2012).
  - Principle Component Analysis (PCA) is a statistical method that reduces the dimensions of the data sets analyzed by connecting correlated parameters and combining those parameters into a set of new and uncorrelated parameters. These parameters are evaluated compared to a fault-free PCA, and a threshold decides whether the operation is faulty or not (Villegas et al., 2010).
  - Linear/Multiple linear/Polynomial regression are statistical methods that in a similar fashion to gray-box modeling regression can connect input predictors to outputs, except now none of the parameters estimating the input/output relation has a physical meaning. An example of typical black-box modeling can be seen in (Rossi and Braun, 1997), where the output states, z_i, of a simple packaged air conditioner are estimated through only three different input parameters; T_{wb}, T_{ra} and $T_{ambient}$ as seen in Equation 2.2 below.

$$z_i = d_1 + d_2T_{wb} + d_3T_{ra} + d_4T_{wb} + d_5T_{wb}^2 + d_6T_{ra}^2 + d_7T_{ambient}^2 + d_8T_{wb}T_{ra} + \ldots \tag{2.2}$$

    What separates black-box regression from gray-box regression is that d_1, d_2, d_3, d_4, d_5 etc have no physical meaning.

  - Partial Least Squares (PLS) constructs the minimum amount of predictor variables from an originally large amount of predictor variables creating a higher stability than most other models even when little data is available (Höskuldsson, 1988).

  - Logistic Regression is a statistical method that aims to predict an outcome variable measured by a dichotomous or binary variable based on one or more independent input variables (Brownlee, 2016).

- Fuzzy Logic labels residuals between predicted and measured values in a human way according to thresholds dependent on how strongly each residual is connected to a fault to reduce the ambiguity (Kulkarni et al., 2009, Mechefske et al., 1996).

2.1.1. Conclusions on literature

Deciding which model approach to apply depends on several factors, but mostly on the available data from operation (both faulty and fault-free) and the criteria imposed in Table 1.1. Models for the compressor have been developed and validated, hence it could prove advantageous to use them rather than spending time and effort developing models that might not prove as accurate.

In (Katipamula and Brambley, 2005b) the FDD methods applied in the Heating, Ventilation, Air- Conditioning and Refrigeration (HVAC&R) industry are outlined. It can be seen that for chillers, air-conditioners, heat pumps and refrigerators process-history based methods are the most applied methods. These are applications with the same underlying working principles as the industrial heat pump of interest. Nevertheless there are several examples of quantitative and qualitative FDD methods for the HVAC&R industry as well. The process-history based methods seen in HVAC&R were all model specific and lacked the adaptability desired by GEA, however FDD can be deployed with databases to cover more equipment model lines. In (Katipamula and Brambley, 2005b) the need for hand-crafted systems was recognized as one of the major issues for process-history based FDD, and some ways to avoid this issue has been suggested. They were all seen to have issues with the diagnostics of multiple occurring faults.

Although the methods above differ, several systems have used a combination of the methods for their FDD programs. The FDD program is constructed by seeing which approach is the most suitable for each individual fault. These are the so-called hybrid methods (Venkatasubramanian et al., 2002c). It has been suggested that to make the most suitable program for each industrial system a hybrid system is the only truly feasible option, as single systems will often prove insufficient for large systems. A hybrid system can deploy different techniques for each component or different techniques for the detection and diagnosis. It has also been suggested that if the system is extensively instrumented, which GEAs system is, then classical limit checks and simplified empirical models are sufficient for detection while rule-based or knowledge-based is often required for the diagnosis (Katipamula and Brambley, 2005a).

Several of the later seen faults apply a process history based fuzzy logic approach which was a combination of simple limit checking of residuals between predicted and measured values.

For the general FDD program for GEAs heat pumps a combination between qualitatively rule-based and case-based reasoning shall be used where expert knowledge from previous faults exist. For the faults where expert knowledge does not exist a process history based approach will be used with the compressor model developed by GEA.

2.2. On-line and off-line detection

An important aspect of the FDD program to be made is its ability to detect the faults while the heat pump system is operating before the faults impose any danger to the system. This is known as the ”Quick detection and diagnosis” from Table 1.1. For many systems it is important to detect and diagnose the fault before it is able to damage the system, this goes especially for more critical systems. It is desirable for GEAs heat pumps to have quick detection and diagnosis.

That implies that most faults should have an approach where it is possible to detect the failure the moment the failure symptom occurs in the data. As it will be apparent in the analysis for some particular faults, this is not necessarily possible. However the algorithms seen later that construct the FDD program are all made in order to detect the fault as it is developing when it is possible. By having a FDD program that is able to perform on-line FDD the FDD program can eventually be programmed

into the control system of the heat pump system, which is the ultimate goal of this project for GEA. By having a FDD program in the control system the control system will be able to control the heat pump system to avoid the failures when they are occurring before they create damage.

However, for the scope of this project the FDD program constructed is off-line and it is not able to detect faults on-line. The goal of this project is to make a data processing tool, the ultimate goal for GEA is to have it integrated into the control system of the the heat pump system. To accommodate for the ultimate goal of GEA each fault is programmed in a manner where the transition to an on-line system does not require any adjustments, where it is possible. Some failure symptoms do not allow for on-line detection, this will be mentioned in the individual failure description.

2.3. Overview of Relevant Programming Options

The modeling effort can be done in several programs and there are several options for language preferences as well. there are several different software options, thus only the major and most commercial softwares have been evaluated in ascending order below.

- **Matlab**; Matlab is an applicable and powerful language that have all the required functions. It can also be linked to Simulink which is an add-on to Matlab that can easily construct a simulated model of systems. There are several examples in literature of Matlab being used for FDD (Kulkarni et al., 2009, Vecchio, 2014, Villegas et al., 2010, Dexter and Pakanen, 2001). Matlab is most applicable for quantitative and qualitative models.
- **Python**; Python is a free software similar to Matlab. Python has its own programing language, thus Python has several different Integrated Development Environments (IDE) that can be very similar to R (introduced later in this section) or Matlab for the actual programing effort, implying that Python is compatible with most FDD methods. GEAs control systems expert have advised to use Python for the FDD program due to its compatibility, there are some examples of Python used for FDD (Wissink et al., 2011, Rosvold, 2017).
- **WinMOD**; Software which is used in order to validate control systems to avoid actually testing systems without sufficient control. It can be used to construct an analytical model which can be compared to the measured data, hence WinMOD is applicable for the quantitative methods.
- **R**, R is popularly used for big data analytics to perform different regressions and neural networks, where the ultimate problem is the size and the noise of the dataset, R is more suitable for process-history based FDD.
- **Modelica**; Modelica can model dynamical systems based on physical equations, an intuitive Graphical User Interface (GUI) illustrates the process by connecting building blocks with equations (Fritzson, 2004). There exist some examples of Modelica used for model construction for quantitative FDD (Delgoshaei et al., 2017).
- **HUGIN**; a program developed especially to construct probabilistic Bayesian Belief Networks (BBN) (Andersen et al., 1989, Madsen et al., 2003).
- **Excel**; Excel is a powerful tool based on a spreadsheet design that allows quite heavy calculations and is especially suitable for medium sized data. However it often proves insufficient when more complicated programs are required. Excel has its own programing language called Visual Basic for Applications (VBA).
- **Stata**, Stata is a software intended for handling of large datasets. Its concepts are similar to R in many ways, but it is less powerful in reducing noise. Stata does however come with some simple matrix programing functions, as with R it will be most useful for process-history based methods.

The choice of the appropriate software or programing language depends on several factors. Some of the approaches listed above are limited only to certain approaches. The software seen to fit best with the desired FDD characteristics imposed by GEA in subsection 1.2 was Python.

3

Compressor prediction tool and initial analysis

GEA has a program available that can predict some of the measured variables in their heat pump systems based on the running conditions of the compressor. This program is designed using a black- box approach further outlined in subsection 2.1, where variables are predicted with nonphysical polynomial regression models. The FDD program will use this prediction tool to predict certain values based on the running conditions, these predicted values can be compared to the actual values for the FDD algorithms. This allows the FDD program to do a feature extrapolation of prior knowledge in a quantitative (gray-box) manner, where the values are coming from a process-history based black-box model (the compressor prediction tool), but compared in a quantitative manner.

The FDD program will be linked with the compressor prediction tool. Every time step the FDD program will use the compressor prediction tool to calculate the outputs. This is done based on the inputs to the tool at that exact time step.

The running conditions together with the outputs of the compressor prediction tool are listed in Table 3.1. Where T_{sh} and T_{sc} are defined as the total superheat and total subcooling in the heat pump system by equation 3.1 and equation 3.2 respectively. The tool can predict other variables, which are the variables needed to detect the faults later introduced in section 4, 5, and 6.

$$T_{sh} = T_{suc} - T_{suc,sat} \tag{3.1}$$

$$T_{sc} = T_{dis,sat} - T_{cond,out} \tag{3.2}$$

Where $T_{cond,out}$ is the temperature of the refrigerant exiting the condenser. The prediction tool is able to predict these values for every time-step based on the running conditions at that time step. The accuracy of the compressor prediction tool is of interest to discover its field of application for FDD analysis. The deviations between the measured and predicted variables should remain at a minimum for the tool to maintain its relevance.

The following subsections will discover and evaluate the compressor prediction tools performance for FDD analysis.

3.1. Field of application

The compressor prediction tool has an operating range that must be precisely defined in order to have an accurate prediction tool. This operating range is defined based on the operating conditions needed as inputs in Table 3.1. The only difference between the operating range for the two different types of compressors is the capacity, which is different for the ”5HP-compressor” and the ”V-compressor” being 100 % and 20 % respectively. The prediction tool requires a certain time period from startup of the compressor until the predictions become sufficiently accurate due to the thermal mass of the system during startup for some of the variables. This period is discussed in subsection 3.3.1, 3.3.2, and 3.3.3 for each relevant variable.

Table 3.1: The inputs to the compressor prediction tool, their corresponding limitations and the outputs from the compressor prediction tool. For the "5HP-compressor" the capacity must be 100%, while for the "V-compressor" the capacity has to be at least 20%.

Parameters	Symbol	Limitations
Input parameters to tool		
Saturated suction temperature	$T_{suc,sat}$	-65°C<$T_{suc,sat}$<90 °C
Saturated discharge temperature	$T_{dis,sat}$	-65°C<$T_{dis,sat}$<90 °C
Rotational speed of motor	N_{rpm}	Must be above 350 rpm
Total superheat	T_{sh}	0 K<T_{sh}<100 K
Total subcooling	T_{sc}	0 K<T_{sc}<50 K
Compressor operating capacity	$Capacity$	Must be 100% or 20 %
Environmental temperature	$T_{ambient}$	-20°C<$T_{ambient}$<45°C
Output parameters from tool		
dis temperature	$T_{PR,dis}$	
Compressor driving power	$P_{PR,e}$	
Power lost to friction in shaft	P_{fric}	
Condenser heat	$\dot{Q}_{PR,cond}$	

3.2. Validation of compressor prediction tool

The deviations between the measured and predicted variables are of importance for the compressor prediction tool and the deviations will be further outlined in this section for each variable of importance.

The heat pump systems can be equipped with two different compressors; the "V-compressor" and the "5HP-compressor". The "V-compressor" is relatively new, thus there are limited amounts of data available as there are only two of the kind in operation. The validation of the compressor prediction tool is mostly done for the "5HP-compressor" as it has an abundance of data available for validation. The limited data from the "V-compressor" is sampled, and assumed for further FDD analysis, however no major conclusions can be drawn from these data.

3.2.1. Discharge temperature

The compressor prediction tool assumes that the compressor has been running at the given running conditions for a longer period. This implies that the compressor prediction tool assumes steady state at the given running conditions, while during startup of the compressor the heat pump system will need some time to heat up. Due to this the starting difference between the measured and predicted discharge temperature will be quite high.

After the deviations converge to a stable value and the system is heated up, the predicted discharge temperature is still seen to be higher than the measured temperature. Now by a constant value as illustrated by Fig. 3.1.

Table 3.2 shows the results from analyzing the difference between $T_{PR,dis}$ and T_{dis} during steady state operation for both compressor types. The results have compared the measured and predicted discharge temperatures in fault-free heat pump systems fitted with both types of compressors. Some

Table 3.2: The experienced differences between $T_{PR,dis}$ and T_{dis} for heat pump systems with a "5HP-compressor" and "V-compressor" during steady state operation.

Evaluation parameters	"V-compressor" heat pump systems	"5HP-compressor" heat pump system
Number of sampled compressors	2	27
$\overline{T_{PR,dis} - T_{dis}}$	5.38 K	3.30 K
$\sigma_{\overline{T_{PR,dis}-T_{dis}}}$	0.33 K	0.88K
$\overline{\sigma_{T_{PR,dis}-T_{dis}}}$	1.79 K	0.95 K

deviance is expected due to the thermal mass of the system and the time delay of the sensors. The

running conditions entered to the compressor prediction tool give a direct value of what T_{dis} would apply when running at these conditions during steady state for a longer time period. The heat pump system will take some time to cool down or heat up when the running conditions of the compressor prediction tool are changed, thus there will not be a direct response in the measured output, in this case T_{dis}. Hence if the compressor prediction tool predicts a certain value for T_{dis}, the sensors will measure this value with a certain time delay.

For further FDD analysis $T_{PR,dis}$ will be adjusted to the findings from Table 3.2 for the "5HP-compressor" and "V-compressor" with an uncertainty, $T_{dis,uncertainty}$, of $\pm$ 0.95 K and $\pm$ 1.79 K respectively. The comparison of the two temperatures for the "V-compressor" later in Fig. 3.4 are adjusted to the findings from Table 3.2, and so are the temperatures in Fig. 3.1 for the "5HP-compressor".

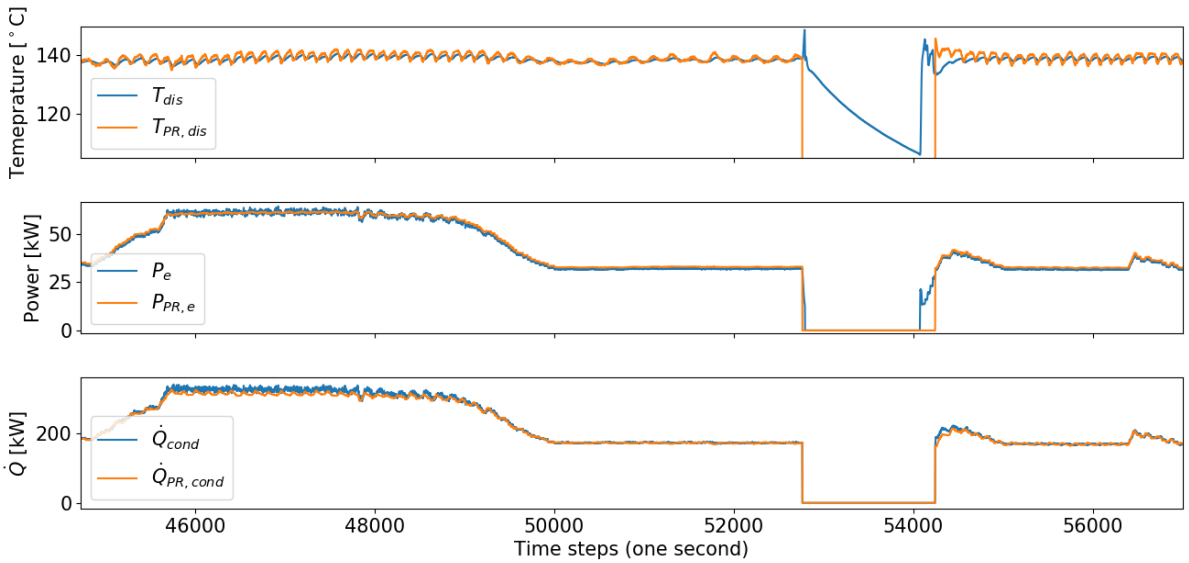

Figure 3.1: Three plots showing from top to bottom the development of the predicted and measured discharge temperature, motor power and condenser heat for the "5HP-compressor" respectively. It is apparent that the discharge temperature and the condenser heat takes some time before the deviations converge to a constant value after a startup. There is a time delay between the T_{dis} and $T_{PR,dis}$, as $T_{PR,dis}$ is more sensitive to changes in the operating conditions than T_{dis} due to issues of thermal mass.

3.2.2. Compressor driving power

Not all heat pump systems are measuring the driving power of the compressor. When the driving power is not measured it can be calculated through an estimation. For the heat pump systems where the driving power is measured, the measurements are of the power drawn from the grid, $P_{e,measured}$. For some clarity of the different power later discussed see the Sankey diagram in Fig. 3.2. The predicted power from the compressor prediction tool, $P_{PR,e}$, is the power required to drive the shaft from the motor.

Heat pump systems without power measurements

The compressor driving power can be estimated through equation 3.3 for a three-phase electric motor based on the variables measured in the heat pump system.

$$P_e = \frac{\sqrt{3} N_{rpm} * I_{motor} * V_{grid}}{C * 60} \tag{3.3}$$

Where C is a constant defined by the heat pump system itself, N_{rpm}, I_{motor} and V_{grid} are the rotational speed in rotations per minute, the motor current measured in Ampere and the supplied grid voltage taken to be 400 Volt. Equation 3.3 is an empirical equation, where C is a nonphysical constant.

Between the electricity grid and the electric motor driving the compressor there is a frequency converter that converts the frequency of the current and the the voltage to that of the motor. The current

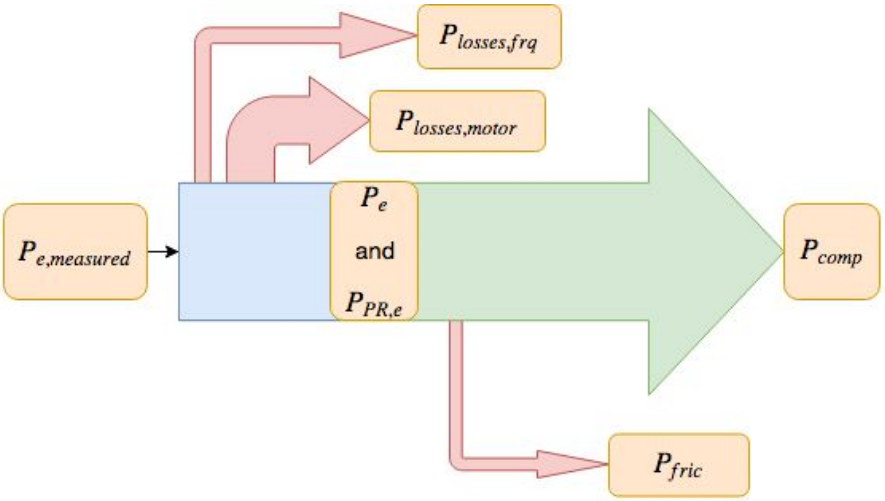

Figure 3.2: A Sankey diagram explaining the losses in the power going to drive the compressor. $P_{losses,frq}$, $P_{losses,motor}$ and P_{fric} are the power lost in the frequency drive, in the electrical motor driving the compressor and to friction lost in the shaft coupling the motor and the compressor.

is measured in the frequency converter, therefore this is not the current drawn from the grid. The voltage is not measured, the grid voltage is assumed for the calculations. However the voltage after the frequency converter is fluctuating. Hence C will differ for the two different compressors. The fluctuating voltage is proportional to the rotational speed of the motor. Thus the empirical equation 3.3 uses the constant voltage supplied by the grid and the rotational input speed to the compressor to account for the fluctuating voltage, the C is then in the units minutes per rotation. C accounts for the efficiency of the frequency converter, the efficiency of the motor and the power factor resulting from the phase shift between the current and the voltage.

C from equation 3.3 was sampled from 11 heat pump systems with a ”5HP-compressor”, all containing two compressors, i.e. 22 different C values. The mean was found to be 48.03, and the average standard deviation was seen to be 0.87, introducing an uncertainty of $\pm$ 1.8%. An uncertainty of $\pm$ 1.8% in C amounts to an uncertainty of $\pm$ 3.9% in $P_{PR,e}$. In addition to this the standard deviation of C in each data set sampled was never seen to be above 1.02, implying that equation 3.3 is a sufficient estimator for the driving power. 1.02 is a reasonable number as the efficiencies of the electrical motor and the frequency converter change with the operating conditions, illustrated in Fig. 3.3. The relationship between the predicted and actual motor power can be assumed to follow equation 3.4 for the ”5HP-compressor” where P_e is not directly measured.

$$P_e = P_{PR,e} \pm 0.039 P_{PR,e} \tag{3.4}$$

Heat pump systems with power measurements

In some heat pump systems the driving power, $P_{e,measured}$, is measured. The measured driving power is the power drawn from the electrical grid. The frequency converter measuring the power is located in the connection between the electricity grid and the motor. The power predicted by the compressor prediction tool, $P_{PR,e}$, is the shaft power required to drive the shaft that runs the compressor.

Thus the predicted and measured power will not be the same, both the frequency converter and the electrical motor have losses, $P_{losses,frq}$ and $P_{losses,motor}$ respectively. The electrical motor producer has limited data on their efficiency during operation, the information known are the three crosses in Fig. 3.3. A second degree polynomial regression model was made to cover the areas not given by the producer, from a running capacity of 50 % and up. The frequency converter has no given data describing its efficiency as it is usually 98% with limited variations.

Hence one can assume that 2% of the power drawn from the grid is lost in the frequency converter as $P_{losses,frq}$. The power loss in the electrical motor, $P_{losses,motor}$, is given by the curve from 3.3. There are only two heat pump systems with the motor power measured, where one has a ”V-compressor”

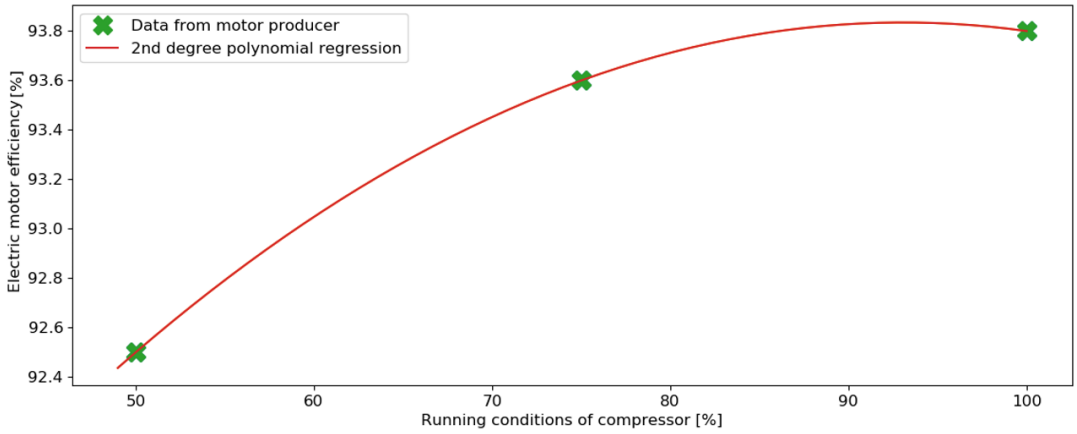

Figure 3.3: Data from the producer of the electrical motor driving the heat pump compressor. The producer only has the three points indicated by green crosses, where the electrical motor efficiency is 92.5%, 93.6% and 93.8% for a capacity of 50%, 75% and 100% respectively. A polynomial fit is assumed to cover the area between the crosses.

and the other one has a ”5HP-compressor”. The deviance between the measured and predicted motor power at the maximum capacity sampled from these two heat pump systems is shown in Table 3.3. From Table 3.3 it can be seen that especially for the ”5HP-compressor” the deviance is higher than

Table 3.3: Table showing how the measurements of the compressor driving power deviates from the predictions made by the compressor prediction tool.

Evaluation parameters	**”V-compressor” system**	**”5HP-compressor” system**
Sampling points	15507	7512
$\overline{(\frac{P_{PR,e}}{P_{e,measured}})}$	0.91	0.59
$\sigma_{(\frac{P_{PR,e}}{P_{e,measured}})}$	0.014	0.021

expected. This data is from a heat pump system where the control system was wrongly adjusted causing the compressor to shut down every 15 minutes and damaged bearings were detected, thus the data collected is corrupt. The sampled heat pump proved to be faulty, as it will be discussed later for Fault 4.3, where a possible symptom was an increase of the driving power to run the compressor. The deviance is due to either a faulty sensor measuring the power, the motor power being higher than expected due to Fault 4.3 or the compressor prediction tool not being able to capture the actual power. The data of the measured power sampled from the ”5HP-compressor” cannot be utilized.

For the ”V-compressor” the results in Table 3.3 show the expected results where the predicted power is 91 % of the measured power with an uncertainty of $\pm$ 1.4 %.

The predicted motor power, $P_{PR,e}$, is expected to be 93.8%-2%=91.8% of the measured power, $P_{e,measured}$. 93.8 % is the efficiency of the electric motor at maximum capacity and 2 % is the expected power loss in the frequency converter.

Thus for the FDD analysis of the ”V-compressor” the motor power measured, $P_{e,measured}$, will be altered to be the power required to drive the shaft, P_e, given by equation 3.5.

$$P_e = P_{e,measured} * 0.918 \pm 0.01397 \tag{3.5}$$

Where the theoretical efficiency of 91.8 % is assumed, should other heat pump systems yield other deviations than what was seen for this specific system.

3.2.3. Condenser heat

The condenser heat is predicted by the compressor prediction tool, however the tool does not take into account if there are two or three compressors acting in parallel or one acting alone, nor does it account for heat losses. The compressor prediction tool uses the running conditions of the compressor to calculate what a heat pump system with one compressor could deliver under these conditions.

The actual condenser heat is not measured, but it can however be estimated through equation 3.6 below based on measured variables.

$$\dot{Q}_{cond} = \dot{m}_r(\Delta h_{vap,r} + \Delta h_{sc,r} + \Delta h_{dis,r}) \tag{3.6}$$

Where $\Delta h_{vap,r}$, $\Delta h_{dis,r}$ and $\Delta h_{sc,r}$ are the latent heat of vaporization of the refrigerant at the discharge pressure, the enthalpy difference between the saturated and measured discharge conditions and the enthalpy difference created by the subcooling of the refrigerant, all measured in kJ/kg, respectively. The mass flow of the refrigerant, $\dot{m}_r$, is estimated through equation 3.7 below.

$$\dot{m}_r = \frac{P_{comp}}{\Delta h_{comp,r}} \tag{3.7}$$

Where Δh_{comp} is the enthalpy difference of the compressor, measured between the suction and discharge conditions in kJ/kg. As Δh_{comp} is based on the data measured at the suction and discharge of the compressor, this will account for the isentropic efficiency of the compressor.

The enthalpies from equation 3.6 and 3.7 are taken at the point specified by the temperature and pressure measured. This implies that the condenser heat is dependent on the accuracy of the discharge temperature and also on other measurements. The FDD program is linked with the program CoolProp which can calculate refrigerant properties based on the pressure and temperature at that point. Thus the program will for every measurement interval, send the necessary temperatures and pressures to CoolProp and retrieve the enthalpy at the specified point.

P_{comp} from equation 3.7 is the actual thermodynamical work done by the compressor per second, while $P_{PR,e}$ and P_e are both the power required to drive the shaft. Therefore the calculated $\dot{m}_r$ must be calculated using P_e subtracted with the power lost through friction in the shaft to acquire P_{comp}. The compressor prediction tool can also predict the power lost to friction in the shaft, P_{fric}. Assuming that these predictions are correct, the mass flow required to calculate $\dot{Q}_{cond}$ can be calculated through equation 3.8.

$$\dot{m}_r = \frac{P_e - P_{fric}}{\Delta h_{comp,r}} \tag{3.8}$$

P_{comp} is the driving power of one compressor, making the calculation of the condenser heat in equation 3.6 for a heat pump system with one compressor.

Table 3.4 shows the results comparing the predicted condenser heat, $\dot{Q}_{PR,cond}$, to $\dot{Q}_{cond}$ for heat pump systems fitted with both types of compressors.

Table 3.4: Comparison of $\dot{Q}_{cond}$ and $\dot{Q}_{PR,cond}$. The data from the heat pump systems with the ”V-compressor” are taken when the power was measured, while the data from the heat pump systems with the ”5HP-compressor” are taken when the power was not measured.

Evaluation parameters	**”V-compressor” systems**	**”5HP-compressor” systems**
Amount of heat pump systems sampled from	1	5
$\overline{(\frac{\dot{Q}_{PR,cond}}{\dot{Q}_{cond}})}$	0.88	1.01
$\sigma_{(\frac{\dot{Q}_{PR,cond}}{\dot{Q}_{cond}})}$	-	0.025
$\overline{\sigma_{\frac{\dot{Q}_{PR,cond}}{\dot{Q}_{cond}}}}$	0.030	0.019

After sampling five different heat pump systems fitted with a ”5HP-compressor” it was seen that $\dot{Q}_{PR,cond}$ was almost identical to $\dot{Q}_{cond}$. After sampling the one heat pump system with a ”V-compressor”

it was seen that $\dot{Q}_{PR,cond}$ was approximately 88% of $\dot{Q}_{cond}$. The deviance is likely to originate from the compressor prediction tool as $T_{PR,dis}$ is also relatively inaccurate for the "V-compressor".

It was concluded that the compressor prediction tool is inaccurate when predicting $\dot{Q}_{PR,cond}$ for the "V-compressor", however it is assumed for future FDD that this inaccuarcy will be constant. It is further assumed that for the "5HP-compressor", $\dot{Q}_{PR,cond}$ can be directly predicted with an uncertainty of 2.5 %.

3.2.4. Coefficient of Performance predictions

The Coefficient of Performance (COP) is an important parameter quantifying the efficiency of the system. The COP can be calculated through equation 3.9, and it is considered as the real COP of the system. The COP predictions are especially considered for Fault 5.9.

$$COP = \frac{\dot{Q}_{cond}}{P_e - P_{fric}} \tag{3.9}$$

The COP is not predicted directly through the compressor prediction tool, but it can be calculated through $P_{PR,e}$ and $\dot{Q}_{PR,cond}$ from the compressor prediction tool with equation 3.10.

$$COP_{PR} = \frac{\dot{Q}_{PR,cond}}{P_{PR,e} - P_{fric}} \pm COP_{uncertainty} \tag{3.10}$$

Where P_{fric} is the power lost to friction predicted by the compressor prediction tool.

The uncertainty of the COP, $COP_{uncertainty}$, will be relatively high as it is directly dependent on $P_{PR,e}$ and $\dot{Q}_{PR,cond}$ and their respective uncertainties. The uncertainties of the COP for the different compressor types are given in Table 3.5 using the findings from the previous 2 subsections. Table 3.5 shows that the COP can be predicted with a higher accuracy for the heat pump systems with a "V-compressor" than for the heat pump systems with a "5HP-compressor". However, this conclusion is on the basis of one heat pump system where $\dot{Q}_{PR,cond}$ was seen to be 88 % of $\dot{Q}_{cond}$. Hence there is not sufficient data to conclude that this goes for other heat pump systems with a "V-compressor".

Table 3.5: Table showing the given uncertainty when calculating the COP for the heat pump systems with the different compressors.

Parameters	**"5HP-compressor" without measured power**	**"V-compressor" with measured power**
P_e uncertainty	3.90 %	1.40 %
$\dot{Q}_{cond}$ uncertainty	2.50 %	3.00 %
$COP_{uncertainty}$	6.41 %	4.40 %

Thus the uncertanty of 6.41 % form the "5HP-compressor" is assumed for all heat pump systems.

3.3. Initiation time until predictions are accurate

During the initiation or startup of the compressor in the heat pump system not all predictions done by the compressor prediction tool will be accurate. The inputs to the compressor prediction tool, defined in Table 3.1, are all either saturated temperatures, running conditions of the compressor (N_{RPM} and $Capacity$) or factors that have a relatively small impact on the predictions.

When starting up a compressor after a longer period of standstill, temperatures are low. During startup the pressures, thus also the saturated temperatures, will increase to its operating conditions at a faster rate than the temperature illustrated by Fig. 3.4.

The compressor prediction tool only sees the saturated temperature inputs, and assumes that the temperatures are already warm. Due to this there will be a period after each standstill, during the startup, where the compressor prediction tool will be inaccurate until the temperature reaches its expected operating conditions. This is illustrated by Fig. 3.4.

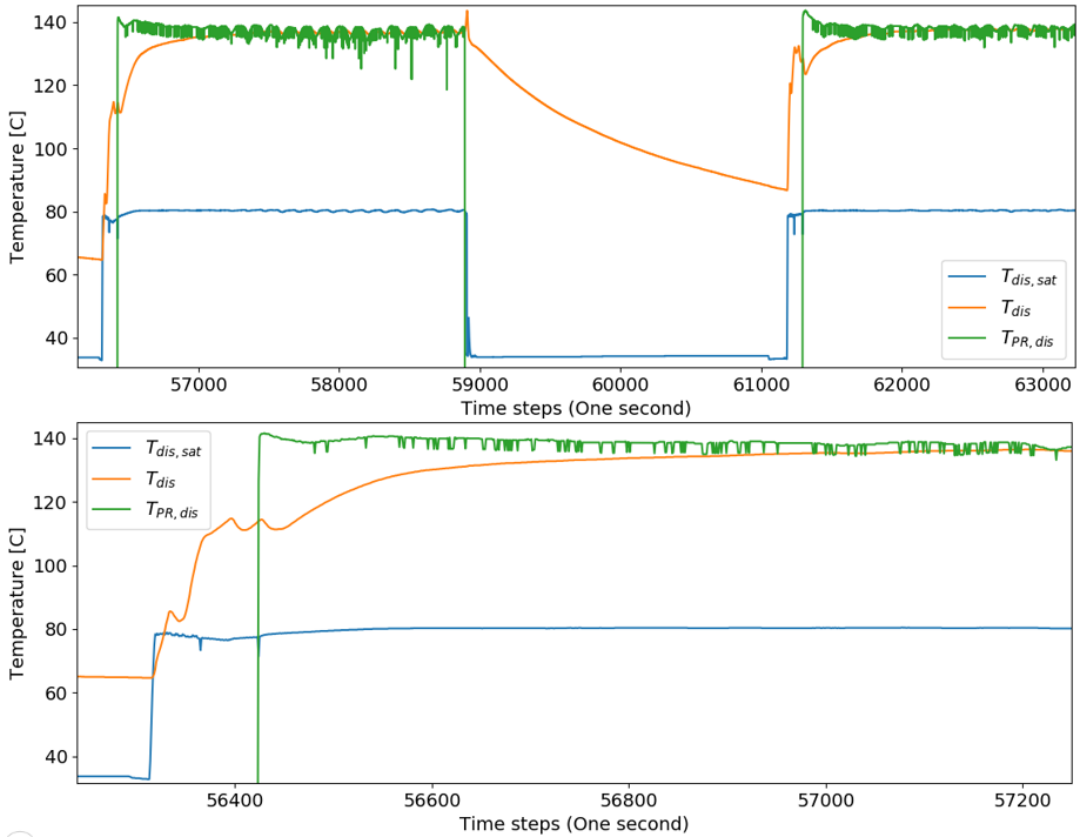

Figure 3.4: The development of T_{dis}, $T_{dis,sat}$ and $T_{PR,dis}$ over time after the startup. $T_{PR,dis}$ is only using the saturated values as input. $T_{dis,sat}$, and hence also $T_{PR,dis}$, reaches its operating conditions long before T_{dis}. The top graph shows two startups that illustrates the issue, while the bottom graph is an enhanced version of the first of the two.

3.3.1. Discharge temperature initiation time

The compressor prediction tool needs a certain time after the compressor starts before it can provide accurate predictions of the discharge temperature. This time and how to predict it will be discussed in this subsection. From Fig. 3.5 it is apparent that the deviations between the measured and predicted discharge temperature, $\Delta T_{PR-measured}$, have an exponential decrease over time following the form described in equation 3.11.

$$\Delta T_{PR-measured} = a * e^{-bt} + c \tag{3.11}$$

Where a, b and c are empirical constants of the graph, t is the time and $\Delta T_{PR-measured}$ is the temperature difference between the predicted and measured discharge temperature of the compressor. This implies that the deviations will converge to an acceptable constant value with time. The acceptable deviations are defined by equation 3.12.

$$\Delta T_{PR-measured}[t] - \Delta T_{PR-measured}[t-1] < 0.002 \tag{3.12}$$

The time step where this occurs, further referred to as t_{conv}, is marked with yellow dots in Fig. 3.5. From Fig. 3.5 it is apparent that the time it takes for the deviations to converge is directly connected to the starting $\Delta T_{PR-measured}$, which is directly linked to the discharge temperature before startup. Startups like the ones in Fig. 3.5 were sampled from several heat pump systems. Furthermore the time until the deviations converged according to equation 3.12 was plotted in relation to the discharge temperature before the startup in Fig. 3.6. From Fig. 3.6 it is apparent that the discharge temperature before the startup directly influences the time it takes before the $\Delta T_{PR-measured}$ converge to an acceptable level. The data from Fig. 3.5 is sampled from 69 different startups where 65 of those had the exponential shape, i.e. 94.2%. These 65 startups were plotted in Fig. 3.6 and based on that two different linear regression models were made. Equation 3.13 dictates the shape of the linear regression

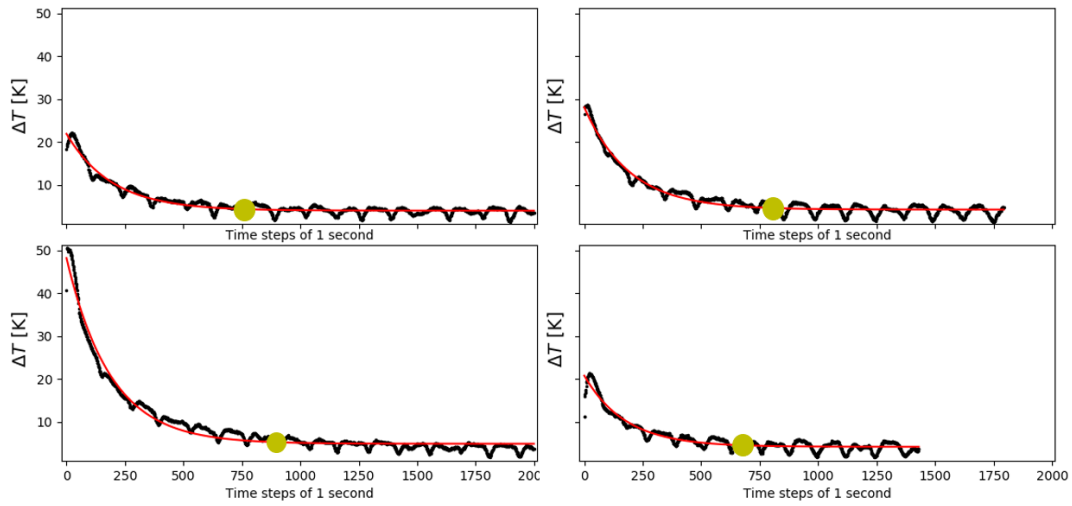

Figure 3.5: The development of the deviation between the $T_{PR,dis}$ and T_{dis} over time after the startup. The red lines are an exponential regression of the deviation with respect to time, while the black lines are the aforementioned deviation.

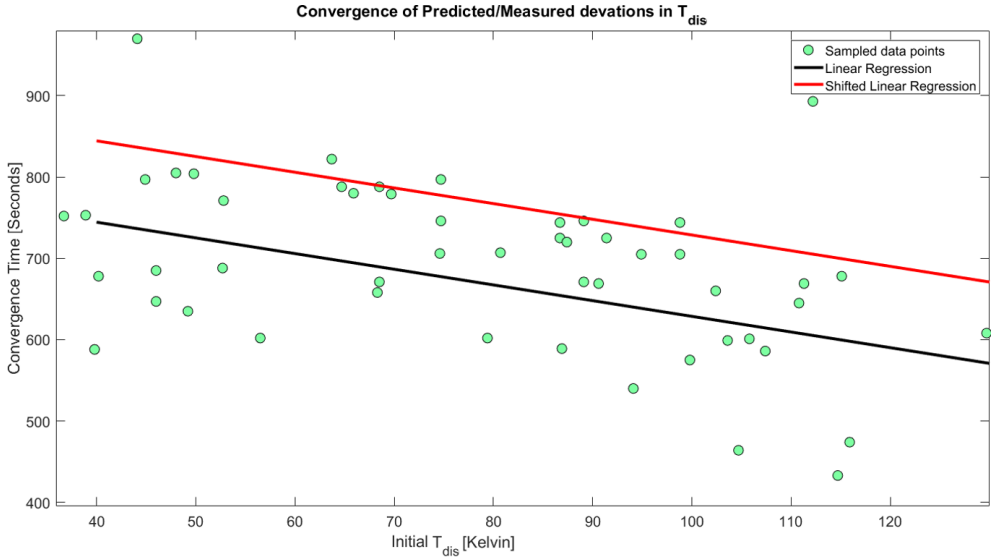

Figure 3.6: The green dots show the relationship between the time it takes for the deviations between $T_{PR,dis}$ and T_{dis} to converge to an acceptable level after a compressor startup defined by equation 3.12. On the x axis is the initial difference between $T_{PR,dis}$ and T_{dis} at startup, and t_{conv} in seconds is on the y-axis. The black and red line are the linear regression for the measured data and the shifted result derived in equation 3.14 respectively.

models.

$$t_{conv,lin} = A + B * T_{dis,initial} \tag{3.13}$$

Where $t_{conv,lin}$ is the convergence time in seconds, $T_{dis,initial}$ is the discharge temperature before the startup, while A and B are constants of the slope. The linear regression model fitted to the data in Fig. 3.6 (black line) had an R squared value of 12.8%.

Shifting the linear regression slope upwards parallel to the original slope can be done by changing the intersection point, A, of the original linear regression model. If the intersection point is increased by 100 seconds, then 92.3% of the measured data will be within the shifted linear regression model, illustrated by the red line in Fig. 3.6.

Thus the shifted linear regression model will prove as the predictor model for $t_{conv,lin}$. The final values used to predict the convergence time can be seen below in equation 3.14.

$$t_{conv,lin} = 921.583 - 1.9287 * T_{dis,initial} \tag{3.14}$$

For further FDD analyses $t_{conv,lin}$ from equation 3.14 will be used to predict when the system has reached steady state oepration.

Predictions of exponential regression model

The deviations between $T_{PR,dis}$ and T_{dis} had an exponential decrease with respect to time depending on the initial difference between T_{dis} and $T_{PR,dis}$. This dependency can be quantified and predicted by looking further at a, b and c from equation 3.11 and their relation with the initial deviation between T_{dis} and $T_{PR,dis}$. From Fig. 3.7 it is apparent that a, b and c can accurately be predicted based on the initial deviation between T_{dis} and $T_{PR,dis}$. Predicting the exponential model through a, b and c will lead to a more precise prediction of the startup sequence.

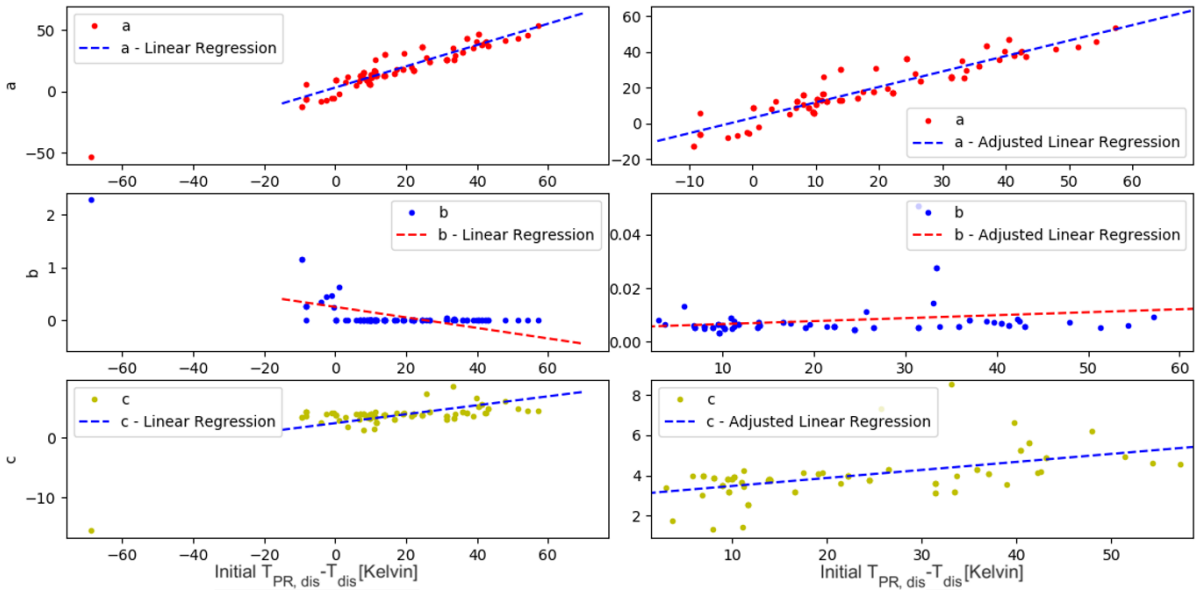

Figure 3.7: a, b and c from equation 3.11 (y-axis) sampled from 98 different startups in relation to $T_{PR,dis} - T_{dis}$ before the compressor prediction tool is initiated (x-axis). The left hand side shows the entire raw data set, while the right hand side shows a, b and c within a defined range where a, b and c can be predicted sufficiently accurate.

On the left side of Fig. 3.7 are all the data points of a, b and c sampled from 98 different startups. The x-axis on Fig. 3.7 is the starting temperature difference between the predicted and measured discharge temperature when the prediction tool is initiated. When this is approaching zero, b becomes fluctuating as seen in the middle graph on the left hand side of Fig. 3.7. However, if the operating range of the initial $\Delta T_{PR-measured}$ is defined from 5 K and upwards, as it is on the right side of Fig. 3.7, then a, b and c from equation 3.11 can accurately be predicted.

When the initial $\Delta T_{PR-measured}$ is below 5 K it indicates that the startup happens at already warm conditions. At these conditions the compressor prediction tool should not need a time difference to predict the discharge temperature accurately.

Fig. 3.8 shows the implementation of the exponential model with the linear regressions from Fig. 3.7. The model generally fits well, however t_{conv} predicted by a, b and c, further called by $t_{conv,exp}$, is not sufficiently accurate as marked by the brown dots in Fig. 3.8. The shifted linear regression model from equation 3.14 gives a sufficiently accurate picture of the convergence time between the predicted and measured discharge temperature as marked by the purple dots in Fig. 3.8 due to its safety margin.

During startups a, b and c given by the linear regression models from Fig. 3.7 can be used to predict the startup sequence in combination with $t_{conv,lin}$. a, b and c can be estimated linearly as seen in Fig. 3.7 by equation 3.15, 3.16 and 3.17 respectively.

$$a = 3.188 + 0.866 * (T_{PR,dis,initial} - T_{dis,initial}) \tag{3.15}$$

$$b = 0.0001107 + 0.00546 * (T_{PR,dis,initial} - T_{dis,initial}) \tag{3.16}$$

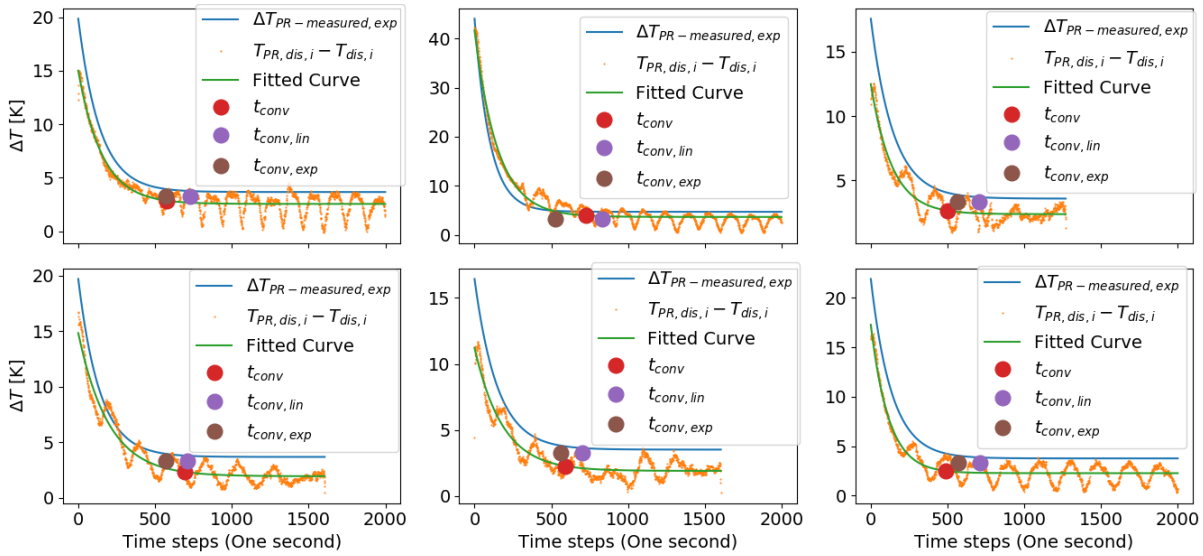

Figure 3.8: 6 sampled startups, the blue line uses the predictions of a, b and c from the linear regressions in Fig. 3.7. The purple dots are the predicted convergence times from the linear regression model in equation 3.14, t_{conv}. The red dots are the actual convergence time from the exponential regression fit for each individual startup, t_{conv}. Lastly the brown dots are the convergence time predicted from the exponential regression fit,$t_{conv,exp}$.

$$c = 3.075 + 0.0400 * (T_{PR,dis,initial} - T_{dis,initial}) \tag{3.17}$$

Analyzing equation 3.15, 3.16 and 3.17 in Fig. 3.8 it is apparent that the first term of equation 3.11, ae^{-bt}, will have the exponential decrease desired. At the first time step e^{-bt} will be approximately one, and $a + c$ dictates the starting value of $\Delta T_{PR-measured}$, hence a is approximately itself inverted. As t increases the term ae^{-bt} will decrease to zero, and the value left will be c. What is apparent from Fig. 3.7 is that c is relatively constant ranging from 3 K to 4.5 K. At the end of the startup $\Delta T_{PR-measured}$ should be constant at 3.3 K as it is a "5HP-compressor". The shape and time of the exponential decrease is dictated by b.

Equation 3.15, 3.16 and 3.17 can be used to predict the exponential curve dictating the temperature difference between the predicted and measured T_{dis}. It is apparent from Fig. 3.8 that t_{conv}, indicated by the red dots, is different from $t_{conv,exp}$, indicated by the brown dots for most startups. In fact $t_{conv,exp}$ is relatively constant in all startups. Table 3.6 shows the results after analyzing 37

Table 3.6: Table showing the results from 37 startups.

Measured differences	**Average**	**Standard Deviation**
$t_{conv} - t_{conv,exp}$	83.97 s	158.6 s
$t_{conv} - t_{conv,lin}$	102.3 s	267.9 s
$\overline{\Delta T_{PR-measured} - \Delta T_{PR-measured,exp}}$	-0.389 K	0.810 K
$\sigma_{(\Delta T_{PR-measured} - \Delta T_{PR-measured,exp})}$	0.903 K	0.435 K

compressor startups. Where $\overline{\Delta T_{PR-measured} - \Delta T_{PR-measured,exp}}$ is the average difference between the exponential regression fit of the recorded data and the exponential regression model predicted through equation 3.15, 3.16 and 3.17 for each startup. $\sigma_{(\Delta T_{PR-measured} - \Delta T_{PR-measured,exp})}$ is the standard deviation between the two models during each startup. They both give an idea of how well the exponential regression model predicted from equation 3.15, 3.16 and 3.17 fits to the measured data.

It is apparent from Fig. 3.9 and Table 3.6 that neither $t_{conv,exp}$ indicated by orange dots nor $t_{conv,lin}$ indicated by blue dots are giving a prediction that can capture the trend in the data. The actual convergence time for each individual startup is indicated by a green cross and has no apparent trend.

Liquid in the discharge line is common during startup and it is not necessarily damaging. Liquid

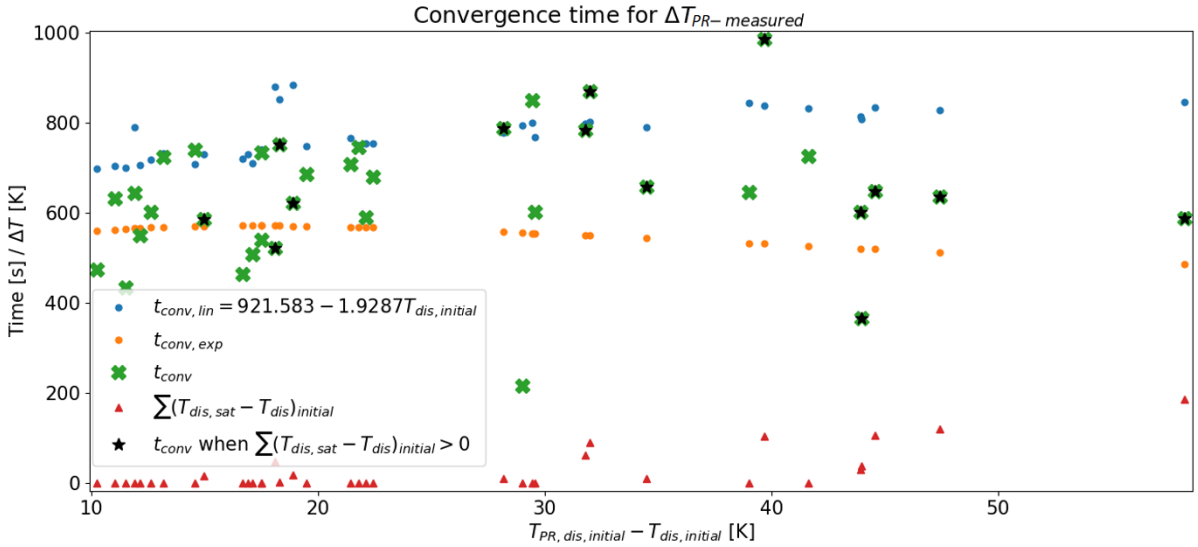

Figure 3.9: Sampled data from 37 startups where t_{conv} from equation 3.12 for each individual startup is given by green crosses, the orange dots are $t_{conv,exp}$ predicted from equation 3.15, 3.16, and 3.17 and the blue dots are $t_{conv,lin}$ predicted through equation 3.14. Instances where T_{dis} was lower than $T_{dis,sat}$ during startup are marked by black stars. The red triangles marks the total sum of $T_{dis,sat}$ minus T_{dis} before and during the startup

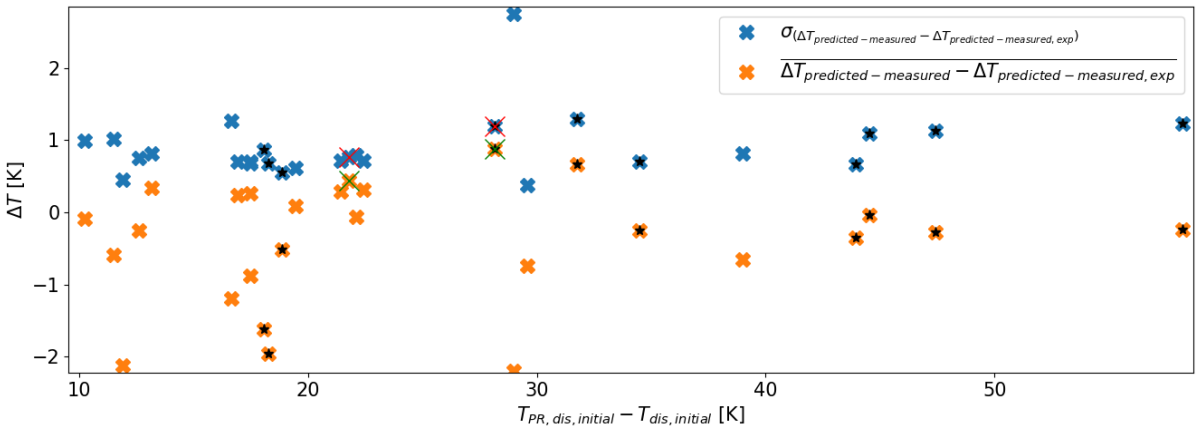

Figure 3.10: The result of analyzing 37 different startups and investigating the difference between the model predicted by equation 3.15, 3.16, and 3.17 and the exponential regression model fitted to the actual data. The black stars marks the startups where condensation was detected in the discharge.

formation will occur when T_{dis} is lower than $T_{dis,sat}$ as in Fig. 3.11. The total sum whenever T_{dis} is lower than $T_{dis,sat}$ of $T_{dis,sat}$ minus T_{dis} before and during startup is indicated in Fig. 3.9 by red triangles. The difference occurs as pressures (thus also saturated temperatures) build up immediately after a startup, while temperatures have a slower build up.

The temperature will increase at a slower rate when there is liquid in the discharge line due to the different heat transfer abilities of gas and liquid. In Fig. 3.11 condensation in the discharge occurs during a startup. This results in T_{dis} dipping and T_{dis} needs more time to reach its operating conditions. There were only 14 cases where condensation was detected in the discharge line, which is not sufficient to build a model or draw any conclusions. The black stars in Fig. 3.9 marks t_{conv} when there was liquid formation in the discharge during startup.

In Fig. 3.10 the orange crosses represents $\overline{\Delta T_{PR-measured} - \Delta T_{PR-measured,exp}}$, which is the average difference between the exponential regression model predicted by equation 3.15, 3.16 and 3.17, and the exponential regression model fitted to the actual data. Whenever this is above zero it is an indication that the startup is happening slower than predicted, as in Fig. 3.12. Two of the startups where

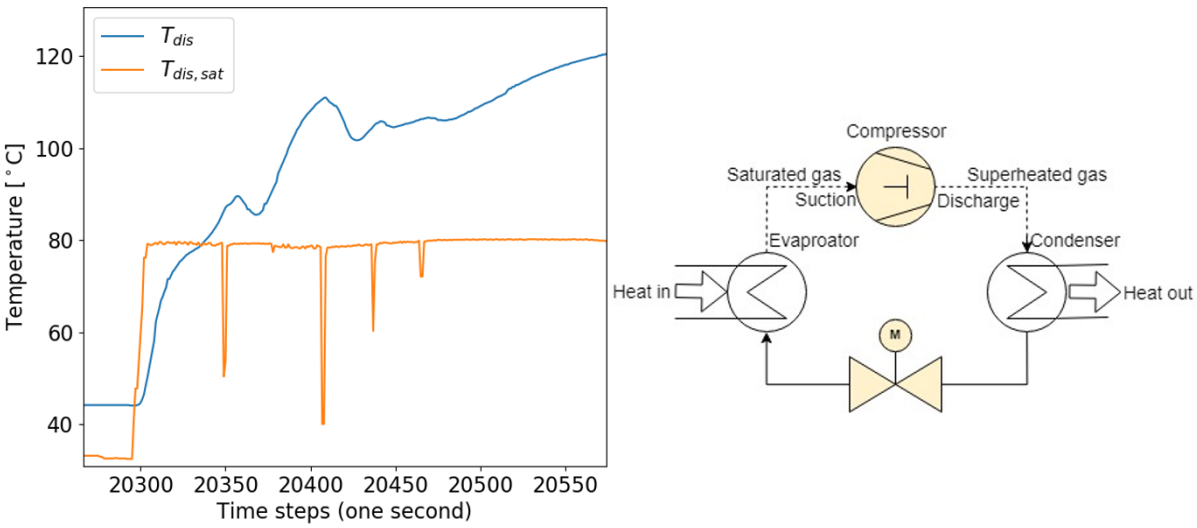

Figure 3.11: The left side shows a graph of condensation happening in the discharge line of a compressor during startup due to $T_{dis,sat}$ beeing higher than T_{dis}. The right side shows a simplified schematic of a heat pump system, where the discharge is indicated.

$\overline{\Delta T_{PR-measured} - \Delta T_{PR-measured,exp}}$ is particularly high, are further examined in Fig. 3.12. What is apparent is that the green line ($\Delta T_{PR-measured}$), is clearly higher than the blue line ($\Delta T_{PR-measured,exp}$). Based on the initial $T_{PR,dis,initial} - T_{dis,initial}$ the data is expected to follow the blue line.

For the FDD analyses the linear predictions of $t_{conv,lin}$ will be used to predict the startup time of the

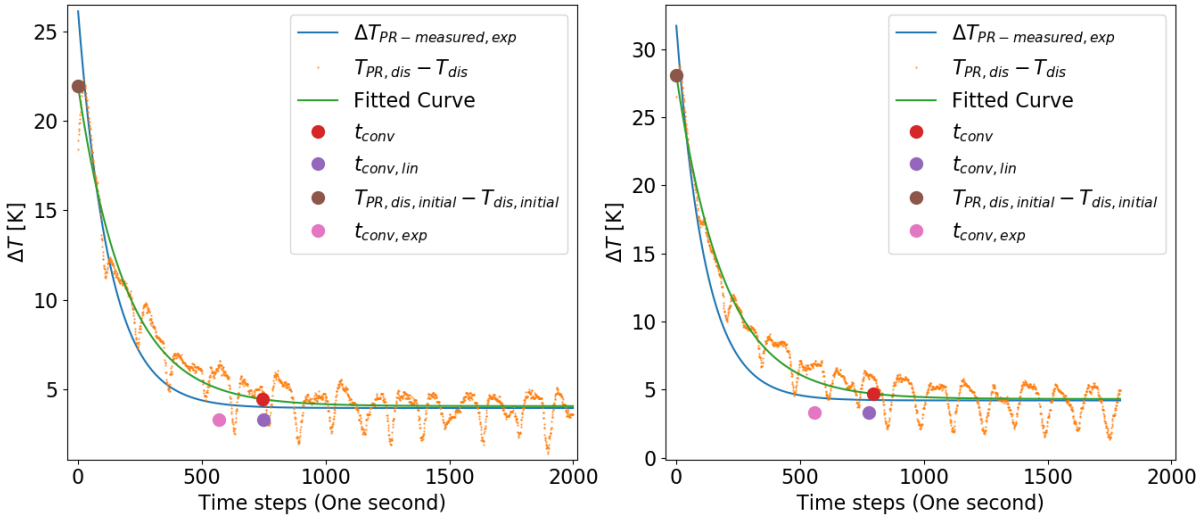

Figure 3.12: Two startups from the same "5HP-compressor" where the startup time was longer than expected. The graph to the right had condensation detected in the discharge. t_{conv} is higher than $t_{conv,lin}$ and $t_{conv,exp}$, and $\Delta T_{PR-measured}$ is clearly higher than $\Delta T_{PR-measured,exp}$. These startups are marked by the green and red crosses in Fig. 3.10. They will be further discussed for Fault 5.7 as a symptom of liquid carry-over causing a delayed increase of T_{dis} during startup.

compressor. The findings are assumed to be valid for both compressor types as there is not enough data available from the "V-compressor" to draw any conclusions.

The results from the one heat pump system operating with a "V-compressor" in Fig. 3.13, shows on the right side a, b and c, b varying more than for the "5HP-compressor". The left side of Fig. 3.13 shows t_{conv} in relation to the starting T_{dis}, where there is no apparent trend.

The only thing that can be concluded about the "V-compressor" is that the startup time could be

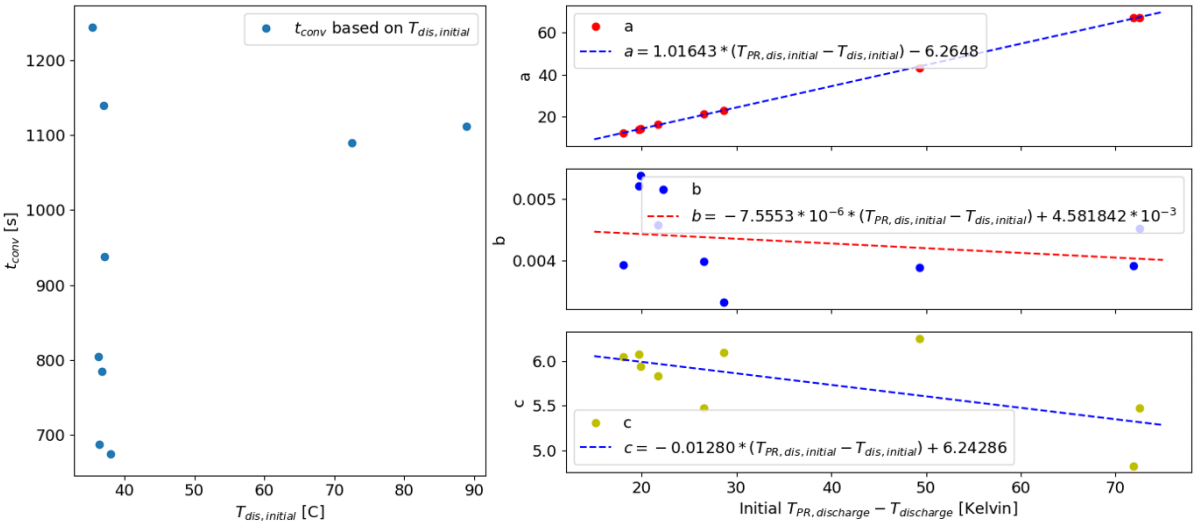

Figure 3.13: The analysis of the startup time for the "V-compressor" sampled from 9 compressor startups of the "V-compressor". The left hand side shows t_{conv} based on $T_{dis,initial}$, the right hand side shows a, b and c from equation 3.11 and the best fit of a linear regression model for a, b and c, based on the initial $T_{PR,dis} - T_{dis}$.

longer for the "V-compressor". This is based on the left hand side of Fig. 3.13. The conclusion is that most dots on the left side of Fig. 3.13 are higher than what was seen in the same plot in Fig. 3.6 for the "5HP-compressor". Hence the startup is expected to last longer for the "V-compressor".

3.3.2. Compressor driving power initiation time

The compressor driving power is not dependent on the rate at which T_{dis} increases during a startup. P_e is however dependent on the capacity steps the compressor does during startup where the operating capacity of the compressor is increased in steps. These steps are done as the compressor activates one cylinder at a time.

Heat pump systems without power measurements

The calculated power is dependent on N_{RPM} and I_{motor}. During a startup there is a direct dependency between I_{motor} and the running capacity of the compressor. This direct dependency is captured by equation 3.3, making the calculations of the driving power accurate at all running capacities, the accuracy during a startup was seen in Fig. 3.1.

The compressor prediction tool requires a running capacity of 100 % for the "5HP-compressor". This avoids the startup issues for the power of the "5HP-compressor".

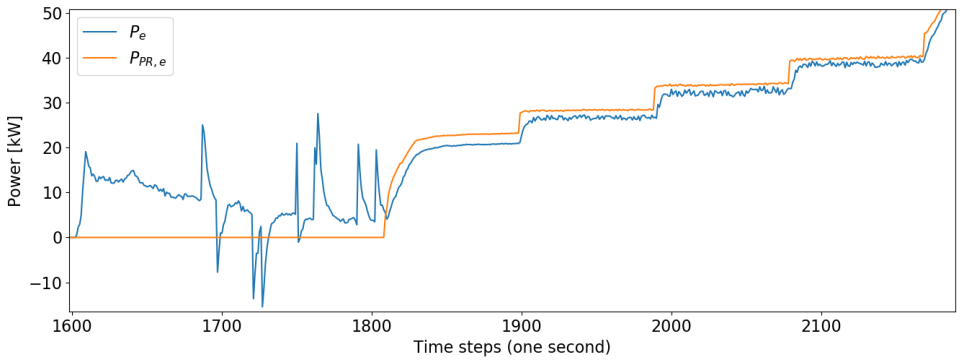

Figure 3.14: Startup of a "V-compressor" showing the predicted driving power, $P_{PR,e}$, and the measured power required to drive the shaft P_e.

Heat pump systems with power measurements

When the compressor does its capacity steps during startup, the predicted compressor driving power is not able to capture the measurements correctly during the first capacity step. For the heat pump systems where the power is measured, one is dependent on comparing the motor powers after the first capacity step. For the "V-compressor" the compressor prediction tool can predict $P_{PR,e}$ after first capacity step, and it is accurate from the second capacity step illustrated in Fig. 3.14.

3.3.3. Condenser heat and COP initiation time

The compressor prediction tool required the time previously discussed as $t_{conv,lin}$ after the compressor starts up to have a constant deviation between $\dot{Q}_{cond}$ and $\dot{Q}_{PR,cond}$. This time is marked by red dots in Fig. 3.15. In Fig. 3.15 the difference between the estimated and predicted condenser heat capacity

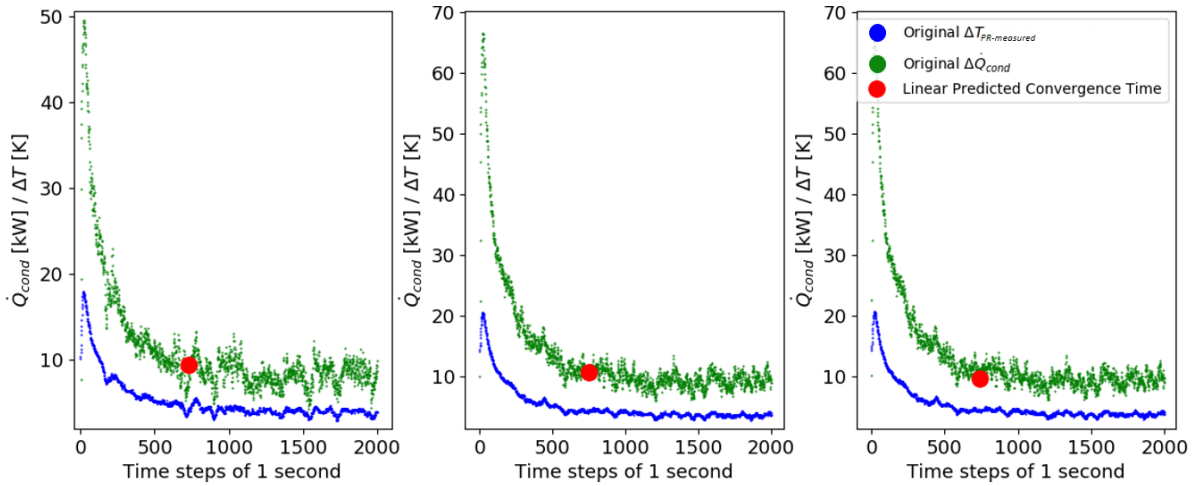

Figure 3.15: 3 sampled startup sequences from a "5HP-compressor". The difference between $\dot{Q}_{PR,cond}$ and $\dot{Q}_{cond}$ is shown by the green line, the difference between $T_{PR,dis}$ and T_{dis} is shown by the blue line. The red dots mark the convergence time using the linear relationship from equation 3.14, $t_{conv,lin}$.

is recorded during 3 different startups in a "5HP-compressor". It was concluded that the predictions of the startup time of the discharge temperature from subsection 3.3.1 are valid for $\dot{Q}_{cond}$. Because $\dot{Q}_{cond}$ is directly depending on the enthalpy at the discharge of the compressor, which again is taken from the measurements of T_{dis} and p_{dis}.

Both $P_{PR,e}$ and $\dot{Q}_{PR,cond}$ are estimated through the compressor prediction tool, meaning that COP_{PR} is dependent on the startup time of both. The COP will be dependent on the same startup time as $\dot{Q}_{cond}$ because P_e does not have a startup time, this is apparent in Fig. 3.16.

The startup time that was found valid for T_{dis} is assumed to be valid for $\dot{Q}_{cond}$ and the COP, as they are both dependent on T_{dis}.

3.4. Initial data analysis

Different faults have different demands of variables and measurement interval and some faults are exclusive to certain compressors or heat pump systems. Therefore an initial analysis is done for each data set to identify the heat pump system and what lies within the system, to see which faults can be analyzed and not. This initial analysis is shown in Fig. 3.17. It is assumed for the analyses to follow in section 4, 5, and 6 that the measuring time step is the same as what is indicated in Table 1.2. It is also assumed for the FDD algorithms to follow that the necessary variables are measured.

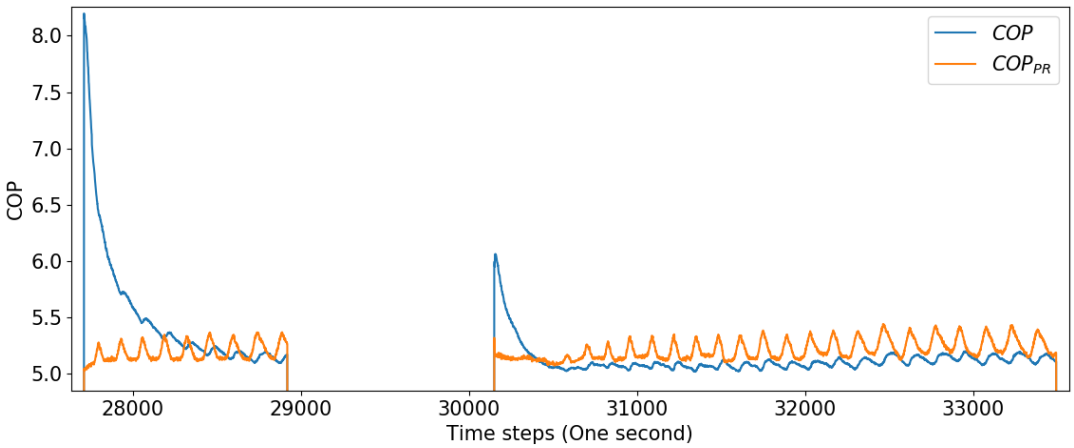

Figure 3.16: The development of the predicted COP and the measured COP during two startups of a "5HP-compressor". The graph contains two startups where it is visible that the predictions need a certain time to become stable.

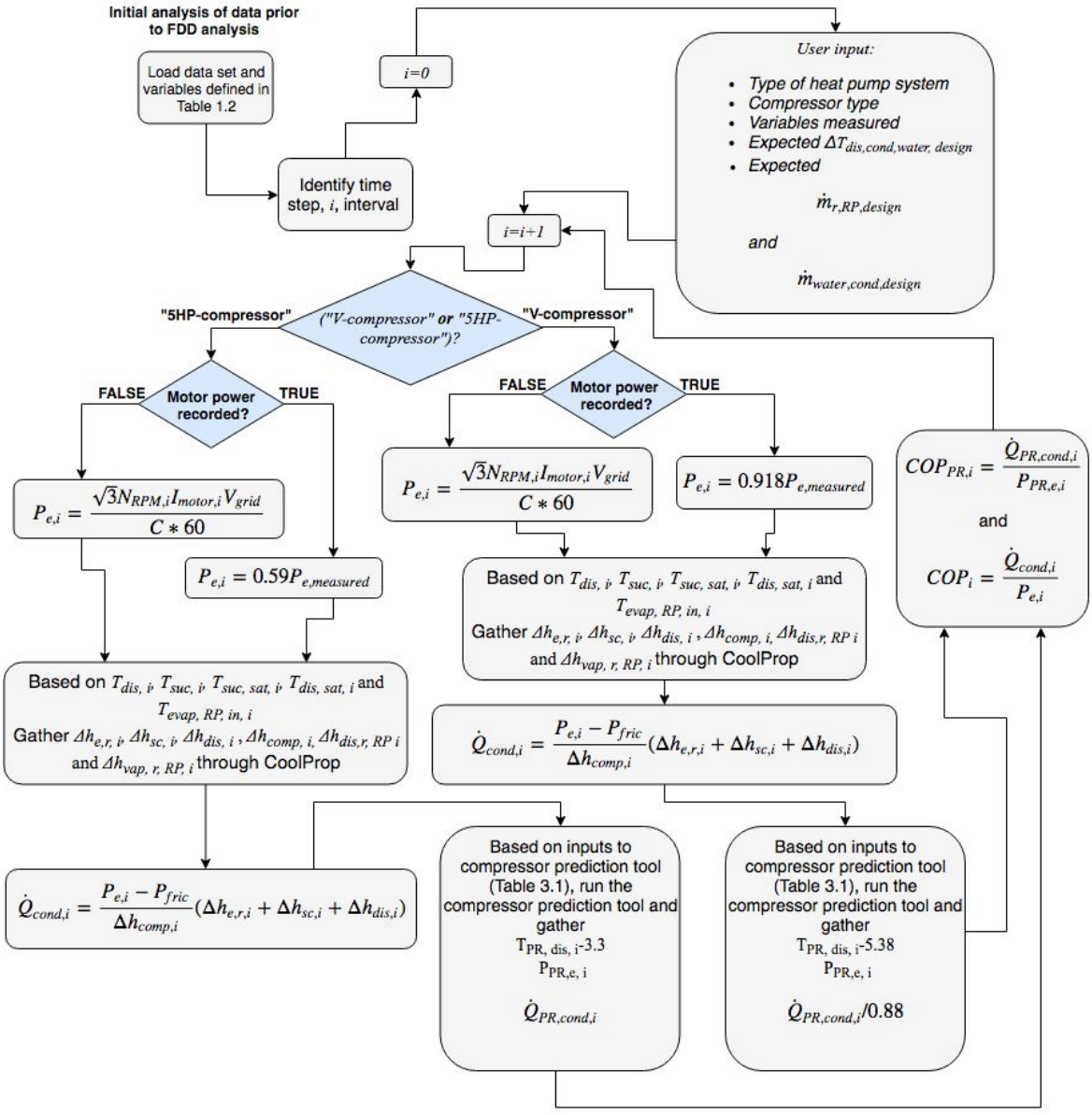

Figure 3.17: The initial analysis of the data required prior to the FDD analysis to identify the system.

4

Compressor Related Faults

Compressor related faults are failures in the heat pump system where the compressor or a component within the compressor is the failure cause. The heat pump systems of relevance are equipped with two different compressor types in Fig. 4.1, referred to as the ”V-compressor” and the ”5HP-compressor”. Both are prone to failures, the ”5HP-compressor” is the older of the two. There are two differences between the compressors that affects the FDD approach; the ”5HP-compressor” has an oil pump mounted on the same shaft circulating oil in the compressor, while the ”V-compressor” has an external oil pump. The second difference is that the ”V-compressor” is proven to resist all back flows, which in principle gives the ”V-compressor” two non-return valves. The ”5HP-compressor” has a slight leak when introduced to a back flow. These differences will become apparent in Fault 4.3, Fault 5.5, Fault 6.1 and Fault 6.5.

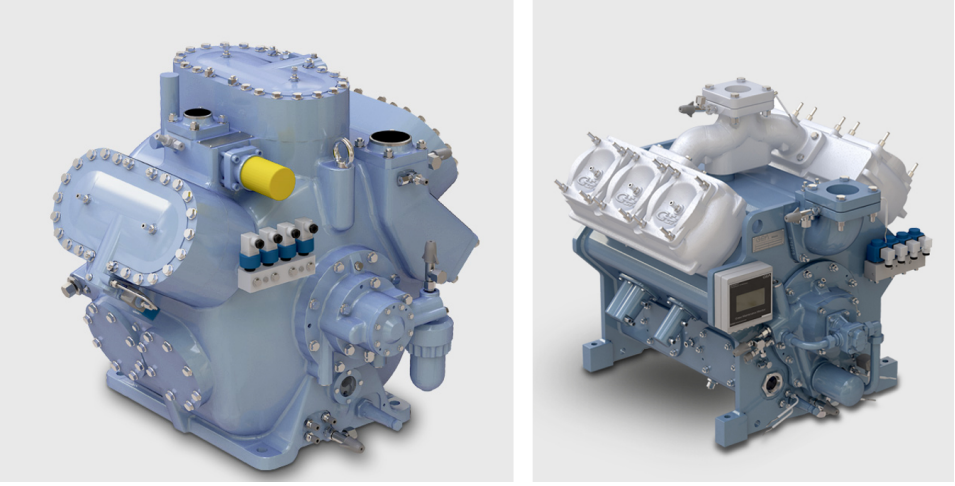

Figure 4.1: The two different types of piston compressors considered. On the left side is the ”5HP-compressor” and on the left side is the ”V-compressor”. They can all be fitted with a variable amount of cylinders.

All faults classified as compressor faults are independent of what type of heat pump system the compressor is mounted on. There are seven individual faults classified as compressor faults where the failure is directly related to the compressor or a part within the compressor, which are all listed in the following subsections.

4.1. Broken bypass valve of the compressor

The bypass valve is the yellow motor driven valve in the schematic of Fig. 4.2. It can be faulty for both the ”5HP-compressor” and the ”V-compressor”. To detect it, a measuring interval of 1 second is required, however a closed bypass valve during shutdown is only detectable for the ”5HP-compressor”. During startup of the compressor the bypass valve is opened for a small time period to allow for

bypassing the gaseous refrigerant. This is done to have an unloaded start of the compressor to reduce the strain on the shaft. During shutdown of the compressor the bypass valve is opened again to equalize the pressures of the compressor, to lower the pressure of the discharge line. Both these behaviors in their ideal case can be observed in Fig. 4.3.

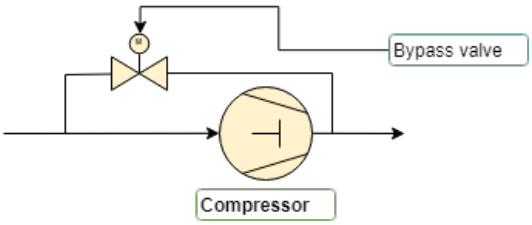

Figure 4.2: The bypass valve that allows for the gaseous refrigerant to bypass the compressor.

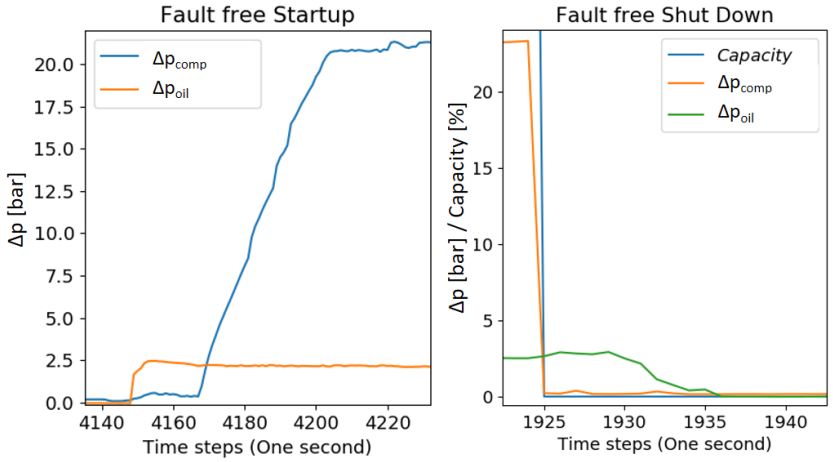

Figure 4.3: The ideal behavior of the bypass valve during startup and shut down of the compressor. The graph to the left shows the desired minimum 10 second lag between the increase of Δp_{oil} (orange line) and the increase of Δp_{comp} (blue line). The graph to the right show the Δp_{comp} (orange line) equalizing immediately after the capacity (blue line) reaches zero, while Δp_{oil} (green line) stays at operating conditions slightly longer.

4.1.1. Fault Description and Symptoms

The bypass valves are subject to temperatures above their prescribed limits, making them prone to damage.

1. The bypass valve remains closed during startup. If the bypass valve does not open during startup the pressure difference over the compressor increases simultaneously as the heat pump is started. Ideally there would be the 10-15 second lag as in Fig. 4.3.

2. The bypass valve remains closed during shutdown. The closed valve is noticeable by the time it takes for the compressor differential pressure to equalize, this should ideally be less than 10 seconds. In Fig. 4.3 it is less than three seconds. This fault only applies for the ”5HP-compressor”, as the bypass valve for the ”V-compressor” has relatively small opening, which causes the compressor differential pressure to take up to five minutes to equalize.

3. After a startup of the compressor the bypass valve never closes and the pressure difference over the compressor never increases. The compressor shuts down eventually due to limit alarms because the compressor differential pressure never reaches the minimum operating conditions.

4.1.2. Failure Detection Approach

The first failure mode is detected by isolating the startup periods of each compressor. During this period the time difference between the startup of the compressor and the compressor differential pressure

starting to increase is recorded. This time difference should be ten seconds or more according to the control system, hence whenever it is less than 10 seconds the fault is detected. The approach is illustrated in Fig. 4.4.

The second fault is detected by the time step where the compressor shuts down, known as the

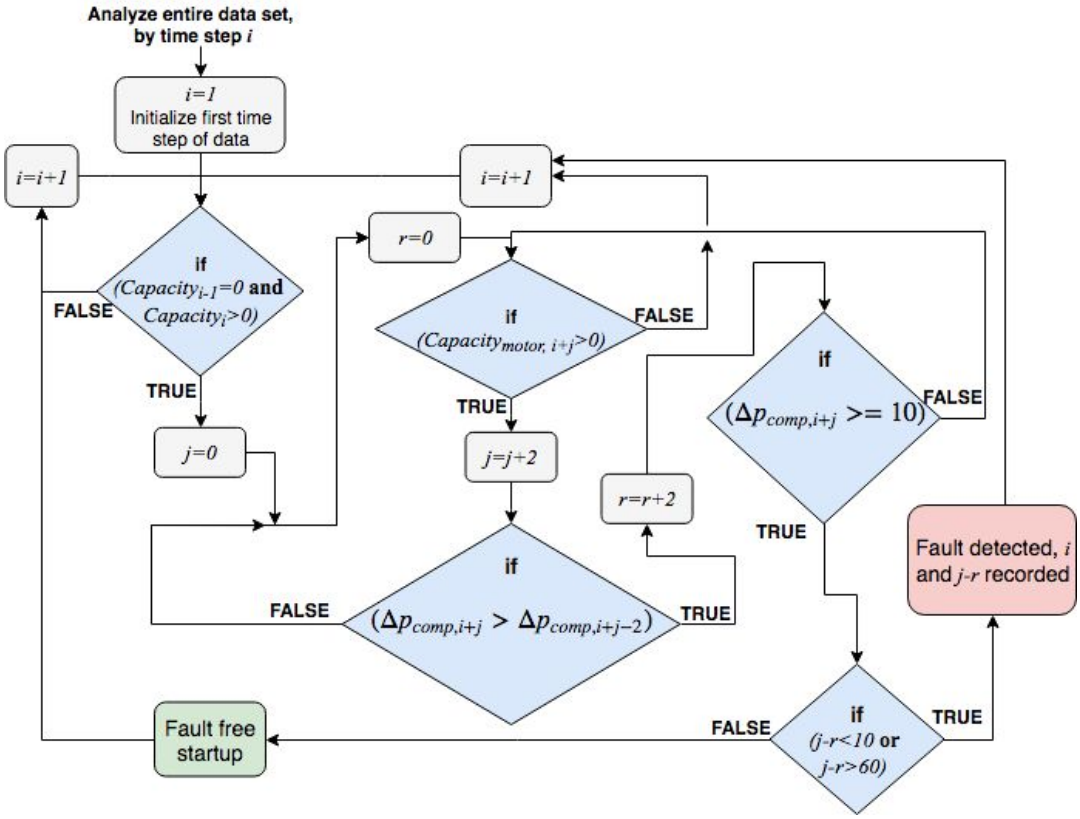

Figure 4.4: The FDD approach to detect a closed bypass valve during a compressor startup. Δp_{comp} is said to be within operating conditions for this fault at 10 bar. The program checks that Δp_{comp} is increasing every 2 seconds and detects the fault if the time difference from when the compressor capacity is initiated and when Δp_{comp} begins to increase is less than 10 seconds or more than 60 seconds.

time step when the capacity reaches zero. The time difference between the known shutdown and the compressor differential pressure equalizing is recorded, in addition to the time step where the compressor differential pressure begins to decrease. The fault is detected if either the compressor differential pressure decrease to less than 10 bar does not begin by 45 seconds, or if the compressor differential pressure decrease lasts for more than 10 seconds as in Fig. 4.5.

The third bypass valve fault is detected by isolating the startup period of the compressor. If the compressor is started, but the compressor differential pressure never reaches above 3 bar after more than 20 seconds of operation. The compressor eventually shuts off and the fault is detected. A warning is issued if the compressor differential pressure takes longer than 25 seconds to reach its operating conditions. This approach is illustrated in Fig. 4.6.

The three failures of the bypass valve are all detected in a qualitative manner using a case-based reasoning approach. The failure is detected by storing the knowledge learned by experts in a database, and seeing how the measured data compares to the trends in the database.

4.1.3. Results

The closed bypass valve during startup and the closed bypass valve during shutdown, the first and second failure mode could be detected in the given manner. Fig. 4.7 shows the first and second failure mode being detected in a heat pump system on the left and right side respectively. The closed bypass

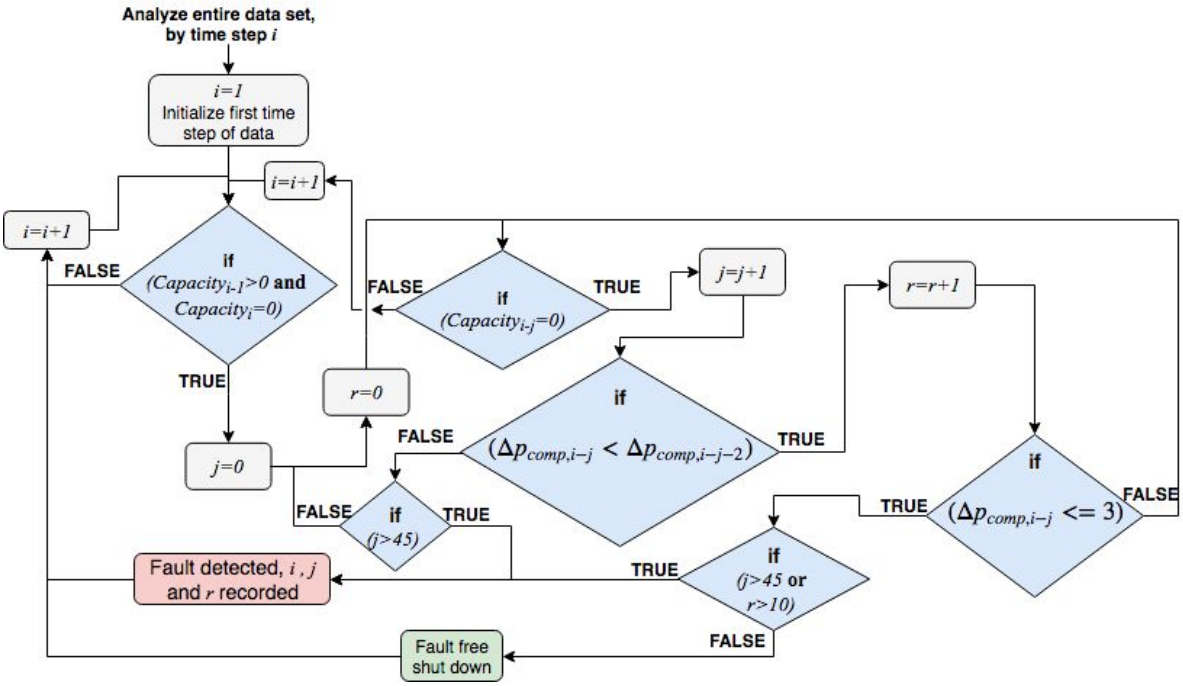

Figure 4.5: The FDD approach to detect a closed bypass valve during shutdown. The FDD algorithm counts every time step the pressure decreases until it is less than 3 bar, which is defined as pressure equalization in this case. r counts how long the decrease lasts, j counts the time passed since the capacity reached zero. If r is higher than 10 seconds or if j is higher than 45 seconds then the fault is detected.

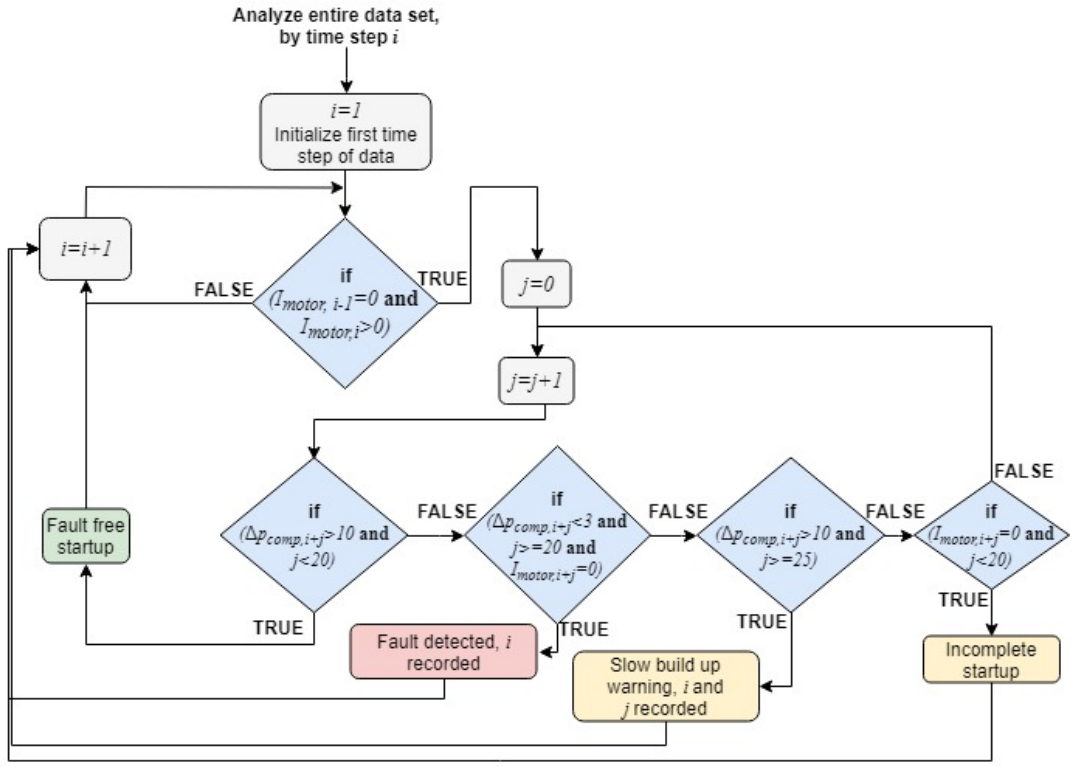

Figure 4.6: The approach to of the FDD program to detect an open bypass valve during startup.

valve during startup is detected repeatedly during every startup, where the recorded time difference is less than three seconds. The closed bypass valve during shutdown is detected once during a shutdown,

the right side of Fig. 4.7. It became apparent that a leaking non-return valve, later introduced as Fault 6.1, had an identical failure symptom to the bypass valve being closed during shutdown, making them impossible to differentiate for the ”5HP-compressor”.

The bypass valve remaining opened during startup, the third failure mode, could not be differentiated from a broken suction valve in the compressor and a problematic startup of the heat sink flow, later introduced as Fault 4.5 and Fault 5.10 respectively. This was due to the three failure modes having identical failure symptoms.

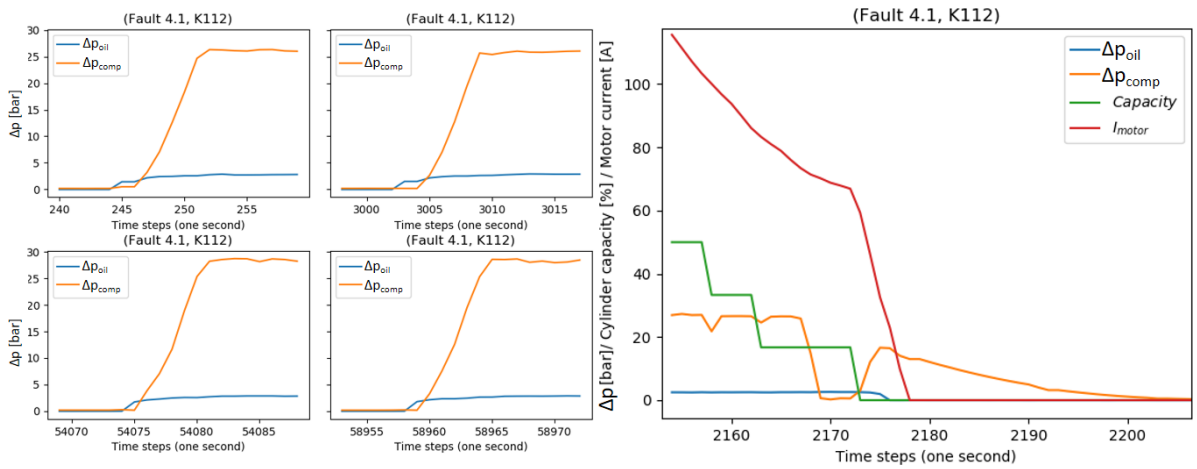

Figure 4.7: A defect bypass valve detected in a heat pump system. The left side shows the bypass valve remaining closed during startup where the time difference between Δp_{comp} (orange line) and Δp_{oil} (blue line) beginning to increase is less than 3 seconds. The right side shows the bypass valve remaining closed shutdown, the capacity (green line) reaches zero, however Δp_{comp} (orange line) was equalized before. Upon inspection this is however an example of a leaking non-return valve, later described in Fault 6.1.

4.2. Defect capacity valve mechanism

During a startup of the compressor the cylinders of the compressor are activated one by one. The running capacity of the compressor is defined as the amount of activated cylinders. There is a direct dependency between the current consumed by the motor and the running capacity of the compressor. Whenever a capacity step is done the motor current should increase accordingly through the capacity solenoid valves as in Fig. 4.8. This is a fault that can occur in both the ”5HP-compressor” and the ”V-compressor” and it requires a measuring interval of one second.

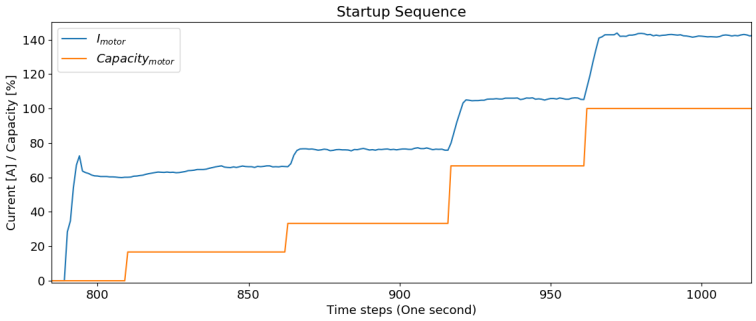

Figure 4.8: Graph from a fault-free startup in one of GEAs heat pumps, the capacity (orange line) is increasing in steps, and the motor current (blue line) is following accordingly.

4.2.1. Failure Description

The physical fault could be due to a number of reasons; incorrect mounting of the valve, broken push handle or a defect capacity solenoid valve.

4.2.2. Failure Symptom

The fault has only one symptom that characterizes it as seen below. The symptom gives an indication that something is not working as intended with the capacity valve mechanism, however it does not indicate what the fault is.

- During startup of the compressor the motor current is directly related to the running capacity of the compressor. At each different capacity step, the motor current deviations remain relatively insignificant compared to its original value and the motor current seems constant as in Fig. 4.8. However, if the fault is present, the motor current will remain unchanged over the capacity step or decrease as in Fig. 4.10.

4.2.3. Failure Detection Approach

The program will detect this fault by analyzing each startup individually. At each startup the average current at each capacity step is recorded. The fault is identified if the difference between the average motor current at two different capacity steps during a startup is less than the standard deviation, $\sigma_{M,k}$, of the motor current in the first of the two capacity steps as explained in Equation 4.1.

$$\sigma_{M,k} = \frac{\sqrt{\sum (M_{k,i} - \overline{M_k})^2}}{N_k} \tag{4.1}$$

Where M_k is the matrix containing all the recorded motor currents at capacity step k, i is the index in that matrix and N_k is the amount of samples, at the given capacity step k. The approach is illustrated in Fig. 4.9, where $Capacity_{motor}$ is the compressor running capacity. Assuming the compressor has a maximum of six different capacity steps during start up indicated as $Capacity^k$.

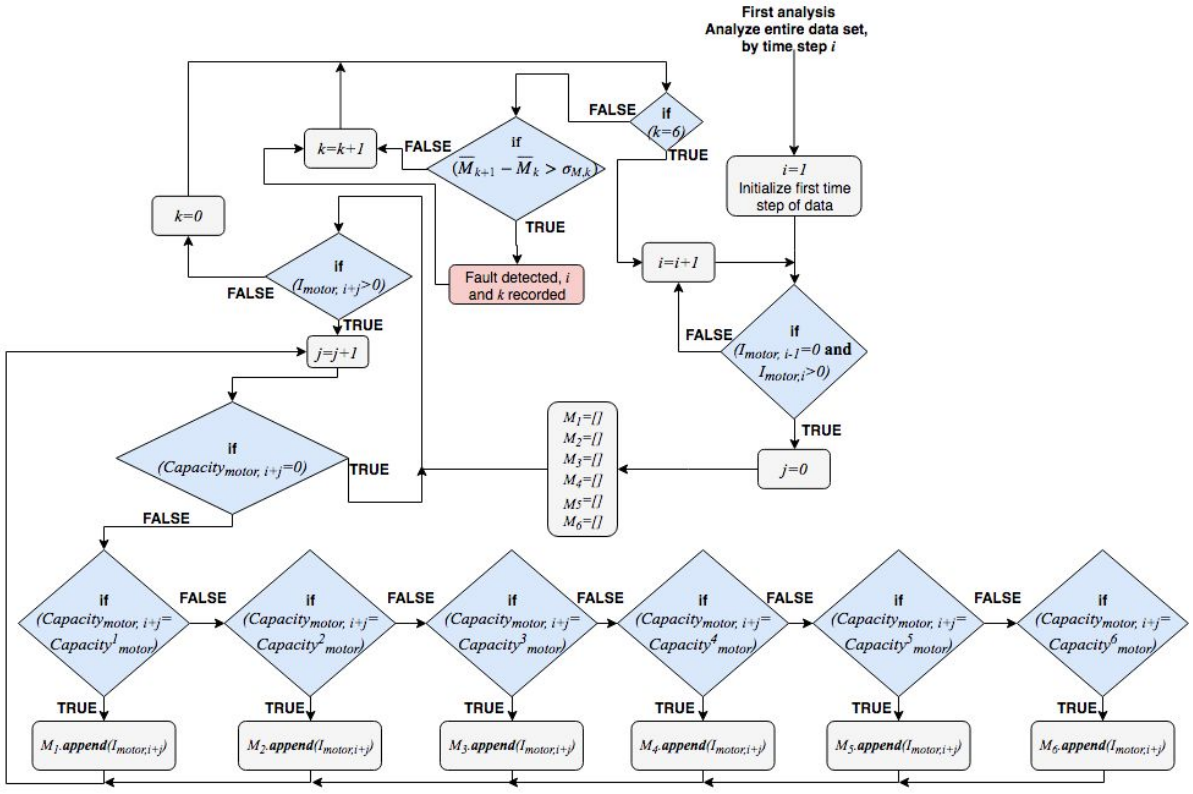

Figure 4.9: The FDD approach of the FDD program to detect the faulty capacity valve mechanism, where $\sigma_{M,k}$ is given by Equation 4.1

.

The failure of the capacity valve mechanism is detected in a qualitative manner using a case-based

reasoning approach. The failure is detected by storing the knowledge learned by experts in a database, and seeing how the measured data compares to the trends in the database.

4.2.4. Results

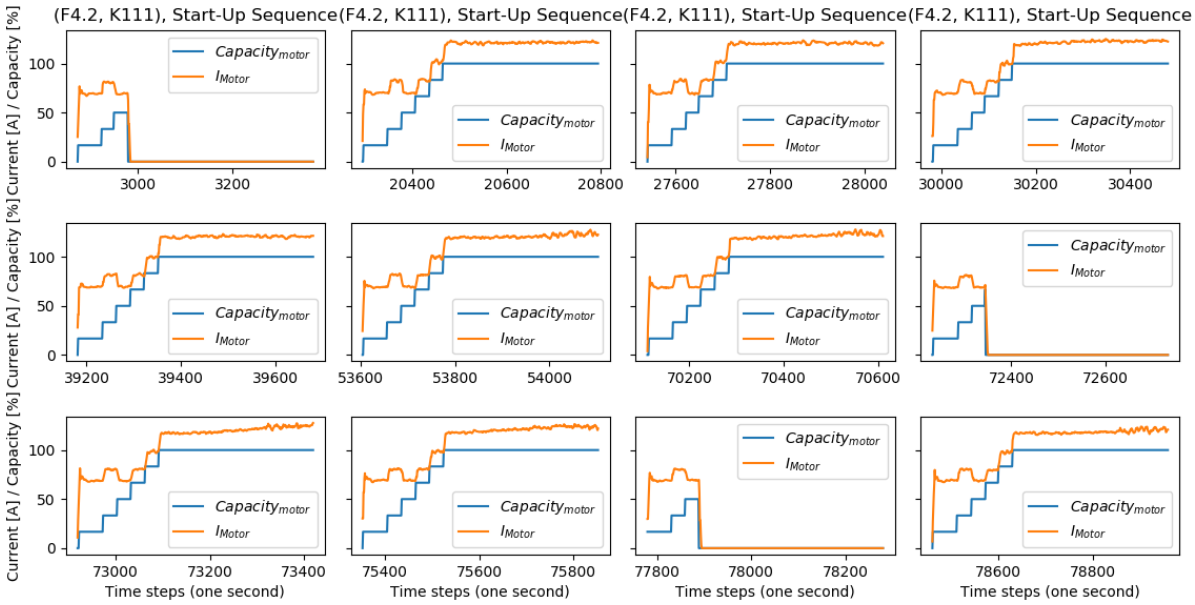

Figure 4.10: Data from a heat pump with faulty capacity valve mechanism occurring. The algorithm recognizes the fault repeatedly at every startup.

The algorithm was able to detect the fault in the example of the fault occurring during all startups of the compressor. The faulty capacity valve mechanism was apparent in the step from the second compressor running capacity to the third in Fig. 4.10. It is however apparent from Fig. 4.8 and Fig. 4.10 that the motor current at the lowest running capacity is fluctuating more than the motor current at the other running capacities. At the lowest running capacity (0%) the shaft has no resistance and the current is more fluctuating. The standard deviation of the motor current at the lowest running capacity will be higher than for the other steps, this leads to a less robust FDD for this particular compressor capacity. The concept of a robust FDD algorithm is explained in Table 1.1.

4.3. Bearing damage due to liquid refrigerant mixed with the oil

This is a problem which is specific to the ”5HP-compressor” and it requires a measurement interval of 10 seconds. The 5HP-compressor is lubricated with an oil that has a specific viscosity which is prescribed for the compressor of the heat pump. The 5HP-compressor has an oil pump mounted on its shaft that circulates oil throughout the system.

4.3.1. Failure Description

Liquid refrigerant mixing with the oil decreases the viscosity and lubrication abilities of the oil, a decrease in the lubrication abilities would over time decrease the lifetime expectancy of the compressor and lead to frequent starts and stops of the heat pump. This could originate from a sudden decrease in the suction pressure which lowers the boiling point of the refrigerant causing it to condensate or refrigerant mixing with the oil or other reasons.

4.3.2. Failure Symptoms

This fault has three different symptoms seen below.

1. The compressor driving power is higher than predicted by compressor prediction tool.

2. The temperature of the oil increases slightly, this is however dependent on the sensor positioning.

3. At low rotational speed the differential oil pressure is too low. The oil pump of the "5HP-compressor" is running at the same shaft speed as the compressor. If the differential oil pressure is too dependent on the rotational speed this fault can be identified as in Fig. 4.11.

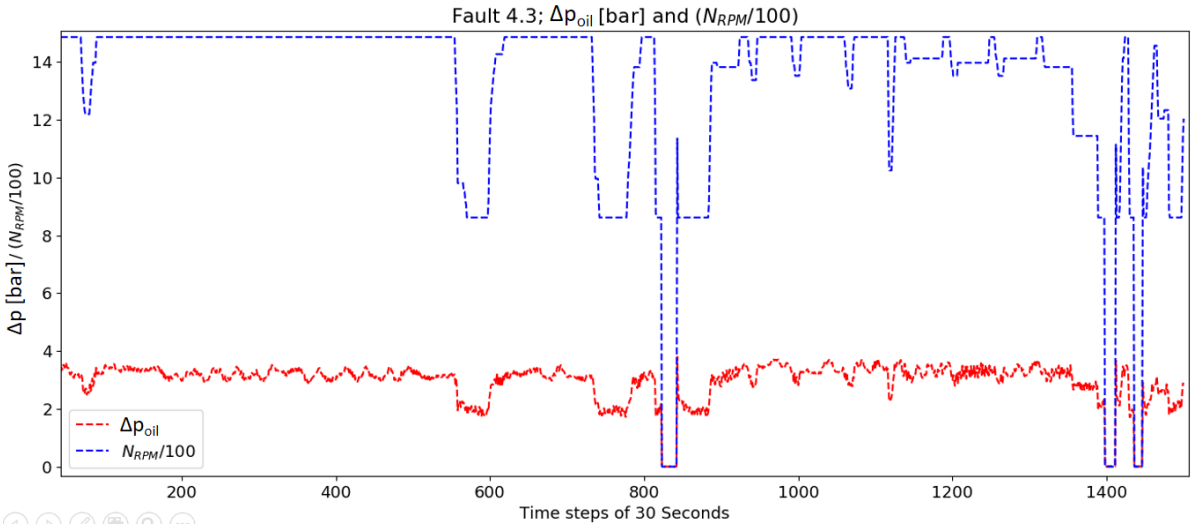

Figure 4.11: Graph of bearing damage detected through the relationship between Δp_{oil} and N_{RPM}. Whenever the rotational speed (dotted blue line) drops then the differential oil pressure (red line) follows and drops too low.

4.3.3. Failure Detection Approach

The high compressor driving power and the oil temperature increase are not visible enough in the data to actually identify a fault. This is proven for the power in Fig. 4.13.

The relationship between Δp_{oil} and N_{RPM} is used to detect the fault in the data. The program records the linear relation between the rotational speed of the motor and the differential oil pressure in the form given by equation 4.2.

$$\Delta p_{oil} = \Delta p_{oil,initial} + N_{rpm}\overline{(\frac{\Delta p_{oil}}{N_{rpm}})_{sampled}} \tag{4.2}$$

Where Δp_{oil}, N_{rpm} and $\overline{(\frac{\Delta p_{oil}}{N_{rpm}})_{sampled}}$ are the differential oil pressure in bar, the rotational speed of the motor in rotations per minute and the sampled linear relation between the two respectively. Furthermore the data from when the rotational speed is zero and running at its maximum is neglected, because the oil differential pressure is varying at the end points. The slope of the linear relation is sampled for 27 different fault-free compressors. The mean of these samples are used as a reference. The FDD program compares the measured slope coefficient to the sampled in Fig. 4.12.

The FDD approach utilizes a process history based gray-box linear regression model to detect the fault combined with qualitative case-based reasoning based on previously seen faults.

4.3.4. Results

$\overline{(\frac{\Delta p_{oil}}{N_{rpm}})_{sampled}}$ was $6.2445 * 10^{-4}$ with a standard deviation from the 27 compressors of $6.7086 * 10^{-5}$, or approximately 10 % of the mean.

In the data containing the fault from Fig. 4.11 it was seen that $\overline{(\frac{\Delta p_{oil}}{N_{rpm}})}$ was approximately 70 % higher than $\overline{(\frac{\Delta p_{oil}}{N_{rpm}})_{sampled}}$, thus the fault threshold used was 60 % to detect the fault, due the the standard deviation of $\overline{(\frac{\Delta p_{oil}}{N_{rpm}})_{sampled}}$.

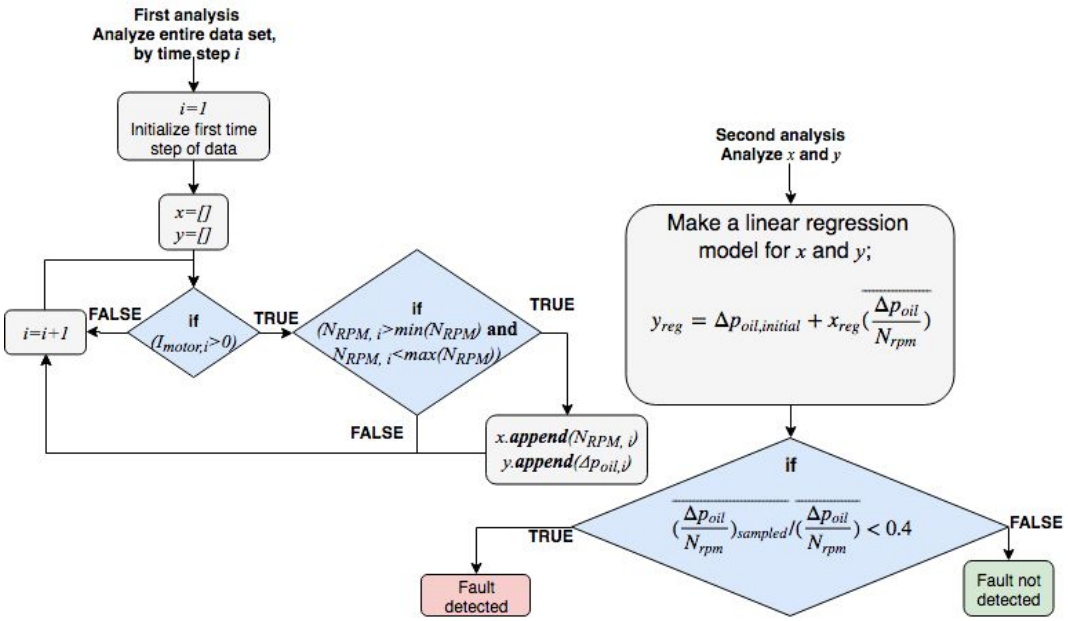

Figure 4.12: The approach of the FDD program to detect bearing damage. The approach is built up in two steps; first Δp_{oil} and N_{rpm} are recorded in the desirable range. Then the program performs a linear regression of Δp_{oil} and N_{rpm} and compares the slope coefficient, $(\overline{\frac{\Delta p_{oil}}{N_{rpm}}})$, to the sampled slope coefficient, $(\overline{\frac{\Delta p_{oil}}{N_{rpm}}})_{sampled}$.

The FDD program was able to detect the fault in one of GEAs compressors, where the operator was unaware of the fault. Fig. 4.13 shows $(\overline{\frac{\Delta p_{oil}}{N_{rpm}}})_{sampled}$ and $(\overline{\frac{\Delta p_{oil}}{N_{rpm}}})$ for the faulty heat pump, where $(\overline{\frac{\Delta p_{oil}}{N_{rpm}}})$ was seen to be $1.780 * 10^{-3}$, which is 64.9% steeper than expected. Hence the fault was detected on the third symptom.

For the first symptom, the fault was not detected, on the right side of Fig. 4.13, the power required to drive the shaft from measurements, P_e, was 1.4 times higher than the power predicted, $P_{PR,e}$. However the data from the right side of Fig. 4.13 is the only data from heat pump system with a "5HP-compressor" where P_e is measured. Hence the efficiency losses in the electrical motor and the frequency converter for the heat pump system with a "5HP-compressor" is unknown. However the power calculated (through equation 3.3), P_e, is identical to $P_{PR,e}$.

It cannot be concluded if bearing damage is detected on symptom one, if the calculations of the driving power are incorrect, or if the power losses prior to the shaft are larger for the "5HP-compressor" than for the "V-compressor".

The FDD approach to detect bearing damage was able to detect the failure in these two instances, however it is dependent on analyzing all the data first. Hence with this approach the FDD algorithm will only detect the fault after it has happened. Thus FDD algorithm to detect bearing damage is not performing well on the quick detection and diagnosis criteria from Table 1.1.

4.4. Defect discharge valve

Each cylinder in both compressors have a discharge valve, shown in Fig. 4.14. The valve ensures that there is no back flow from the discharge line when sucking the refrigerant before compressing. To detect this fault a measurement interval of 30 seconds is required.

4.4.1. Failure Description

Should the discharge valve be broken then the piston is sucking gas from the discharge line and recompressing this gas, due to the leaking valve.

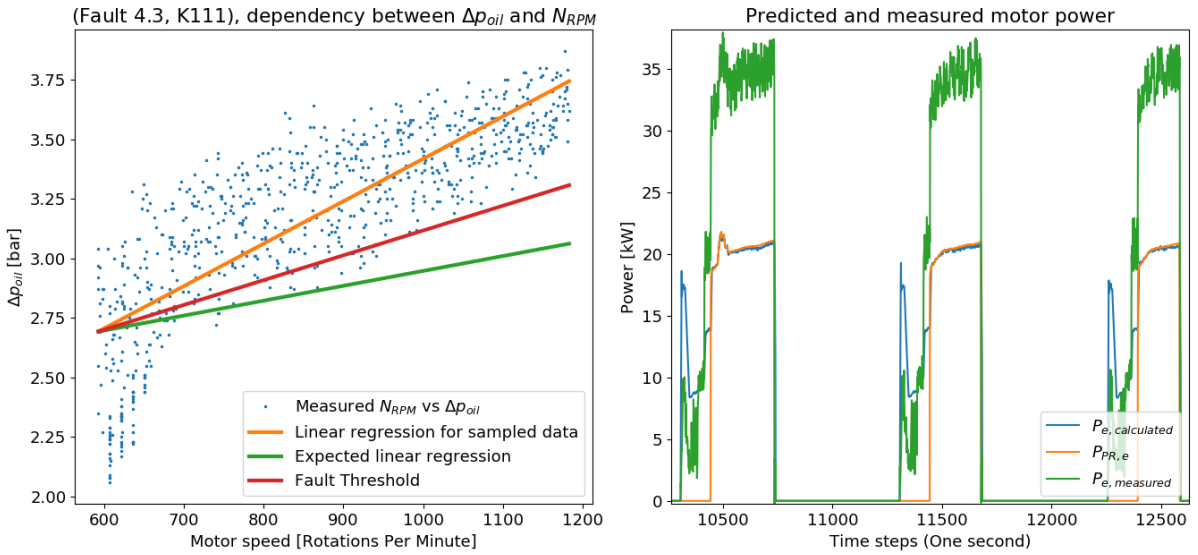

Figure 4.13: A result from the FDD algorithm for bearing damage. The image on the left side is the fault detected through the third symptom; the orange line is showing $(\overline{\frac{\Delta p_{oil}}{N_{rpm}}})$, while the green line is showing $(\overline{\frac{\Delta p_{oil}}{N_{rpm}}})_{sampled}$. The fault has been detected as the orange line is 64.9 % steeper than the green line. The graph on the right hand side shows the predicted motor driving power, $P_{PR,e}$, and the driving power calculated through equation 3.3, P_e, and the unaltered measured power drawn from the grid, $P_{e,measured}$, in the same heat pump.

4.4.2. Failure Symptom

The fault is recognizable through the symptom below.

- The discharge temperature of the compressor with the faulty discharge valve is higher than expected.

4.4.3. Failure Detection Approach

The periods of steady state operation at maximum capacity are isolated using the linear prediction of the startup time. The discharge temperature is recorded and compared to the discharge temperature predicted by the compressor prediction tool. The uncertainty between $T_{PR,dis}$ and T_{dis} from the compressor prediction tool, $T_{dis,uncertainty}$, was sampled to be $\pm$ 0.95 K and $\pm$ 1.79 K for the "5HP-compressor" and the "V-compressor" respectively.

$$T_{dis} > T_{PR,dis} + 3 + T_{dis,uncertainty} \tag{4.3}$$

The fault threshold is taken to be 3 K in addition to the uncertainty. The fault is detected when the threshold in equation 4.3 is exceeded for more than 5 % of the steady state operation period.

The FDD program utilizes a process history based fuzzy logic approach where the residual between the predicted and measured T_{dis} is weighted by how often the fault threshold is exceeded.

4.4.4. Results

A defect discharge valve has never been recorded in a heat pump system, thus the fault threshold is not proven. The algorithm was tested for data from 27 different "5HP-compressors". The fault was never detected, making the FDD algorithm robust in the sense that it never falsely detects the fault. However, it cannot be known whether or not the FDD algorithm would detect the fault if it is occurring.

4.5. Defect suction valve

Each cylinder in both the "5HP-compressor" and the "V-compressor" have a suction valve, illustrated in Fig. 4.14, to ensure no back flow to the suction line when compressing the refrigerant.

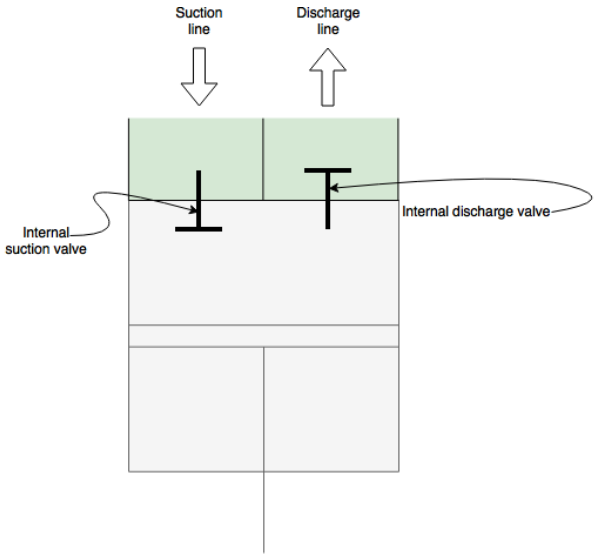

Figure 4.14: Internal piston compressor illustration showing the internal suction and discharge valves in the piston compressor.

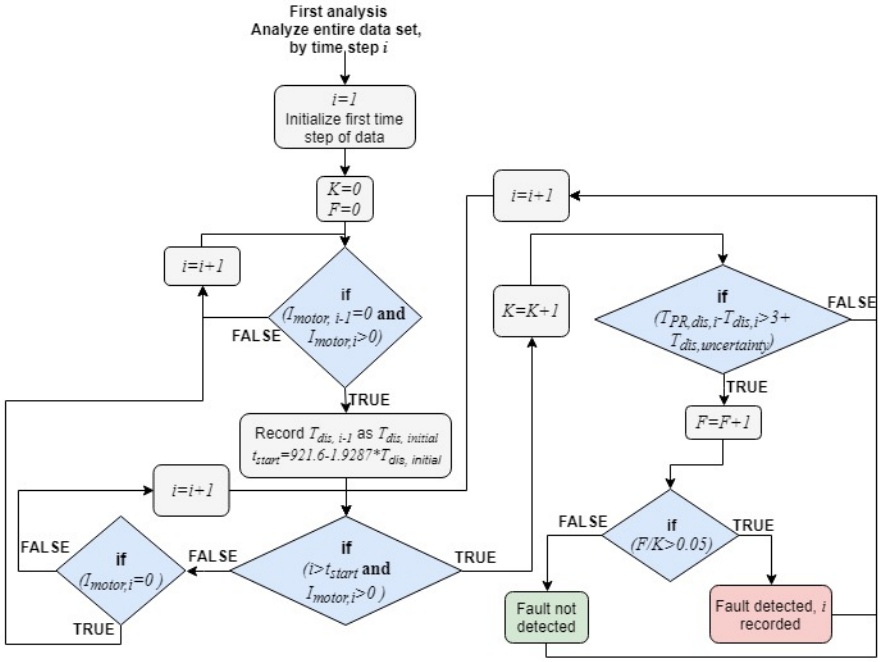

Figure 4.15: The approach of the FDD program to detect a defect discharge valve, the failure threshold is shown as $T_{dis,uncertainty}$+3 K.

4.5.1. Failure Description

When the piston compresses the refrigerant, the refrigerant leaks through the suction valve, and the piston has no resistance from the gas. If the wrong valve ring is fitted, the suction valve can leak.

4.5.2. Failure Symptoms

A defect suction valve is detectable by the two symptoms listed below.

1. The power consumption of the compressor will be approximately $\frac{1}{N_{cylinders}} * 100\ \%$ lower than expected for each cylinder with a broken valve. $N_{cylinders}$ is the amount of cylinders in the compressor.
2. The compressor differential pressure never builds up to the operating conditions as shown in Fig.

4.16. Note that this is the same symptom as for the bypass valve never closing during a startup (item 3 of Fault 4.1).

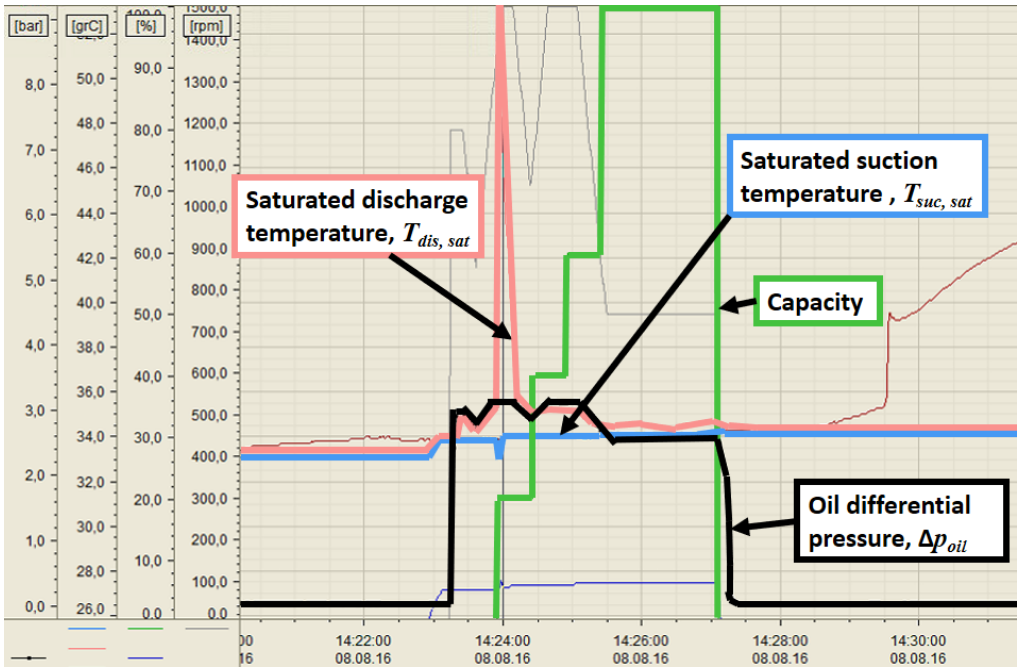

Figure 4.16: Example of a defect suction valve leading to slow build up of Δp_{comp}. $T_{dis,sat}$ (red line) remains at approximately the same value as $T_{suc,sat}$ (light blue line) during operation when Δp_{oil} (black line) has a non-zero value. Assuming that only one cylinder has this problem the short peak of $T_{dis,sat}$ is most likely due to the other cylinders operating normally.

To detect the first symptom a measurement interval of 30 seconds is required, while a measurement interval of 1 second is required for the second symptom.

4.5.3. Failure Detection Approach

The first symptom can be detected by isolating the steady state operating conditions when the compressor is running at maximum capacity. Here the predictions from the compressor prediction tool are identical to the measurements. The program can detect the fault if the measured compressor driving power is lower than the driving power predicted by the compressor prediction tool. The residual between the two should be more than the collected uncertainty added with 12.5 % for more than 5% of the steady state operation period to detect the fault. A comparison between the measured and predicted driving power of the compressor can be seen in Fig. 3.1 and Fig. 4.13.

The "V-compressor" has the most cylinders, being eight, thus $\frac{1}{8} * 100$ %=12.5% is the failure threshold. The uncertainty of the motor power calculations and predictions of $\pm$3.9% and 1.4% for the "5HP-compressor" and the "V-compressor"respectively is added to the threshold, making the fault threshold 16.4% and 13.9% respectively.

The approach of the FDD algorithm is illustrated in Fig. 4.17, where $P_{e,i}$ and $P_{PR,e,i}$ are the calculated or measured compressor motor power and the predicted compressor motor power in kW at time step i respectively. While $Capacity_i$ and $I_{motor,i}$ are the running capacity of the compressor in % and the motor current in Ampere respectively.

A delayed increase of Δp_{comp} is detected in the same way as a defect bypass valve remaining open during startup (item 3 of Fault 4.1). It is worth noting that this symptom alone is not enough to detect a defect suction valve. If this symptom occurs individually it could be either a defect suction valve, a bypass valve remaining open during startup or a defect butterfly valve allowing a too high mass flow of cold water to the condenser during startup (the second symptom of the later introduced Fault 5.10).

The FDD program utilizes a process history based fuzzy logic approach where the residual between

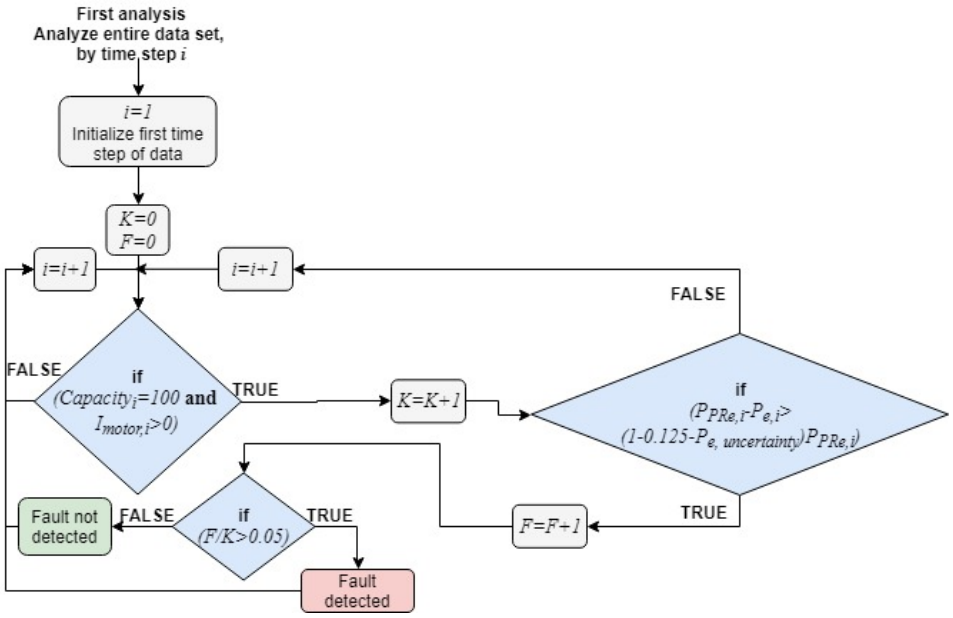

Figure 4.17: Approach to detect a defect suction valve through a low compressor driving power. $P_{e,uncertainty}$ is the uncertainty between P_e and $P_{PR,e}$ which is 0.039 when the power is not measured, and 0.01397 when the power is measured.

the predicted and measured P_e is weighted by how often the fault threshold is exceeded for the first failure mode.

The second failure mode is detected in a qualitative manner using a case-based reasoning approach. The failure is detected by seeing how the measured data compares to the trends in the database storing the knowledge learned by experts.

4.5.4. Results

There is only one example with visual data available of the differential pressure in the compressor never building up in Fig. 4.16. The fault threshold of 12.5% + 3.9% = 16.4 % was never confirmed. Only when both symptoms are detected a defect suction valve can be isolated. The second symptom can be other faults.

4.6. Leaking overflow valve

The discharge and suction lines have an overflow or relief valve between them to regulate the pressure difference in the compressor. The overflow valve is used whenever the pressures in the compressor are getting too high to reduce pressures. A leaking overflow valve is a problem in both the ”5HP-compressor” and the ”V-compressor”, where a measurement interval of 1 second is required to detect the fault.

4.6.1. Failure Description

A leaking overflow valve results in the compressor compressing and sucking the same volume of refrigerant during each reciprocation, where the volume of the refrigerant overheats. An overheated refrigerant could for example lead to damaging the bypass valve (Fault 4.1).

4.6.2. Failure Symptom

A leaking overflow valve is detectable through one symptom as seen below.

- The suction temperature will increase above its expected values during constant operating conditions as in Fig. 4.18 up until the heat pump is shut off, where the suction superheat will be at least above 5 K.

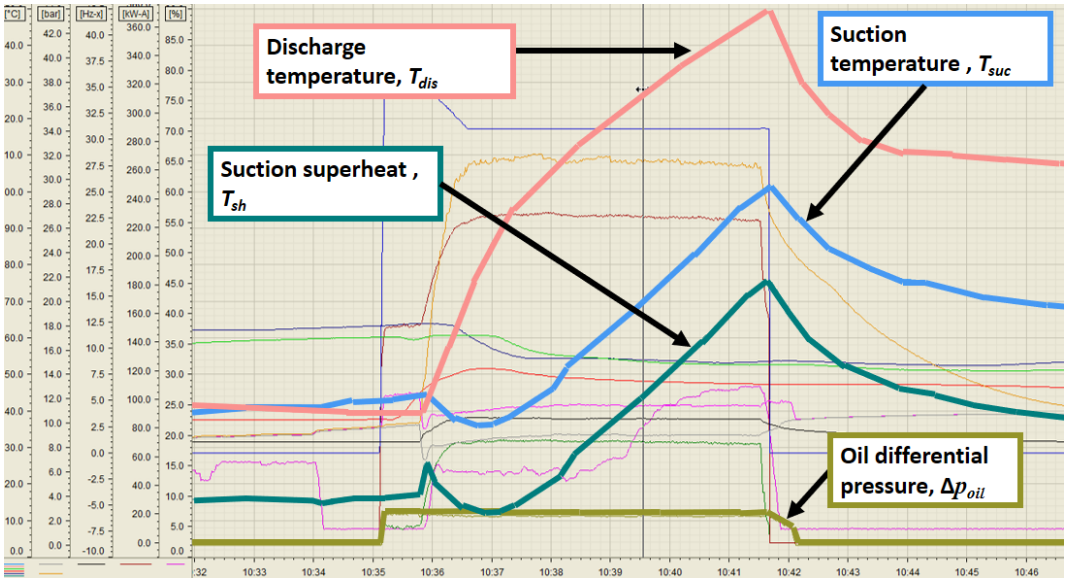

Figure 4.18: Example of a leaking overflow valve in a ”V-compressor”, during non-changing operating conditions the suction and discharge temperatures (light blue line and light red line respectively) are increasing until the compressor reaches a shut-off limit.

4.6.3. Failure Detection Approach

The program isolates the shutdown, then goes backwards and checks if the suction temperature was increasing every two seconds for more than the last 120 seconds before the shutdown. In addition the temperature difference between the saturated suction temperature and the measured suction temperature, i.e. the suction superheat of the compressor, around the shutdown should be above 5 K, the FDD approach is illustrated in Fig. 4.19.

The failure is detected in a qualitative manner using a case-based reasoning approach. The failure is detected by seeing how the measured data compares to the trends in the database storing the knowledge learned by experts.

4.6.4. Results

There are no data containing a leaking overflow vale, therefore one cannot know for certain that the algorithm will work. However from the graph in Fig. 4.18, the suction temperature is seen to be increasing for the last four minutes before the shutdown, while having a suction superheat at shut down of approximately 70 K. The weakness of this algorithm is the time frame, in the example of the fault the increase is lasting for four minutes.

A false fault was created in a data set to simulate the behavior seen in Fig. 4.6, where the suction temperature was continuously increasing until the heat pump was switched off. The FDD program recognized both symptoms in Fig. 4.20. The program recognizes that the suction temperature is increasing for the last 139 seconds and at shutdown the suction superheat is above 5 K when the compressor shuts down.

4.7. Operating with a fluctuating torque in the coupling shaft

The torque of the shaft coupling the electric motor and the compressor can be seen to have high fluctuations. The high fluctuations will only occur during certain low rotational speeds of the motor. It is further not known why it is occurring. However there is reason to believe that it is either a frequency converter not suited to operate at these frequencies or the shaft is operating at its natural frequency.

Both the ”5HP-compressor” and the ”V-compressor” can have this problem, the required measurement interval will be further discussed in this subsection.

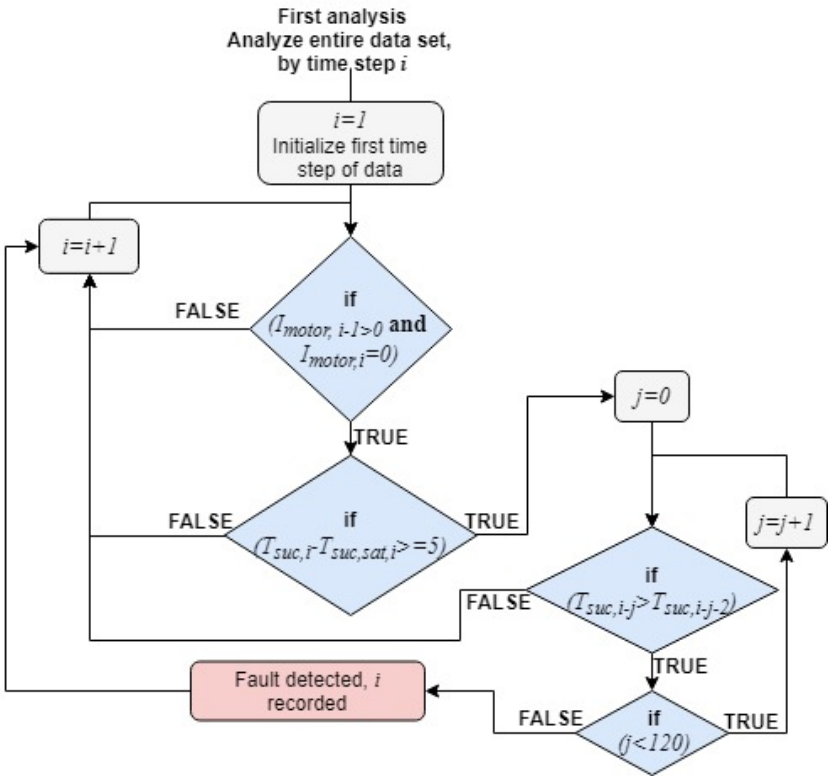

Figure 4.19: Approach of the FDD program to detecta leaking overflow valve by counting backward from a known shut down and investigating the suction temperature.

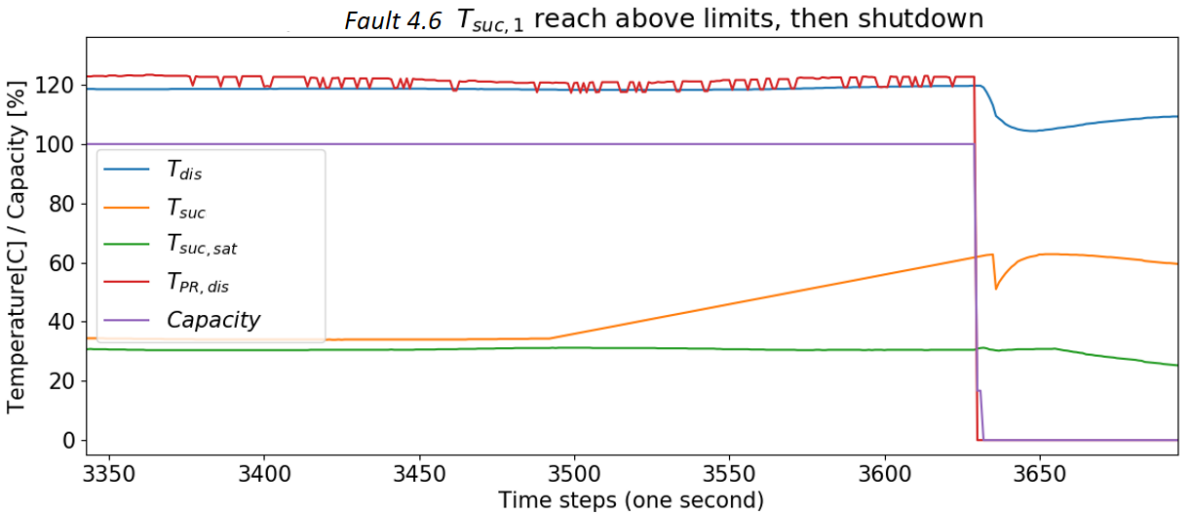

Figure 4.20: Example of how a broken overflow valve would look like being recognized by the program in a data set modified to contain leaking overflow valve.

4.7.1. Failure Description

The control system of the heat pump system will request a certain N_{RPM} which is the recorded N_{RPM}. If this corresponds to the natural frequency of the shaft, then the experienced N_{RPM}, τ_{shaft} and P_e will be fluctuating in an undesirable manner due to resonance.

Should the motor be operated with a fluctuating torque this can be damaging for the shaft, and its lifetime expectancy. Operating with a fluctuating torque is seen to introduce vibrations that again can cause damage to the shaft, the compressor and the motor.

4.7.2. Failure Symptom

High fluctuations in the torque of the shaft can be recognized by the symptom below for the heat pump system where the torque in the coupling shaft is measured.

- If the requested rotational speed of the motor remains constant while the torque is fluctuating this is a symptom that the motor is operated at the natural frequency of the shaft or the frequency drive is not suited for the operational frequency.

The rotational speed measured is the speed requested by the control system, while the recorded torque is however the experienced torque on the shaft. Fig. 4.21 shows a heat pump system where high fluc-

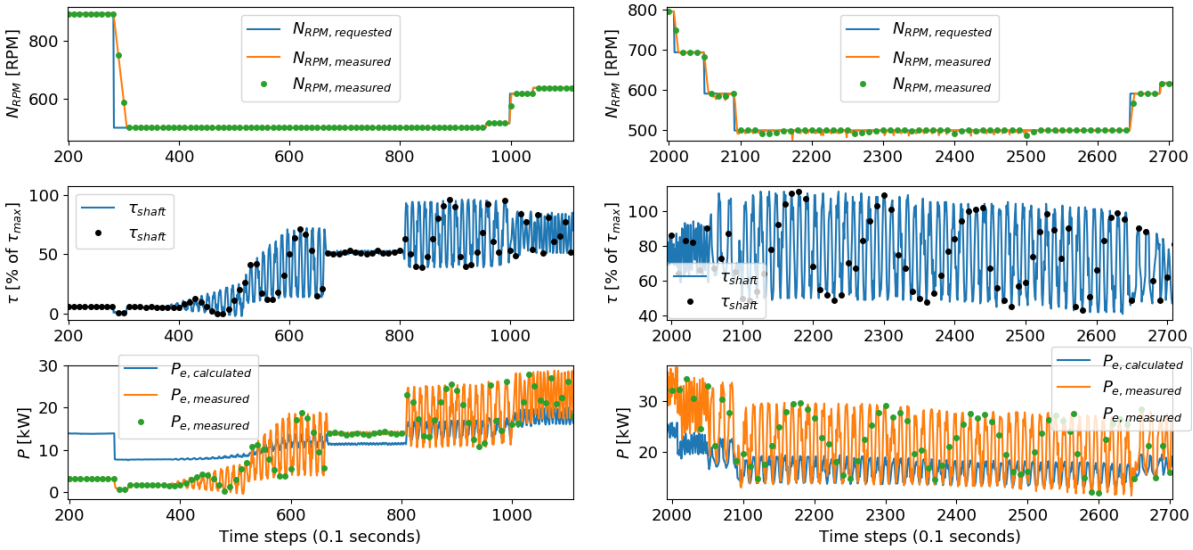

Figure 4.21: An example of a heat pump system with a fluctuating torque. A constant N_{RPM} leads to relatively large variations in τ_{shaft} for no apparent reason. The left side illustrates the difference between ideal and faulty behaviour, time step 700 to 800 shows ideal behaviour, where a constant N_{RPM} leads to a relatively constant τ_{shaft}. However after time step 800, N_{RPM} remains constant while τ_{shaft} is fluctuating from 40 % to 90 % of its maximum value. The right hand side show a time interval where the experienced N_{RPM} was fluctuating, causing the undesirable fluctuations in τ_{shaft}. It is worth noting that the data measured every second (green and black dots) in the bottom right graph have a sinusoidal curve. This happens if the measuring frequency is at least half of the original signal frequency.

tuations in the torque was experienced. This is from a heat pump system where after a longer period of unstable operation the service engineer suspected that the torque had high variations due to vibrations. To further examine the heat pump, the system was fitted with special sensors that measure every 0.1 seconds. In addition extra sensors where fitted to examine the experienced N_{RPM} and not only the N_{RPM} requested by the control system.

The fault became apparent, the requested N_{RPM} remained constant, and the measured τ_{shaft} was seen to have high fluctuations. The left side of Fig. 4.21 illustrates the issue well; the requested N_{RPM} remains constant, and from time step 650 to time step 810 τ_{shaft} behaves as expected during ideal operation. After that τ_{shaft} is seen to have high variations.

The black and green dots in Fig. 4.21 are measuring the value every second. In a normal heat pump system only the information from the black and green dots would be available and some of the fluctuations might not be visible in the black and green dots. However it is worth noting that the fluctuations in the bottom right graph are stable enough for the black and green dots to follow a sinusoidal wave. It is also worth noting that P_e remains constant, this is the power calculated, which is based on N_{RPM} and I_{motor} and constants. This is also a confirmation that the problem is occurring as P_e is seen to be relatively constant while $P_{e,measured}$ is seen to be fluctuating.

4.7.3. Failure Detection Approach

When operating at a fluctuating N_{RPM} it can be difficult to detect that τ_{shaft} is fluctuating. The typical values of N_{RPM} ranges between 500 and 1500 rpm, which translates to 8.33 to 25 rotations per second,

which translates to a frequency of 0.12 to 0.04 Hz. If the motor is operated at the natural frequency then once or more per rotation the shaft will get an increased amplitude and an increase of τ_{shaft}. To be able to detect small changes in τ_{shaft} at least once per rotation a higher measuring accuracy would be required. Measuring twice per rotation would be the minimum, i.e. measuring every 0.02 seconds. However, by only looking at the dots in Fig. 4.21 the fault can still be recognized.
If the original signal is a sinusoidal wave with constant fluctuations, then the sinusoidal wave will still be recorded with the same amplitude, but a different period, as seen in the bottom right graph of Fig. 4.21.

The FDD program must isolate the periods of a constant N_{RPM}, during these periods the FDD program

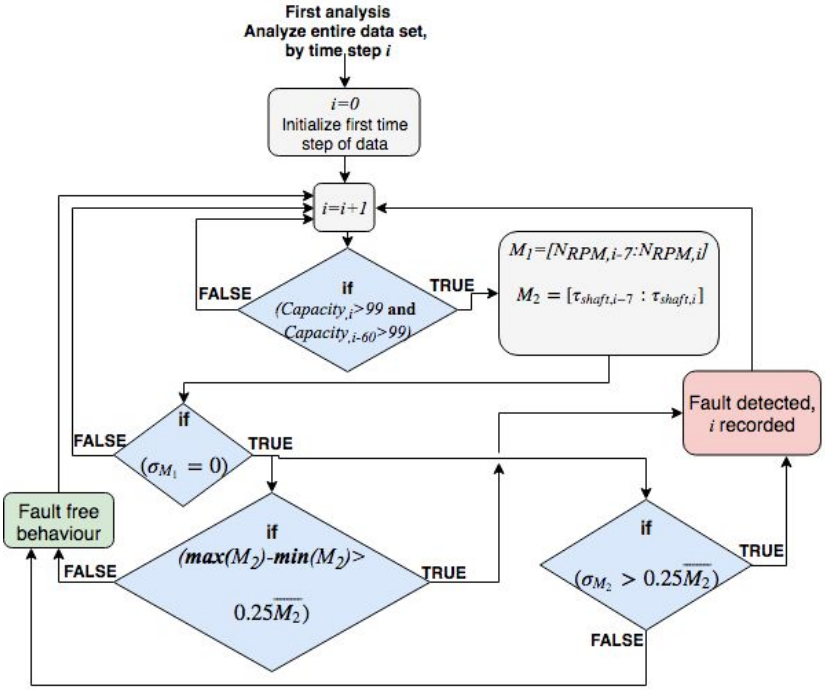

Figure 4.22: The approach of the FDD algorithm to detect a fluctuating torque. To avoid the variations in τ_{shaft} during the capacity steps during startup the algorithm ensures that the compressor has been running at 100 % capacity for the last minute. This is under the assumption that the measuring time step interval is 1 second.

will isolate the last 7 measured values for τ_{shaft} and check that N_{RPM} was constant for the last 7 time steps.

The fault is detected in two manners. If the difference between the minimum and maximum of the last seven measured τ_{shaft} is higher than 25 % of the average τ_{shaft} from the same period, the fault is detected.

If the standard deviation of the 7 last values of τ_{shaft} is higher than 25 % of the average of the 7 last values of τ_{shaft} then the fault is detected.

The approach of the FDD program can also be seen in Fig. 4.22. The FDD program utilizes a qualitative limit checking and case-based reasoning where the program looks for a specific trend whenever a limit or threshold defined from priori knowledge is exceeded.

4.7.4. Results

For the data set from Fig. 4.21 the FDD program was able to detect the fault when only analyzing the data given by the dots measuring every second in Fig. 4.21. In the results Fig. 4.23, the right hand side shows the entire original data set with a time step interval of 0.1 second, while the left hand side shows the data set when modified to only analyzing the values every tenth time step.

At this point the true origin of the fault is not known, as the problem have recently been discov-

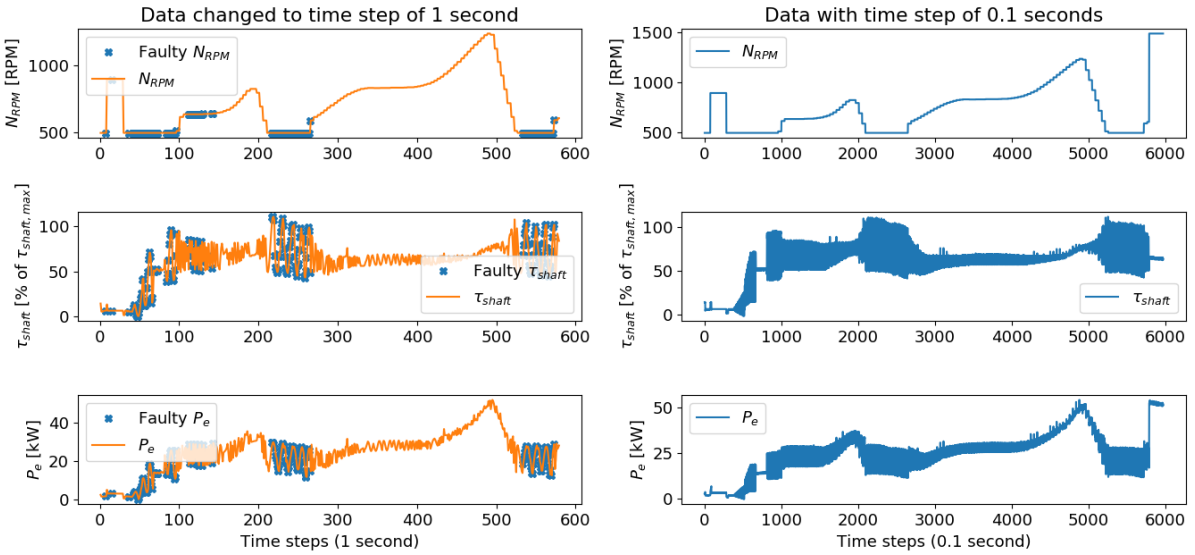

Figure 4.23: Results from analyzing a heat pump system known to contain a fluctuating torque. The right hand side shows the original data with a measurement time interval of 0.1 second, while the left side shows the FDD analysis of the same data measured every tenth time step. Whenever N_{RPM} remains constant for more than 7 seconds the FDD program analyses τ_{shaft} for the past 7 seconds and compares it to the fault thresholds. The blue crosses on the left hand side marks whenever the fault was detected.

ered for the first time in a heat pump system. The service engineers of this heat pump have several different hypotheses, but none have been confirmed or denied. For the sake of the FDD program the fault is detected as a fluctuating torque.

Conclusions about the required measurement interval to detect a fluctuating torque

The conclusion for the fluctuating torque was that fluctuations in τ_{shaft} can be detected with a measuring interval of 1 second. However the FDD algorithm would be stronger with a measurement interval of 0.02 seconds. When measuring every second the FDD program is dependent on the fluctuating τ_{shaft} to fluctuate for a longer time period.

5

Operational Faults

Operational faults are faults typically occurring during operation of the heat pump system. Operational failures are not the failure of a component or part of the heat pump being broken, but rather operation of the heat pump system in an unintended manner which can lead to damage and other failures. There are 11 faults classified as operational faults, where some faults are specific for specific heat pump system setups or compressors.

5.1. Condensation of the refrigerant inside the crankcase

This is a fault that can occur for all heat pump systems and compressors, detection of the fault requires a measurement interval of 1 second. During stand still of the compressor the crankcase heater heats the oil in the compressor to maintain the refrigerant in an evaporated state in the crankcase of the compressor, by maintaining a superheat in the suction line of at least 5 K.

5.1.1. Fault Description

The refrigerant can condensate if the crankcase heater is not operated correctly. Due to density differences the refrigerant will accumulate as a liquid layer on top of the oil. The oil temperature is monitored, however the heat is not dispersed evenly from the internal heater as shown in Fig. 5.1 due to a low heat conductivity of the oil. The temperature transmitter, located close to the internal heater, will read temperatures above the evaporating temperature of the refrigerant at the crankcase pressure. However there will be a time delay before these temperatures reach the refrigerant. The problem arises when starting the compressor with liquid refrigerant in the oil, the oil mix has a different viscosity and does not lubricate well, this can ultimately lead to bearing damage (Fault 4.3).

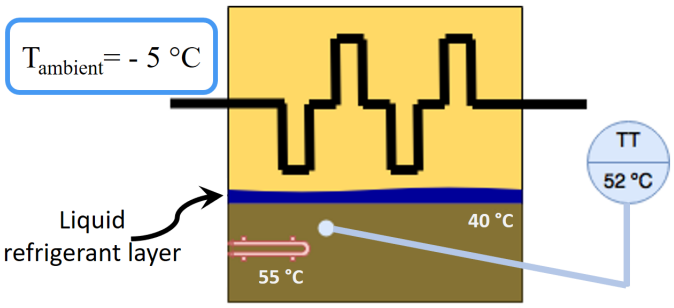

Figure 5.1: Simplified schematic of compressor crankcase illustrating the issue of condensing refrigerant

5.1.2. Failure Symptoms

The fault is detectable through the symptoms shown below.

1. During startup the saturated suction temperature will be higher than the actual suction temperature illustrated in Fig. 5.2.

2. If the saturated discharge temperature is higher than the measured discharge temperature during startup and the compressor never runs at the maximum capacity this could mean that some liquid could be left in the cylinder heads as in Fig. 5.2.

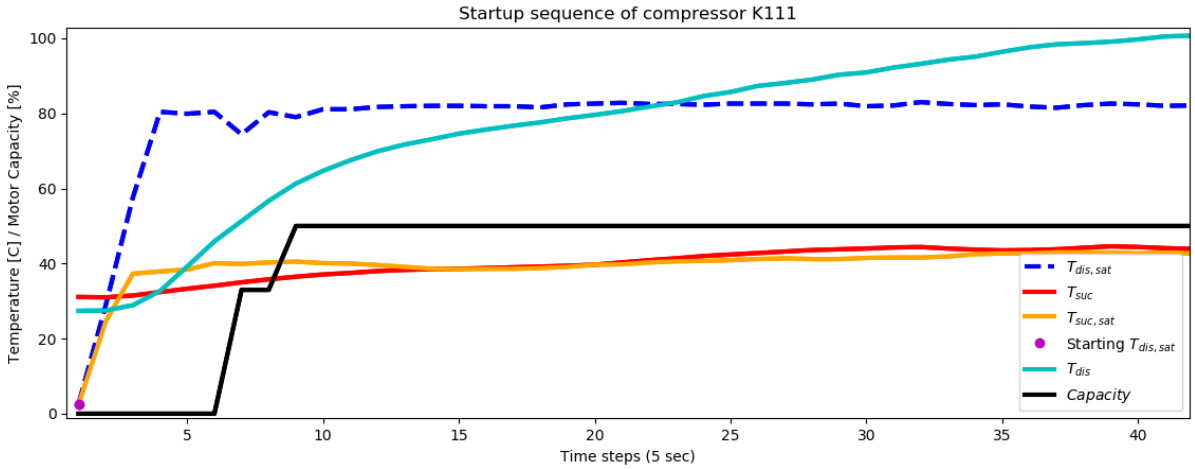

Figure 5.2: Condensation in the crankcase during startup of a compressor. For a short time period after startup $T_{suc,sat}$ (orange line) is higher than T_{suc} (red line), allowing for condensation in the suction line of the compressor. $T_{dis,sat}$ (dotted blue line) is also higher than T_{dis} (light blue line) during startup and afterwards the capacity (black line) never reaches its maximum (100 %).

3. If the saturated suction or the saturated discharge temperatures are higher than the measured suction or the measured discharge temperature during standstill when the discharge and suction is equalized as explained by equation 5.1.

$$2 + (T_{suc,sat}\ or\ T_{dis,sat}) > T_{suc}\ or\ T_{dis} \tag{5.1}$$

4. The ambient engine room temperature, $T_{ambient}$, is too far away from the saturated suction temperature during standstill as seen in equation 5.2.

$$T_{suc,sat} - T_{ambient} > 10K \tag{5.2}$$

5. If the oil temperature is decreasing too quick upon startup.

5.1.3. Failure Detection Approach

To detect the fault during startup with condensation in the discharge or the suction line the FDD program identifies the startups and looks for the two first symptoms as illustrated in Fig. 5.3. For both symptoms the program identifies how long the fault thresholds was exceeded.

To detect condensation during standstill the FDD program will record perform a simple limit check. If equation 5.1 or equation 5.2 are true during standstill then the fault is detected and the FDD program will record the time step and the fault proving temperature difference. The fifth symptom is not sufficient on its own to detect the fault, as a decreasing oil temperature during startup does not necessarily indicate a fault.

All symptoms are detected through a qualitative simple-rule based reasoning looking for a specific residual between two parameters, where priori knowledge defines the residual as faulty or fault-free.

5.1.4. Results

The program is able to detect the fault through the first four symptoms, the last symptom proved insufficient. There was only data available from the first and second symptom for validation, the example from Fig. 5.2.

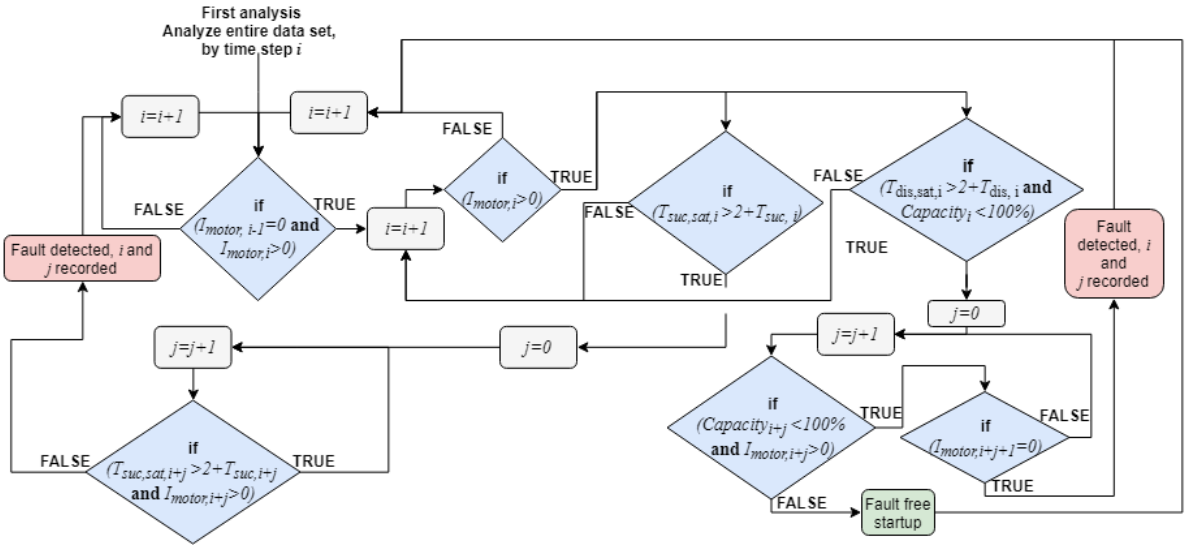

Figure 5.3: The FDD approach to detect condensation in the crankcase during startup.

5.2. Air in the condenser due to leakage in refrigeration plant

A leakage in the refrigeration plant is only a problem for the heat pump configured as an add-on to a refrigeration plant in an open type configuration as seen in Fig. 1.3. The pressures experienced in the refrigeration plant can be below atmospheric pressures, a leak will introduce air into the piping. Due to the open type heat exchanger the air is ultimately introduced in to the heat pump system. To detect the fault a measurement interval of 30 seconds is required.

5.2.1. Failure Description

The air ultimately accumulates in the condenser as a non-condensible adding more mass transfer resistance for the refrigerant. This is further increasing the pressure of the refrigerant due to Dalton's law seen in equation 5.3 stating that the total pressure, p_{total} is equal to the individual pressures of the ideal gasses present added up.

$$p_{total} = p_{air} + p_r \tag{5.3}$$

Where p_{air} and p_r is the partial pressure of the air and the refrigerant present in the condenser in bar respectively.

5.2.2. Failure Symptom

Air in the condenser is detectable by the symptom below.

- The temperature difference between the water exiting the condenser and the condensing temperature of the refrigerant is too high as illustrated in Fig. 5.4.

This symptom is occurring during steady state operation. During the compressor startup, the discharge pressure and hence also the saturated discharge temperature will build up slowly and $T_{dis,sat}$ will not be as stable as seen in Fig. 5.4. Therefore the startup time prediction from equation 3.14 in subsection 3.3.1 is used for the FDD approach in Fig. 5.5.

5.2.3. Failure Detection Approach

The expected temperature difference between the water exiting the condenser and the condensing temperature of the refrigerant, $\Delta T_{dis,cond,water,design}$ is taken as a design input. This temperature difference will differ per heat pump system.

The fault detection threshold is given by equation 5.4. For the fault to be detected the measured difference, $\Delta T_{dis,cond,water}$, should be larger than $\Delta T_{dis,cond,water,design}$.

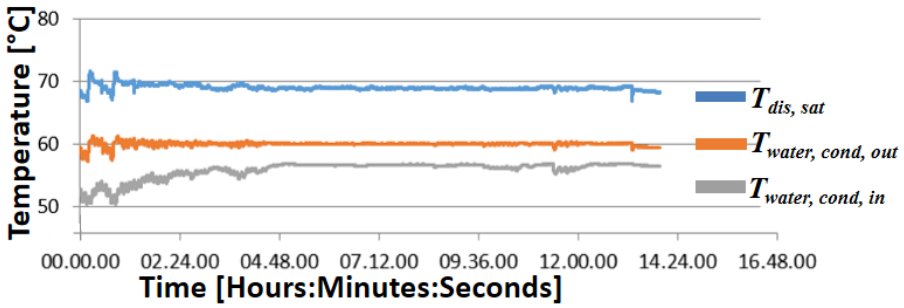

Figure 5.4: Example of air in the condenser, it can be seen that the temperature difference between the outlet of the water stream (orange line) and the condensing temperature (blue line) is approximately 9 K, ideally it should be approximately 1.4 K for this heat pump system as explained later.

The temperature difference between the two should be more than the maximum standard deviation in any of the measured data sets, $\sigma_{\Delta T,sampled}$, plus the average standard deviation of all the measured heat pumps, $\sigma_{\overline{\Delta T},sampled}$.

When equation 5.4 is true for more than 25 % of the steady state period the fault is detected.

$$\Delta T_{dis,cond,water,i} > \Delta T_{dis,cond,water,design} + \sigma_{\overline{\Delta T},sampled} + max(\sigma_{\Delta T})_{sampled} = \Delta T_{dis,cond,water,design} + 2.25 \tag{5.4}$$

Where $\Delta T_{dis,cond,water,i}$ is the temperature difference between the saturated discharge temperature and the water exiting the condenser at time step i. The approach of the FDD program is illustrated in Fig. 5.5.

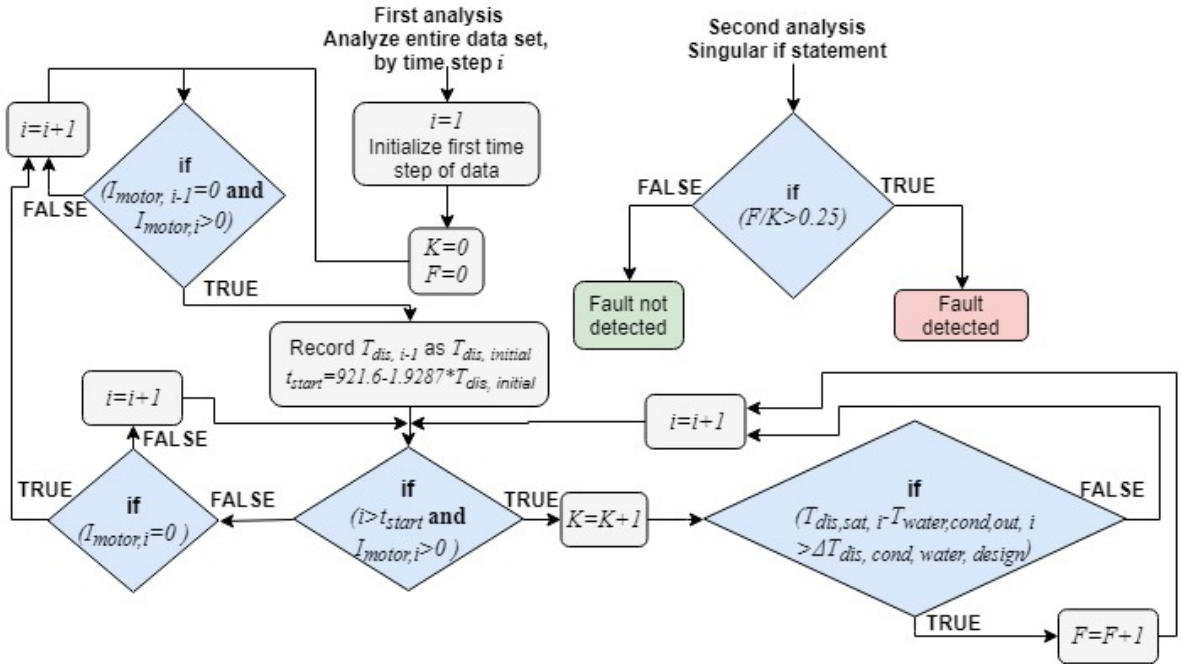

Figure 5.5: FDD approach to detect air in the condenser. The detection of the fault is dependent on two analyses.

It is worth noting that $\sigma_{\overline{\Delta T}}$ and $max(\sigma_{\Delta T})_{sampled}$ are both relatively high compared to the expected differences, i.e. there is a high uncertainty in the measurement of $\Delta T_{dis,cond,water}$. Therefore $\sigma_{\overline{\Delta T}}$ and $max(\sigma_{\Delta T})_{sampled}$ were added, and the threshold has to be exceeded for 25 % of the operating period or more. The 25 % is to be certain that the fault is apparent and re-occurring, and not only happening for a few seconds due to uncertainties in measurements.

The fault is detected through a qualitative simple-rule based reasoning looking for a specific residual between two parameters, where priori knowledge defines the residual as faulty or fault-free.

5.2.4. Results

A heat pump system was analyzed where the fault was known, there was data available from before and after the fault was detected. After the fault was detected, the condenser was emptied of air, and the data from after the cleaning of the condenser showed that $\Delta\overline{T_{dis,cond,water}}$ after operation was 1.38 K, which will be assumed as $\Delta T_{dis,cond,water,design}$ for this heat pump system. This totals to a fault threshold of 3.63 K.

The data from before the fault was detected were analyzed. Whenever $\Delta T_{dis,cond,water}$ is above the 3.63 K for more than 25 % of the operational time the fault is detected. In Fig. 5.6 air in the condenser was detected, the threshold is exceeded for 100% of the operational time. In the graph both the expected $T_{water,out,cond}$ based on the measured $T_{dis,sat}$ and the threshold of 3.63 K, and the threshold for when the fault is detected are shown as the orange and purple line respectively.

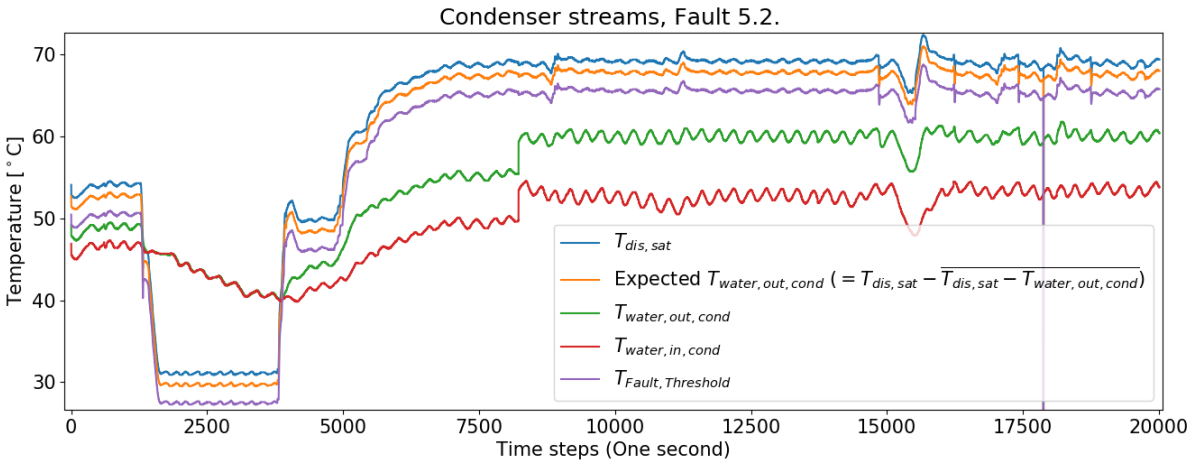

Figure 5.6: Example from air in the condenser being detected by the FDD program. The expected $T_{water,out,condenser}$ is shown as the orange line calculated as $T_{dis,sat} - 1.38$. The fault threshold is the minimum allowed value of $T_{water,out,cond}$, shown as the purple line being $T_{dis,sat} - 3.63$.

5.3. Fluctuations in the incoming heat source flow

For the heat pump functioning as an add on to a refrigeration plant the flow of the refrigerant in the refrigeration plant is often used to defrost the evaporators of the refrigeration plant. Part of the refrigerant is rerouted to the evaporators for defrosting purposes, giving away its heat to the evaporators. A simplified scheme showing the refrigerant being used for defrosting is illustrated in Fig. 5.7.

A decreased flow of the heat source affects the evaporating properties of the refrigerant, which again is directly linked with the suction line of the compressor. This fault can occur for a water cooled heat pump as well, if there are too many variations in the water entering the evaporator. The fault is independent of the compressor type and requires a measurement interval of 1 second to be detected.

5.3.1. Failure Description

The mass flow of the heat source is lower than expected because it is being used to defrost air-coolers or the temperature of the heat source flow has too high fluctuations. This lowers the suction pressure of the heat pump compressor. The sudden pressure decrease also lowers the boiling point of the refrigerant, which can lead to problems with the refrigerant dissolved in the oil, and potential bearing damage (Fault 4.3). If this happens frequently it can ultimately shorten the lifetime expectancy of the

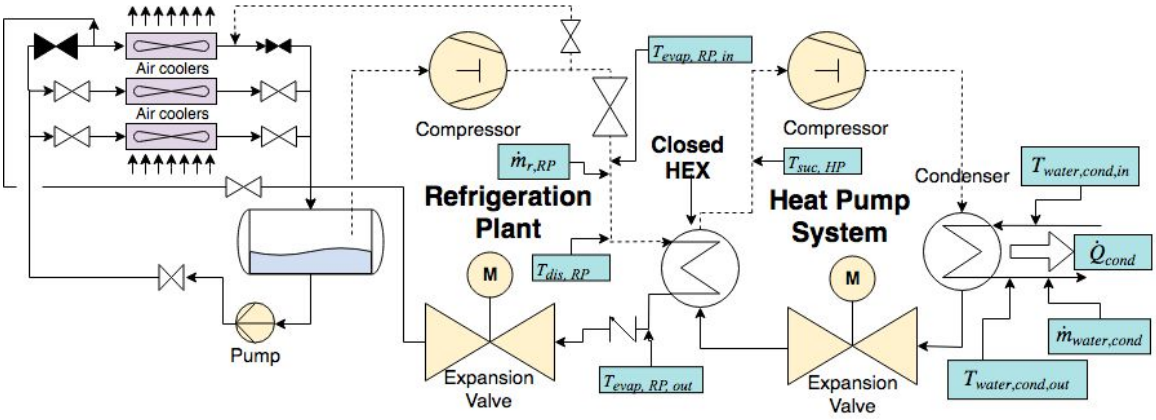

Figure 5.7: A detailed schematic of the heat pump used for as an add-on for refrigeration plants. The discharge gas of the compressor in the refrigeration plant is used to defrost the air coolers, reducing the flow of refrigerant to the inter cooler which can result in fluctuations of the incoming heat source flow.

heat pump and more so the compressor.

5.3.2. Failure Symptoms

High fluctuations in the incoming heat source flow is an issue for heat pumps working as an add on to a refrigeration plant. The heat source is then dependent on the refrigeration plant operation, which also has several possible failure modes. The fault can be detected by the symptoms below.

1. The entering heat source temperature, $T_{evap,RP,in}$, is varying more than its design specification of 2 K per minute on average.

2. The mass flow of the refrigerant in the refrigeration plant, $\dot{m}_{r,RP}$, is too low as it is being used for defrosting. The allowed flow is 50-110% of the design flow.

3. The mass flow of the refrigerant is varying more than its design specification of 10 % per minute.

4. The saturated suction temperature of the heat pump compressor, $T_{suc,sat,HP}$, drops accordingly to the entering heat source temperature, but with a time delay, as seen in Fig. 5.8. $T_{suc,sat,HP}$ has design specifications dictating that it should not vary more than 2 K per minute.

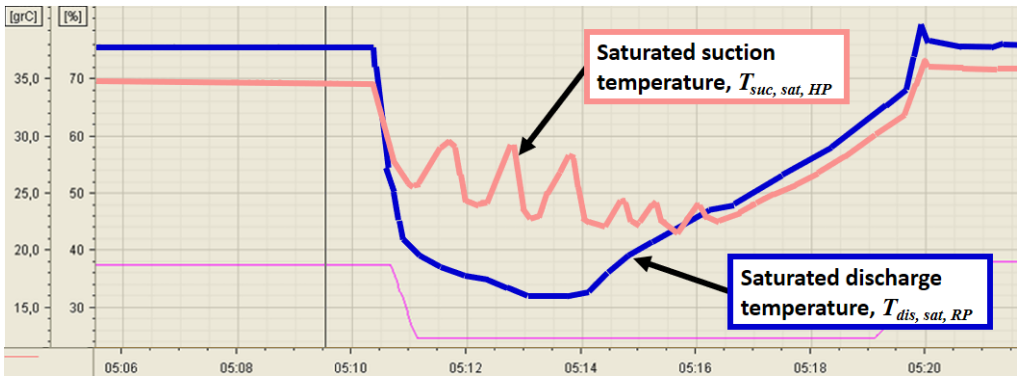

Figure 5.8: The saturated suction temperature in the heat pump (red line) drops by 8 K in 40 seconds due to the discharge pressure of the refrigeration plant (blue line) dropping in a system with a closed type HEX. For a heat pump system with an open type HEX the two values would have been identical.

5.3.3. Failure Detection Approach

The mass flow of the refrigerant in the refrigeration plant is not directly measured, but it can be estimated through equation 5.5 for a system with an open type HEX.

$$\dot{m}_{r,RP} = \frac{\dot{Q}_{cond} - P_{comp}}{\Delta h_{dis,r,RP} + \Delta h_{vap,r,RP}} \tag{5.5}$$

Where $\Delta h_{dis,r,RP}$ is the enthalpy difference between the actual discharge and the saturated discharge of the refrigeration plant. The enthalpy at the discharge is collected using the recorded temperature of the incoming heat source flow, $T_{evap,RP,in}$, and the suction pressure recorded in the heat pump system. $\Delta h_{vap,r,RP}$ is the latent heat of vaporization taken at the outlet temperature of the refrigeration plant refrigerant exiting the evaporator, $T_{evap,RP,out}$. Equation 5.5 is under the assumption that the subcooling of the refrigerant in the refrigeration plant is negligible. In addition equation 5.5 can only be used for a heat pump system working as an add-on to a refrigeration plant with an open type HEX, thus the second and third symptom can only be detected for this type of heat pump system.

For the actual calculations of the mass flow from equation 5.5 the startup time predictions of the condenser heat has to be considered. Although the mass flow going through the condenser will be constant itself during the startup period, the calculation of it will fluctuate until after the startup time.

To detect fluctuations in the mass flow or temperature of the entering heat sink or the saturated suction temperature, the FDD program takes the mean of each variable every 60 seconds. This is done over past 60 seconds, which effectively changes the time step to one minute. The FDD program further checks that the temperatures do not vary more than 2 K per time step and the mass flow does not vary more than 10 % of its own value per time step.

A mass flow too far away from the design flow is detected with a limit check of the mass flow of the heat source. Checking that the mass flow is within 50-110 % of the design flow.

Since the fault has 4 highly intertwined symptoms the FDD algorithm scores higher on the isolability from Table 1.1 if all are detected. Especially the fluctuations in the mass flow and temperature of the entering heat sink and the saturated suction temperature are directly intertwined.

The fault is detected in qualitative rule based limit checking to predefined thresholds.

5.3.4. Results

The calculations of the mass flow of the heat source entering the evaporator is directly dependent on several other variables that can be faulty. The mass flow calculations are dependent on two different enthalpies at the suction of the heat pump compressor and $\dot{Q}_{cond}$ and P_{comp} which are dependent on 5 different enthalpies. Which makes the mass flow calculations dependent on 7 different enthalpies in total. Due to this $\dot{m}_{r,RP}$ can be seen to be varying if any number of other faults are occurring.

Due to the uncertainties derived for P_e and $\dot{Q}_{cond}$, the mass flow of the heat source will have a total uncertainty of 3.90 % and 3.00 % for the ”5HP-compressor” and the ”V-compressor” respectively.

There was one example where the saturated suction temperature was fluctuating in Fig. 5.10, where $T_{suc,sat}$ makes a sudden jump of 3.08 K over one minute. This is the same example as later seen for Fault 6.3.

However there were no data available of an add-on heat pump with an open type HEX where the temperature of the entering refrigerant from the refrigeration plant was measured. The later introduced Fault 5.6 is a similar fault dictating the allowable fluctuations in the secondary flow of the condenser. The results from Fault 5.6 can be assumed to be applicable for the fluctuations in the incoming heat sink flow as well.

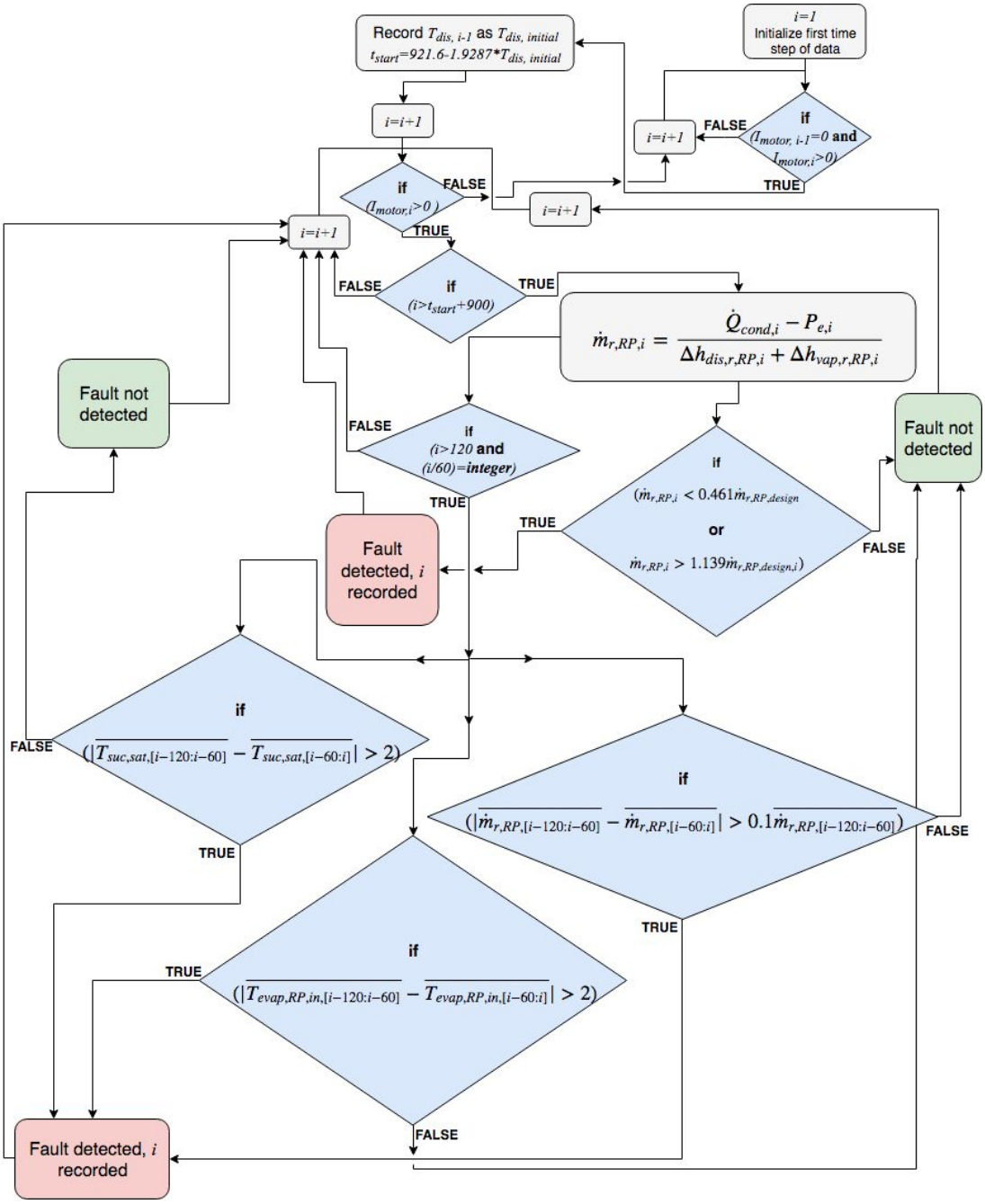

Figure 5.9: The approach to detect too high fluctuations in the heat sink flow, note that the algorithm investigates all symptoms simultaneously.

5.4. Constantly running on the limitations of the field of application

Both the ”5HP-compressor” and the ”V-compressor” have a maximum allowable discharge pressure where safe operation and the given lifetime expectancy can be assured. The control system of the heat pump controls N_{rpm} in order to ensure that p_{dis} is within its limits. This fault is independent of the heat pump system configuration.

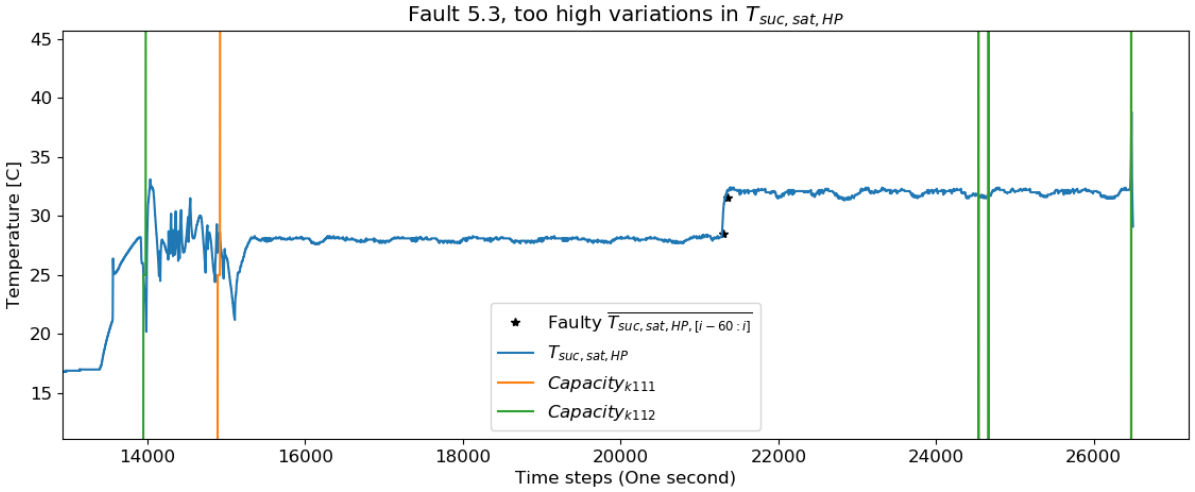

Figure 5.10: An example of high variations of the $T_{suc,sat}$ in a heat pump system. The black stars marks where the fault was identified, the black stars is the average $T_{suc,sat}$ over the last 60 time steps up until that point. As expected $T_{suc,sat}$ has high fluctuations in the startup, however the FDD algorithm only analyzes the time after a compressor startup.

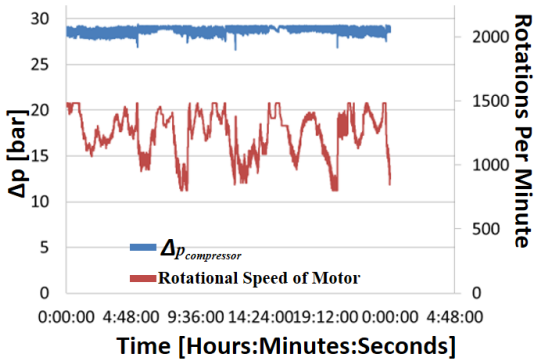

Figure 5.11: The figure shows an example of a compressor running on the limitation of operation. Δp_{comp} (blue line) is varying right below the maximum pressure lgimit and N_{RPM} (red line) is limited and decreased frequently to control Δp_{comp}.

5.4.1. Failure Description

Operating on the limits of the compressor leads to a decrease in the lifetime expectancy of the compressor due to a higher strain on various components. The control system shuts off the compressor if the discharge pressure reaches a certain limit, which differs per compressor. At 0.5 bar below that limit the rotational speed is limited to the current rotational speed and at 0.3 bar below the limit the rotational speed is lowered to decrease the discharge pressure. If this fault occurs often it will lead to frequent starting and stopping of the compressor, which further lowers the lifetime expectancy. The discharge pressure rising too high could be due to sudden increases in the water temperature entering the condenser, too warm water entering the condenser or wrong settings in the control system of the heat pump system.

5.4.2. Failure Symptoms

The fault is recognized by the symptom below.

- Each compressor has a prescribed maximum discharge pressure, $p_{dis,design}$. If the measured discharge pressure is within 0.5 bar of that relatively often, then the control system of the compressor will limit the rotational speed to control the pressure difference, as shown in Fig. 5.11.

5.4.3. Failure Detection Approach

The FDD program is able to detect this fault by isolating the periods of steady state operation defined when the discharge pressure is at operating conditions.

To detect the symptom, the program will make a linear regression model of N_{RPM} from the time step where p_{dis} has a local maximum within 0.8 bar of $p_{dis,design}$ and for the next 120 seconds. If N_{rpm} is seen to be decreasing in the linear regression model by 1.5 rpm or more per second the fault is detected. This approach is further outlined in Fig. 5.12. 0.8 bar is chosen as the failure threshold to account for uncertainties in the sensor measurements.

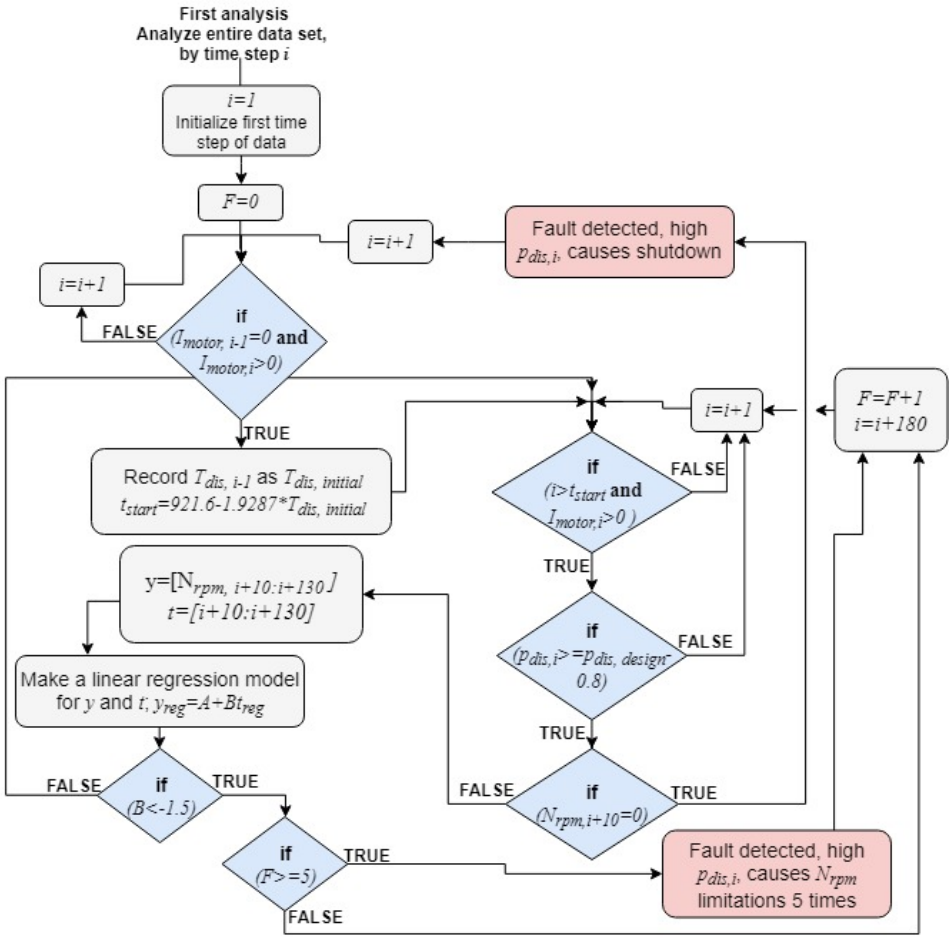

Figure 5.12: FDD algorithm to detect operating at the limits of p_{dis} note that N_{RPM} has to be limited due to a high p_{dis} five times for the fault to be detected. The fault is detected during the steady state operation period.

After investigation it became apparent that it generally took no more than 10 seconds from the high p_{dis} was detected for the first time until N_{RPM} was lowered. Therefore the linear regression is made from 10 seconds after p_{dis} is registered above the threshold for the first time.

The FDD program utilizes a combination of a process history based black-box linear regression and a qualitative limit checking and case-based reasoning. The program looks for a specific linear regression trend whenever a limit or threshold is exceeded.

5.4.4. Results

The fault was detected in one example in Fig. 5.13, the compressor was shut off twice due to high discharge pressures, and N_{RPM} was lowered 16 times. On the right side of Fig. 5.13 p_{dis} is steadily increasing over time until it reaches its limits. This is most likely due to the incoming water to the condenser being too warm, and the refrigerant is not able to cool down sufficiently in the condenser.

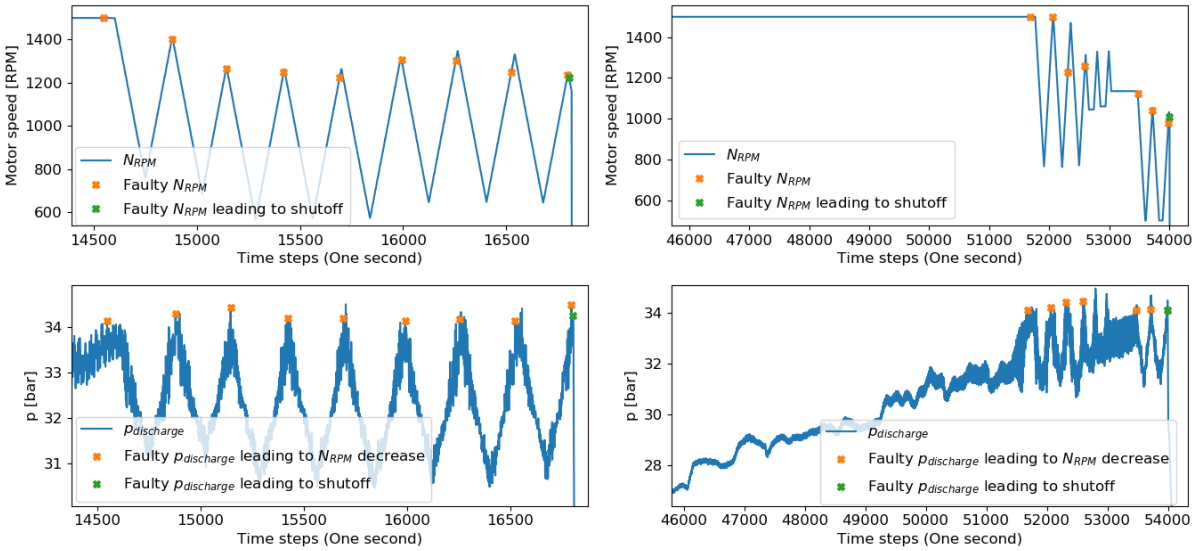

Figure 5.13: Two examples, shown on the left and right side where the top is N_{RPM} and the bottom is P_{dis}, of a compressor operating on its limits being detected in a heat pump system. In the example on the right side the pressure steadily increases over time until it reaches a certain limit where the control system begins to decrease N_{RPM} to decrease p_{dis}. The orange stars mark wherever the FDD algorithm detected that the control system of the heat pump has lowered N_{RPM} to maintain P_{dis} within its limits. The green stars mark wherever the control system has shut off the compressor due to high P_{dis}.

5.5. Compressor not lubricated after periods of longer standstill

The ”5HP-compressor” has an oil pump connected to the same shaft as the compressor. After periods of longer standstill the compressor must be lubricated with oil before startup to ensure safe operation. This is a problem only occurring for the ”5HP-comrpessor” as the ”V-compressor” has an external oil pump that frequently lubricates the system when the compressor is not operating. The fault requires continuously measured data from the last month with a measurement interval of 5 seconds.

5.5.1. Failure Description

If the compressor is not lubricated with oil through an external oil pump prior to operation of the compressor it may lead to dry operation of the heat pump that ultimately damages the compressor bearings (Fault 4.3).

5.5.2. Failure Symptom

This fault is detected by the symptom below.

- Pre-lubrication is detected by monitoring the differential oil pressure during stand-still of one compressor. If the differential oil pressure has a value in the proximity of its normal operating value during stand-still pre-lubrication is being performed.

5.5.3. Failure Detection Approach

The program would require continuous data logged from the periods of stand-still, the standstill should be at least a month. During these longer periods the program will look for a non-zero value in the differential oil pressure. If the differential oil pressure remains below a threshold of 1.2 bar for the entire standstill up until a startup the fault can be identified. The approach is a typical example of a qualitative limit checking FDD approach.

5.5.4. Results

There was no available data containing continuously logged data with a measurement interval of 5 seconds from one month or more. This would require over half a million measuring points, hence the algorithm could not be validated.

However for the future on-line FDD program in the control system the FDD program should compare how long the standstill period has been. If there was a case of Δp_{oil} having a value around 1.2 bar,

and the data does not have to be continuously stored.

5.6. Fluctuations in the incoming heat sink flow

The secondary flow in the condenser has certain maximum allowable fluctuations. Several of the GEA heat pump systems are connected to a larger industrial system where the incoming heat sink flow is coming from another process. Therefore, all heat pumps have maximum allowable fluctuations in the secondary flows. This is a fault that can occur independent of all compressor types and independent of the heat source. It is more common for systems where the heat sink flow is coming from another process.

5.6.1. Failure Description

If the temperature or the mass flow of the entering heat sink fluctuates too much, the heating capacity becomes unstable. This can affect the efficiency or delivered heat of the heat pump system, or it can lead to unstable subcooling (Fault 5.11). Sudden increases of the water temperature could lead to a high discharge pressure on the limitations of operation (Fault 5.4). The maximum fluctuations allowed in the secondary streams are dictated in the documentation of each heat pump system. They are all dependent on the design specifications of the system.

5.6.2. Failure Symptoms

1. The incoming heat sink temperature, $T_{water,cond,in}$, is fluctuating more than its maximum allowed temperature fluctuations of 2 K per minute.

2. The mass flow of the water entering the condenser, $\dot{m}_{water,cond}$, should not vary more than 10% per minute.

3. The mass flow of the water should be 50-110% of the design flow.

The mass flow of the water through the condenser, $\dot{m}_{water,cond}$, is not directly measured, but as the condenser heat is known, the mass flow can be calculated through equation 5.6.

$$\dot{m}_{water,cond} = \frac{\dot{Q}_{cond}}{\Delta T_{water,cond} c_{p,water}} \tag{5.6}$$

Where $\Delta T_{water,cond}$ is the temperature difference between the water entering and exiting the condenser measured in K. The specific heat capacity of the water, $c_{p,water}$, is taken at atmospheric pressure and at the temperature of the water entering the condenser. The pressure of the water flow through the condenser is not measured. Therefore atmospheric pressure is assumed as it will have a relatively small effect on $\dot{m}_{water,cond}$.

5.6.3. Failure Detection Approach

The fault is detected with the same approach as for the fault of too high fluctuations in the heat source flow and temperature (Fault 5.3). However recording different variables.

The FDD program takes the mean of the temperature and the mass flow of the entering heat sink every 60 seconds over the past 60 seconds in blocks. This effectively changes the time step to one minute. The FDD program further checks that the temperatures do not vary more than 2 K per minute and the mass flow does not vary more than 10 % of its own value per minute.

The FDD program can only start analyzing after the startup time linearly predicted (as mentioned later in Fault 5.10 the startup of the water flow in the condenser can have highly varying both flow and temperature during startup).

The flowchart explaining how the algorithm detects the fault is the same as in Fig. 5.9. The fault is detected in qualitative rule based limit checking to predefined thresholds.

5.6.4. Results

$\dot{Q}_{cond}$ has its derived uncertainties, to detect the mass flow deviating too far away from the design flow this uncertainty must be added to the fault threshold of 50-110 %. The derived uncertainty of $\dot{Q}_{cond}$ is 2.51 % and 3.00 % for the "5HP-compressor" and the "V-compressor" respectively. Using these uncertainties gives the new fault threshold as 47.49-112.51 % and 47-113 % for the "5HP-compressor" and the "V-compressor" respectively.

Too high variations in $T_{water,cond,in}$ was detected twice in a heat pump system, illustrated in Fig. 5.14. The fault was detected by high variations in $T_{water,cond,in}$, while $\dot{m}_{water,cond}$ was not faulty. This is visible in the top four graphs of Fig. 5.14, where black stars marks the detected fault. $\dot{m}_{water,cond}$ is only

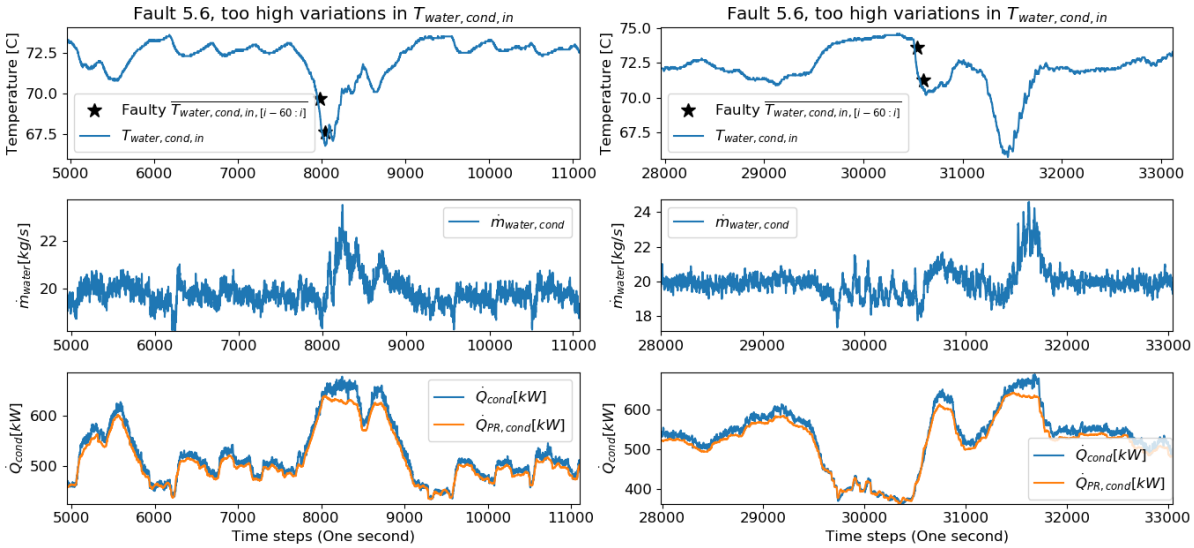

Figure 5.14: Two examples of fluctuations in $T_{water,cond,in}$. In the two graphs in the middle $\dot{m}_{water,cond}$ is increasing due to a decreasing $T_{water,cond,in}$. In the two bottom graphs $\dot{Q}_{cond}$ has an increase due to the decreasing $T_{water,cond,in}$, and it can be concluded that the actual $\dot{m}_{water,cond}$ is probably constant, but it is varying due to its dependency with $T_{water,cond,in}$.

fluctuating due to the fluctuations in $T_{water,cond,in}$, which directly affects the calculated $\dot{m}_{water,cond}$ through equation 5.6. This is reflected in the top four graphs of Fig. 5.14.

The moment the fault is detected $\dot{Q}_{cond}$ and $\dot{Q}_{PR,cond}$ are deviating from each other more than usual, visible in the bottom two graphs of Fig. 5.14. This is an indication of undesirable operation being present as $\dot{Q}_{cond}$ and $\dot{Q}_{PR,cond}$ have different response times to sudden changes of variables.

5.7. Liquid carry-over during operation

During operation of the compressor liquids could carry-over from the evaporator to the compressor. Liquids in the suction line of the compressor can be damaging for the compressor.

Liquid carry-over is occurring during steady state operation (the later introduced Fault 6.4 is liquid transferring away from the evaporator during shutdown). Liquid carry-over during operation is a problem independent of the heat pump system setup and compressor type that requires a measurement interval of 1 second.

5.7.1. Failure Description

Liquid carry-over occurs during operation when the liquid in the evaporator travels away from the evaporator to the compressor. Liquids in the compressor suction line can cause direct damage to the internal parts of the compressor and it is undesirable.

5.7.2. Failure Symptoms

The fault can be detected through the two symptoms below.

1. During startup the discharge temperature takes longer to reach its operating conditions. This is a symptom of liquid carry-over occurring during the previous operation period leading to liquids remaining in the suction of the compressor.
2. When the compressor reaches its operating conditions both the superheat and the compressor discharge temperature will be lower than expected.

5.7.3. Failure Detection Approach

A slow increase of T_{dis} during startup can be detected in two ways. Either by looking at the expected time for the discharge temperature to reach its operating conditions, t_{conv}. Or by looking at how well the expected exponential model predicting $\Delta T_{PR-measured,exp}$ fits to the data measured, by $\overline{\Delta T_{PR-measured} - \Delta T_{PR-measured,exp}}$. Two models were designed to predict the compressor startup based on the compressor prediction tool. Based on the initial T_{dis} and $T_{PR,dis}$, an exponential and a linear model can predict the startup sequence the first 2000 seconds (subsection 3.3.1).

The linear model can predict the time it takes for the residual between T_{dis} and $T_{PR,dis}$, $\Delta T_{PR-measured}$, to converge to an acceptable level, $t_{conv,lin}$. The exponential model can predict $\Delta T_{PR-measured}$ for the first 2000 seconds after a startup. With a relatively high uncertainty it can predict the time it takes for $\Delta T_{PR-measured}$ to converge to an acceptable level, $t_{conv,exp}$.

The actual convergence time, t_{conv}, was in 92.3 % of the startups sampled less than the linearly predicted $t_{conv,lin}$.

The exponential model could accurately predict $\Delta T_{PR-measured}$ for each time step after startup, where the average difference between the measured and predicted $\Delta T_{PR-measured}$ was 0.4 K.

Therefore the linear model will be used to detect the fault based on t_{conv} and $t_{conv,lin}$, while the exponential model will be used to detect the fault based on $\overline{\Delta T_{PR-measured} - \Delta T_{PR-measured,exp}}$.

Thus for a startup liquid carry-over can be detected whenever equation 5.7, equation 5.8 and equation 5.9 are true.

$$t_{conv} > t_{conv,lin} - 102.3 + 139.98 = t_{conv,lin} + 42.28 \tag{5.7}$$

$$t_{conv} > t_{conv,exp} + 83.97 + 158.6 = t_{conv,exp} + 242.57 \tag{5.8}$$

$$\begin{aligned} \overline{\Delta T_{PR-measured} - \Delta T_{PR-measured,exp}} > \\ \overline{\Delta T_{PR-measured} - \Delta T_{PR-measured,exp}}_{sampled} + \\ \overline{\sigma_{\Delta T_{PR-measured} - \Delta T_{PR-measured,exp}}} = 0.514 \end{aligned} \tag{5.9}$$

The approach to detect the slow build up of T_{dis} during startup through equation 5.7, equation 5.8 and equation 5.9 is illustrated in Fig. 5.15.

The fault can also be detected through a low discharge temperature during steady state operation in a similar manner as for the broken discharge valve (Fault 4.4) using the same threshold of 3 K added with the uncertainty of $T_{PR,dis} - T_{dis}$, $T_{dis,uncertainty}$.

The FDD approach for liquid carry-over utilizes a process history black-box approach through a regression model working on predefined thresholds from process-history based sampling.

5.7.4. Results

There were no known examples of either symptoms of liquid carry-over from the evaporator. There was however one example in Fig. 5.16 where the startup time, t_{conv}, was detected as faulty. However this was due to condensation in the discharge line during startup. Fig. 5.16 shows two startups that were particularly slower than expected, the results from the FDD program on these two startups are shown in Table 5.1. The fault was only detected for the startup on the right side of Fig. 5.16.

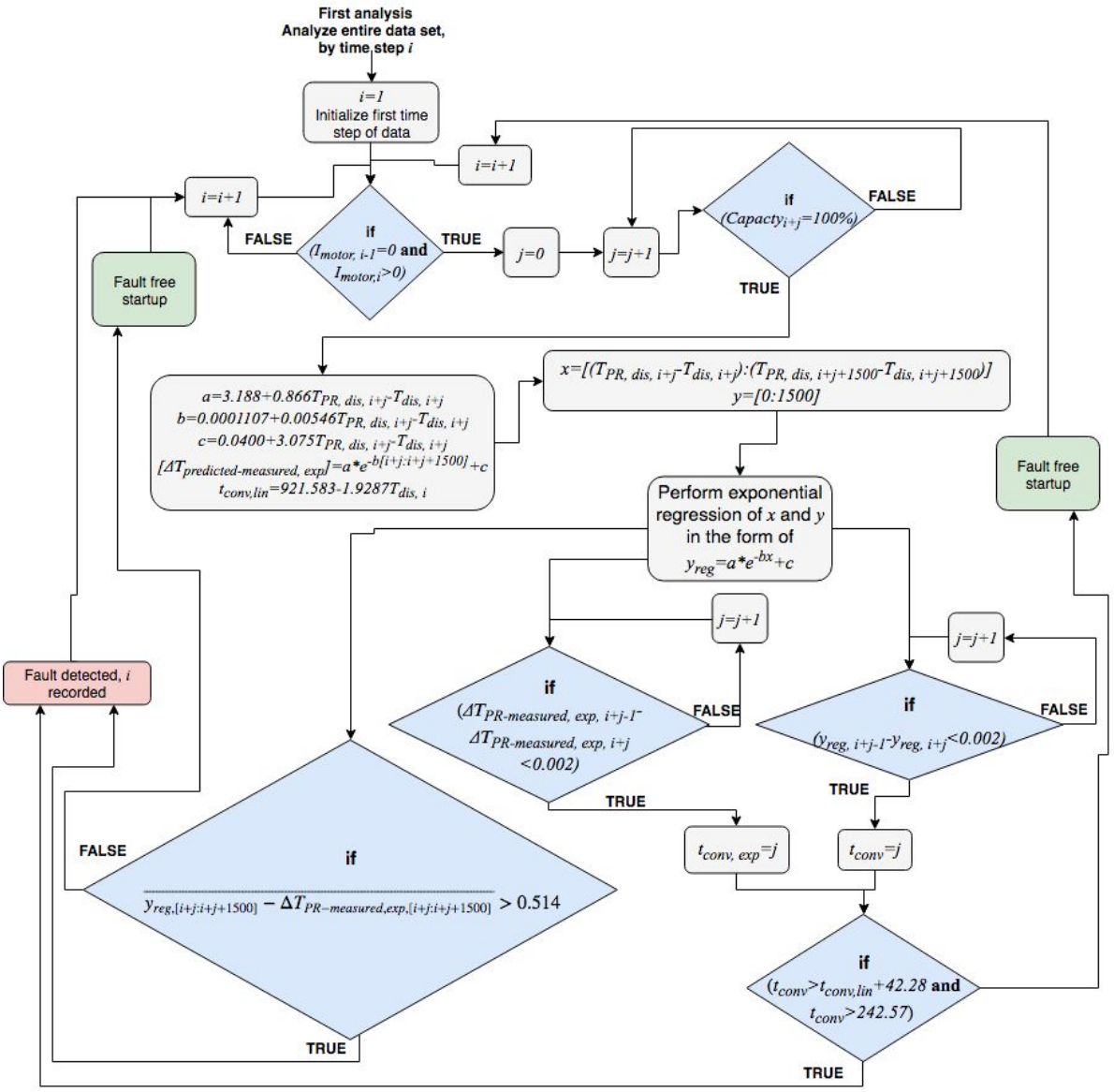

Figure 5.15: The approach to detect liquid carry-over through a slow build up of T_{dis} during startup. It is worth noting that when the exponential models are created the FDD algorithms performs 3 analyses in parallel. y_{reg} is the exponential regression fitted to the measured data of each individual startup.

Table 5.1: Results from the two slow startups shown in Fig. 5.16

Parameter	Fault thresholds	Result from the left side of Fig. 5.16	Result from the right side of Fig. 5.16
$t_{conv,lin} - t_{conv}$	<-42.28 s	3.76 s	-19.49 s
$t_{conv,exp} - t_{conv}$	<-242.57 s	-178 s	-240 s
$\Delta T_{PR-measured} - \Delta T_{PR-measured,exp}$	>0.514 K	0.441 K	0.882 K

Neither of the startups in Fig. 5.16 are detected through t_{conv}. It is clear from the graph on the right side of Fig. 5.16 that $\Delta T_{PR-measured}$ is higher than $\Delta T_{PR-measured,exp}$ for most of the startup time by a significant amount. t_{conv} is however very close to being detected. It is not known if the heat pump system had a problem with liquid carry-over during operation or not, the discharge temperature was not lower than expected during steady state operation.

Condensation in the discharge was discussed in subsection 3.3.1, and its effect on t_{conv} is not precisely

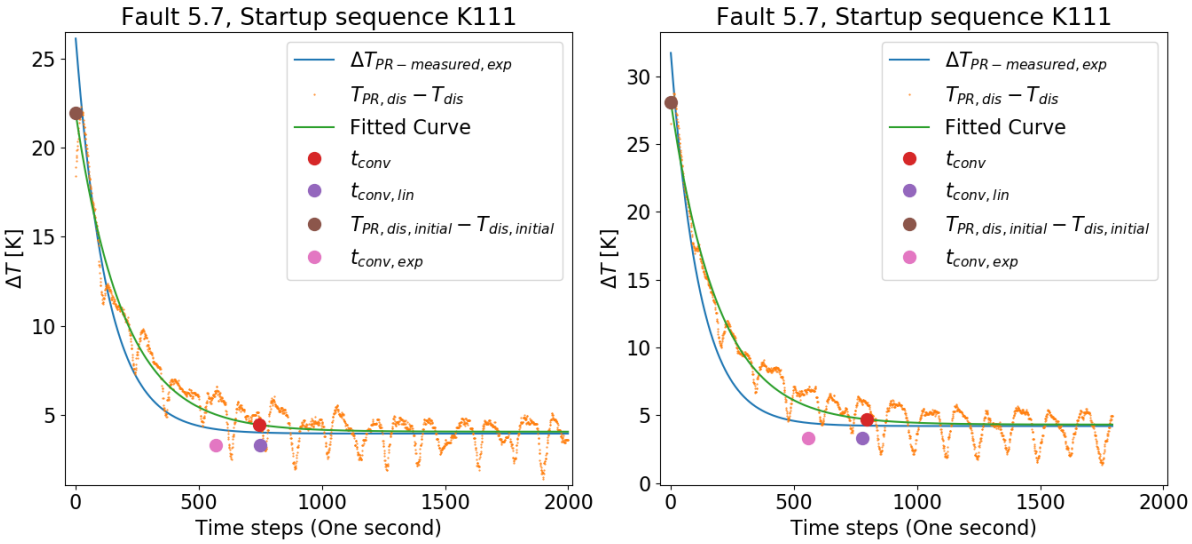

Figure 5.16: Two startups from the same "5HP-compressor" where the startup time was longer than expected. The graph to the right had condensation detected in the discharge, a total of 8.6 K over 4 seconds. All possible indications are saying the startup to the right is slower than predicted, t_{conv} is higher than $t_{conv,lin}$ and $t_{conv,exp}$ and $\Delta T_{PR-measured}$ is clearly higher than $\Delta T_{PR-measured,exp}$, meaning that the predictions were indicating that the startup should have been faster than what is recorded. The results from the FDD algorithm on these two startups are shown in Table 5.1.

known, however it can be assumed that it would increase t_{conv} noticeably. The FDD program will, if a slow build up of T_{dis} during starup is detected, also say how much, if any, condensation was in the discharge line and provide the graph from Fig. 5.16 for every startup.

5.8. Low condenser heat

Each individual heat pump system is expected to deliver a certain amount of heat while running at certain operating conditions. There should be a direct relationship between the running conditions and the condenser heat. Low condenser heat is a typical result of other faults and can occur independently of the compressor type and the heat pump setup. To detect the fault, a measurement interval of 30 seconds is required.

5.8.1. Failure Description

Should the heat pump deliver less heat than expected over longer periods of time, it is not a direct failure of a component, but rather a system not performing to its specifications. If the heat pump does not deliver the expected amount of heat, then GEA is not delivering as promised.

This lack of performance could be a result of any number of failures previously discussed. In fact most of the faults described in section 4, section 5 and section 6 will result in a low condenser heat or a low COP as it will be explained later (Fault 5.9). For example air in the condenser (Fault 5.2), a broken suction valve (Fault 4.5) or fouling in the evaporator or condenser will lead to a low condenser heat.

5.8.2. Failure Symptom

- The condenser heat delivered by the heat pump system is lower than the condenser heat predicted by the compressor prediction tool.

5.8.3. Failure Detection Approach

The condenser heat predicted by the compressor prediction tool, $\dot{Q}_{PR,cond}$, tends to be identical to the condenser heat calculated, $\dot{Q}_{cond}$, for the "5HP-compressor". For the "V-compressor" $\dot{Q}_{PR,cond}$, tends to be 88.16 % of $\dot{Q}_{cond}$. The condenser heat calculated is dependent on 10 different measured variables, introducing a relatively high uncertainty.

To detect the fault the FDD program isolates the linearly defined steady state operating period of the compressor. If equation 5.10 is true for more than 60 % of this period the fault is detected.

$$\dot{Q}_{cond} < \dot{Q}_{PR,cond} - \dot{Q}_{PR,cond,uncertainty} \tag{5.10}$$

Where $\dot{Q}_{PR,cond,uncertainty}$ is the uncertainty between $\dot{Q}_{cond}$ and $\dot{Q}_{PR,cond}$ being 2.5% and 3.0% of $\dot{Q}_{PR,cond}$ for the "5HP-compressor" and "V-compressor" respectively. The approach to detect a faulty low condenser heat is in principle the same approach as to detect a broken discharge valve (Fault 4.4). By seeing how often a simple limit check is exceeded. The algorithm approach to detect a defect discharge valve through a limit check is illustrated in Fig. 4.15. It can be applied to detect a low condenser heat.

The FDD approach utilizes process history based gray-box or fuzzy logic approach to differentiate a faulty from fault free residual between $\dot{Q}_{cond}$ and $\dot{Q}_{PR,cond}$.

5.8.4. Results

Low condenser heat can be a result of several different faults. Air in the condenser (Fault 5.2) should be detected through a low condenser heat, as it affects the temperature difference of the heat sink flow. The heat sink flow does not absorb the expected amount of heat due to this decrease in the temperature difference. Investigating the heat pump system where air in the condenser was detected it became apparent that the threshold that defines $\dot{Q}_{cond}$ (equation 5.10) as faulty was exceeded 14.11 % of the steady state period. The fault was not detected. In Fig. 5.17 $\dot{Q}_{cond}$ is noticeably less than $\dot{Q}_{PR,cond}$, however it is varying so much that a faulty low condenser heat cannot be detected. Further

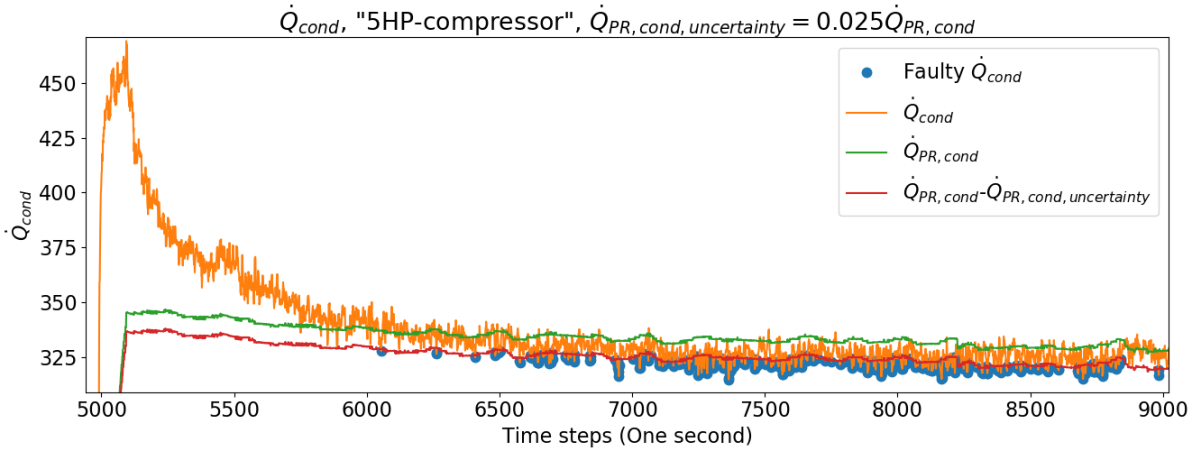

Figure 5.17: An example of a "5HP-compressor" with air in the condenser (Fault 5.2) where a low $\dot{Q}_{cond}$ is expected, but not present. The green line, $\dot{Q}_{PR,cond}$, is the predicted condenser heat, the orange line, $\dot{Q}_{cond}$, is the calculated condenser heat and the red line is the fault threshold defined by equation 5.10. The example is from a "5HP-compressor", thus $\dot{Q}_{PR,cond,uncertainty}$ is $0.025\dot{Q}_{PR,cond}$. The fault is detected whenever $\dot{Q}_{cond}$ is below the fault threshold, which is marked by a blue dot at that point, for more than 60% of the operating time. Note that after a startup the fault detection only begins when the residual between $T_{PR,dis}$ and T_{dis} converged.

the FDD program must consider two things; how much is the condenser heat affected by air in the condenser and is the fault threshold precise enough.

Air in the condenser will create a mass transfer resistance, and the water outlet temperature from the condenser will be lower than expected, air in the condenser is detected if the difference between $T_{dis,sat}$ and $T_{water,cond,out}$ is too high. Assuming a constant mass flow of water, a lower temperature of the outlet water from the condenser lowers the condenser heat through equation 5.11.

$$\dot{Q}_{cond} = \Delta T_{water,cond} \dot{m}_{water,cond} c_{p,water} \tag{5.11}$$

Following this analogy the condenser heat should be noticeably less as $\Delta T_{water,cond}$ is 3 times lower than expected in the heat pump that had air in the condenser. The effect air has on the condenser

heat and also the COP is discussed further in subsection 5.9.3.

The fault threshold was chosen as the recorded standard deviation of $\dot{Q}_{cond}$ and 60 % of the steady state operational time. 60 % was chosen as a relatively high number. There will be a time delay between $\dot{Q}_{PR,cond}$ and $\dot{Q}_{cond}$ arising from the direct response of the compressor prediction tool and the delayed response of the heat pump system to changes in the running conditions. This time delay causes the fault threshold to be exceeded often, Fig. 5.18 illustrates this for a fault free situation. It

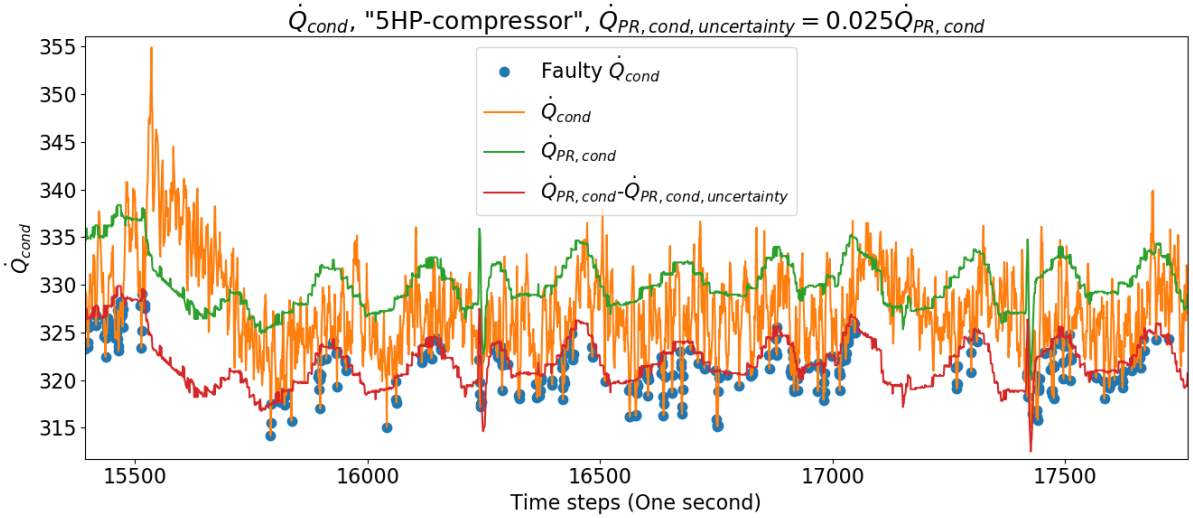

Figure 5.18: Due to the time time delay between $\dot{Q}_{PR,cond}$ (green line) and $\dot{Q}_{cond}$ (orange line) that causes the fault threshold from equation to be exceeded often when the fault is not necessarily present. The graph is from a heat pump system with a "5HP-compressor" where the fault threshold from was exceeded 14.11%.

was concluded that it is preferable to have a FDD program that remains robust and is able to adapt quickly to changes in the system as mentioned in Table 1.1. Therefore the fault threshold was taken as the measurement uncertainty being exceeded for 60 % or more of the steady state operation period to detect when $\dot{Q}_{cond}$ is noticeably lower for longer time periods.

5.9. Low efficiency

The heat pump systems delivered by GEA are expected to deliver a certain amount of heat per amount of energy consumed. This efficiency or performance of the heat pump can be quantified through the COP. The COP is also given by the compressor prediction tool. The calculation method and accuracy of the COP and the COP predicted by the compressor prediction tool are discussed in subsection 3.2.4. A low COP is typically a result of other faults and can occur independent of the compressor type and the heat pump setup. To detect the fault, a measurement interval of 30 seconds is required.

5.9.1. Failure Description and Symptom

The fault is occurring if the heat pump is delivering a COP lower than promised. This implies that the heat pump is consuming too much energy, however if $\dot{Q}_{cond}$ is too low (Fault 5.8) it implies that the heat pump is not delivering enough heat. Due to the interacting nature of $\dot{Q}_{cond}$ and the COP it is important to analyze and see how they affect each other. Both a too low $\dot{Q}_{cond}$ and a too low COP are usually a result of other seen faults, the link between the previously seen faults, and these issues will be further discussed in the following subsections.

5.9.2. Failure Detection Approach

The COP is directly dependent on the uncertainty of the motor power and the uncertainty of the condenser heat estimated.

In total the uncertainty in the COP calculations, $COP_{PR,uncertainty}$, adds up to 6.41 % and 4.40 % for the "5HP-compressor" and the "V-compressor" respectively derived in Table 3.5 in subsection 3.2.4. The FDD approach for detecting a low COP will be done in the same manner as for detecting a low

$\dot{Q}_{cond}$, which again is the same approach as for detecting a defect discharge valve (Fault 4.4), with a simple limit check. During steady state the fault threshold is dictated by equation 5.12.

$$COP < COP_{PR} - COP_{PR,uncertainty} \tag{5.12}$$

The low COP is detected as a fault when the fault threshold is exceeded for 60 % of the steady state operation period, the same threshold which is used to detect a faulty low $\dot{Q}_{cond}$.

The FDD approach utilizes process history based gray-box or fuzzy logic approach to differentiate a faulty from fault free residual between the measured and predicted COP.

5.9.3. Results

Fig. 5.19 shows the COP and COP_{PR} together with the fault threshold in a heat pump system where the fault was not detected. In Fig. 5.19 the fault threshold was exceeded for 0.299 % of the steady state opeartion period. The fault threshold is exceeded some time steps, but this is due to the time delay arising from the delayed response of the heat pump system and the direct response of the variables predicted by the compressor prediction tool.

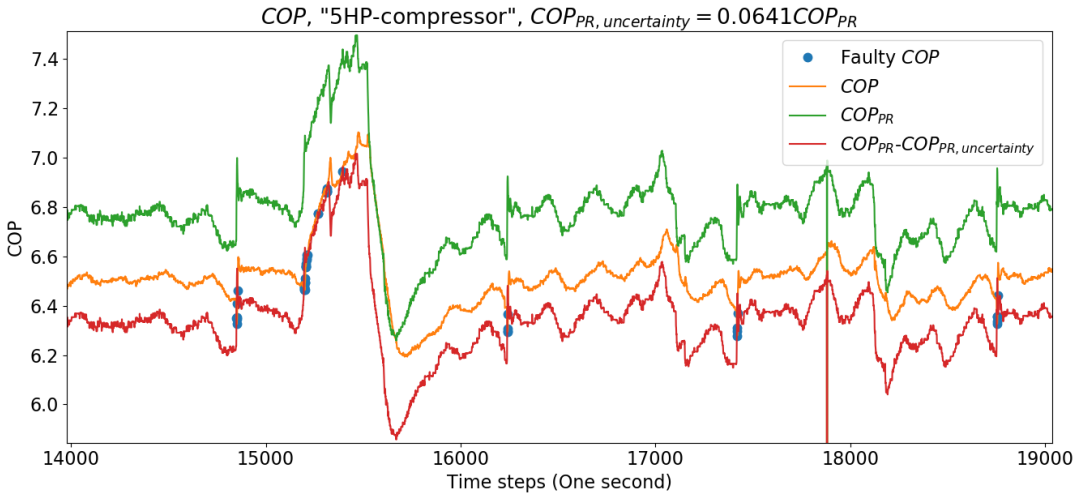

Figure 5.19: Data from the same heat pump system with a "5HP-compressor" as in Fig. 5.18, where a faulty COP was not detected. Due to the direct and delayed response of the compressor prediction tool and the heat pump system the fault threshold (equation 5.12) will be exceeded when the COP is clearly within the threshold. Therefore the fault threshold has to be exceeded 60 % of the time for the COP to be clearly below the threshold most of the time and a faulty low COP detected.

Analyzing the heat pump system where air in the condenser was detected (Fault 5.2), it is apparent from Fig. 5.20 that air in the condenser has a bigger impact on the condenser heat, on the right side, than the COP, on the left side. The results from the analysis of $\dot{Q}_{cond}$ and the COP in the heat pump system known to have air in the condenser are shown in Table 5.2. It is apparent from Table 5.2 that

Table 5.2: The results after analyzing a heat pump system known to contain air in the condenser, the bottom two rows should be above 60 % for either $\dot{Q}_{cond}$ or the COP to be recognized as faulty. The column to the right shows the fault threshold that must be exceeded for the fault to be detected.

Results	**"5HP-compressor" 1**	**"5HP-compressor" 2**	**Fault Threshold (For a "5HP-compressor")**
$\frac{COP}{COP_{PR}}$	98.16 %	96.16 %	<93.593 %
$\frac{\dot{Q}_{cond}}{\dot{Q}_{PR,cond}}$	99.42 %	98.89 %	<97.493 %
Frequency of $COP < COP_{PR} - COP_{PR,uncertainty}$	0 %	0.299 %	>60 %
Frequency of $\dot{Q}_{cond} < \dot{Q}_{PR,cond} - \dot{Q}_{PR,cond,uncertainty}$	0.3369 %	14.11%	>60 %

the FDD program was not able to detect a faulty low $\dot{Q}_{cond}$ or a faulty low COP.

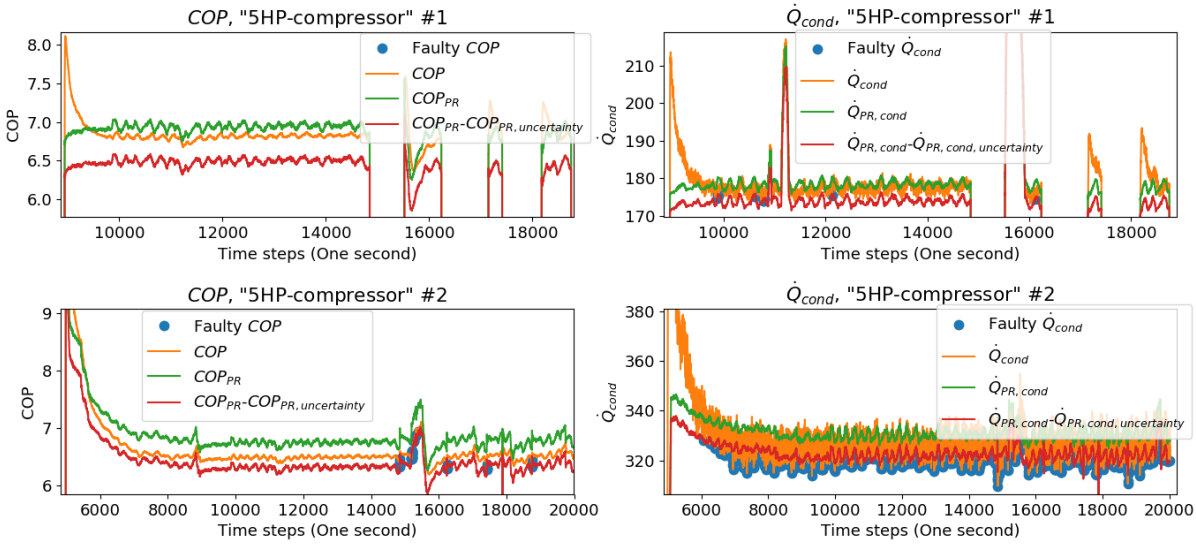

Figure 5.20: Data from the two "5HP-compressors" in the heat pump system known to contain air in the condenser. The top and bottom photo shows the COP and $\dot{Q}_{cond}$ for "K111" and "K112" respectively. The fault thresholds for the COP and $\dot{Q}_{cond}$ are illustrated by a red line. The COP is shown on the left side and $\dot{Q}_{cond}$ on the right side, it is apparent that air in the condenser is more visible in $\dot{Q}_{cond}$ (Fault 5.8). The calculated COP on the top and bottom left side proved to be 94.9% and 92.9 % respectively of the COP predicted on average, while the top and bottom right graphs proved that $\dot{Q}_{cond}$ was 96.1 % and 95.4 % respectively of $\dot{Q}_{PR,cond}$ on average.

Conclusions about the effect of air in the condenser on $\dot{Q}_{cond}$ and the COP

It can be concluded that air in the condenser (Fault 5.2) is more visible in $\dot{Q}_{cond}$ than in the COP as a fault. This is mainly due to the uncertainty and hence the fault threshold which are higher for $\dot{Q}_{cond}$ than for the COP. It is worth noting that should there be air in the condenser it would result in a lower condenser heat (as explained in Fault 5.8). However, it will also result in a higher motor power as the compressor will have to overcome the increased condensing pressure due to Dalton's law. Hence the COP should be more affected by air in the condenser than $\dot{Q}_{cond}$, but the uncertainty of the COP does not allow for FDD. This is confirmed by Table 5.2 where the COP is further away from COP_{PR} than what $\dot{Q}_{cond}$ is from $\dot{Q}_{PR,cond}$.

However, neither $\dot{Q}_{cond}$ nor the COP are detected as faults in the heat pump system known to have air in the condenser. In fact they are seen to be well within the expected values. A possible explanation could be that the air in the condenser affects the inputs to the compressor prediction tool and hence also COP_{PR}. Air in the condenser would affect the saturated discharge temperature, as the measured pressure would be the combined pressure of the air and the refrigerant, p_{total}, in the condenser. The saturated discharge temperature is however dependent on the the pressure of the refrigerant in the condenser alone.

Thus the conclusion is: in a heat pump system containing air in the condenser, the FDD program should detect a faulty low $\dot{Q}_{cond}$ and COP. However if $\dot{Q}_{cond}$ and the COP are not detected as faults it does not necessarily mean that there is no air in the condenser present, as many other factors come to play.

5.10. Problematic startup of the heat sink flow

The heat sink flow has one butterfly valve to control it in Fig. 5.21. The butterfly valve is fully closed during standstill of the heat pump system. The butterfly valve is controlled from the control system of the heat pump system, while the heat sink pump is controlled individually by the heat pump user.

During startup of the heat pump system the heat sink flow has two failure modes. During ideal behaviour the centrifugal heat sink pump should start up a few minutes before the compressor, while the butterfly valve is closed to build up the temperature of the water. The butterfly valve is further meant to throttle the flow after it is opened This is a problem independent of the compressor type and

the heat pump system type which requires a measurement interval of 1 second.

5.10.1. Failure Description

The first failure mode occurs during standstill when the butterfly valve is closed by the control system. The failure occurs if the heat pump user is running the centrifugal water pump in Fig. 5.21, during standstill. The water pump builds up a high discharge pressure and hence also temperature. When the heat pump is started, the butterfly valve is opened and the warm water is introduced in to the condenser. Should the water be too warm it will start boiling the refrigerant. Hence the refrigerant pressure will increase until it triggers a safety valve which will start releasing the refrigerant to the environment to lower the pressure.

During startup the water can also be too cold if the heat pump operator did not start the water pump. The butterfly is meant to throttle the water flow to decrease the mass flow to. This is done to ensure that the refrigerant gives away sufficient heat for the compressor to build up a differential pressure.

The second failure mode occurs when the butterfly valve is broken. It will result in a heat sink flow being too cold and too high which again will lower the discharge pressure of the compressor. This ultimately leads to a delayed or never occurring build up of the discharge pressure of the compressor.

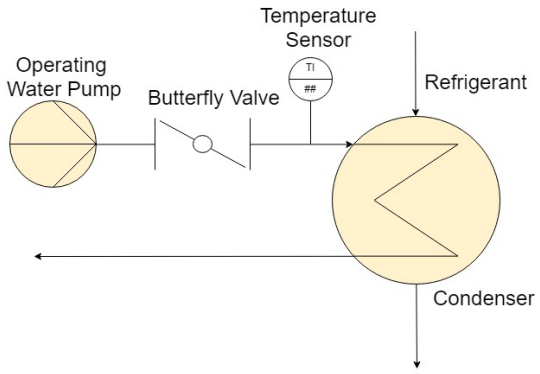

Figure 5.21: Schematic showing a potentially problem in the condenser water flow.

5.10.2. Failure Symptoms

The water temperature sensor is placed after the butterfly valve this sensor will not record high temperatures until the valve is actually opened and it is too late. A problematic startup of the heat sink flow is detectable by the symptoms below.

1. A short, sudden and delayed increase of the water temperature entering the condenser and a sudden increase in the discharge pressure of the compressor during standstill.

2. The compressor differential pressure never builds up to the minimum limit of operation after a startup while temperature of the water entering the condenser is colder than during normal operation.

5.10.3. Failure Detection Approach

A delayed increase of the compressor differential pressure could be due to other failures than the problematic heat sink startup. The bypass valve remaining open during startup (item 3 of Fault 4.1) or a defect suction valve (Fault 4.5) are also detected through a delayed build up of Δp_{comp}. However, together with the entering heat sink temperature the fault can be isolated. The threshold that defines the water to be too cold was taken to be whenever it is lower than the saturated suction temperature.

The failure is detected in a qualitative manner using a case-based reasoning approach. The failure is detected by storing the knowledge learned by experts in a database, and seeing how the measured data compares to the trends in the database.

5.10.4. Results

To detect the first failure mode the sensor placement should be on the other side of the butterfly valve to be able to detect the fault for on-line FDD. With the current sensor placement a FDD program can only detect the fault after it has occurred, when the butterfly valve is opened. At this point the fault is inevitable. This is the only fault that causes the safety valve to go off, thus if it happens the failure cause is known. Hence a FDD algorithm for the first failure mode was not made. An off-line FDD algorithm that can detect the fault when it is too late would not capture the goal of this project, to construct a FDD program for future on-line failure detection.

There were no existing data from a delayed build up of Δp_{comp} due to cold water in the condenser. However several heat pump systems had a delayed build up of Δp_{comp} due to other faults. If a delayed build up of Δp_{comp} is the only recorded failure symptom, it cannot be concluded which failure it is. However, if a delayed build up of Δp_{comp} is occurring when $T_{cond,water,in}$ is lower than $T_{suc,sat}$, then the reason is isolated as a problematic cold water startup.

5.11. Unstable subcooling

Certain heat pump setups have three heat exchangers performing the task of one condenser. Three separate heat exchangers act as a de-superheater, a condenser and a subcooler shown in Fig. 5.22. This heat pump setup is prone to failures arising from variations in the incoming heat sink flow or temperature. The fault is independent of the compressor type and the heat pump system, however it is more often seen in heat pump systems as the one in Fig. 5.22. Detecting the fault requires a measurement interval of 1 second.

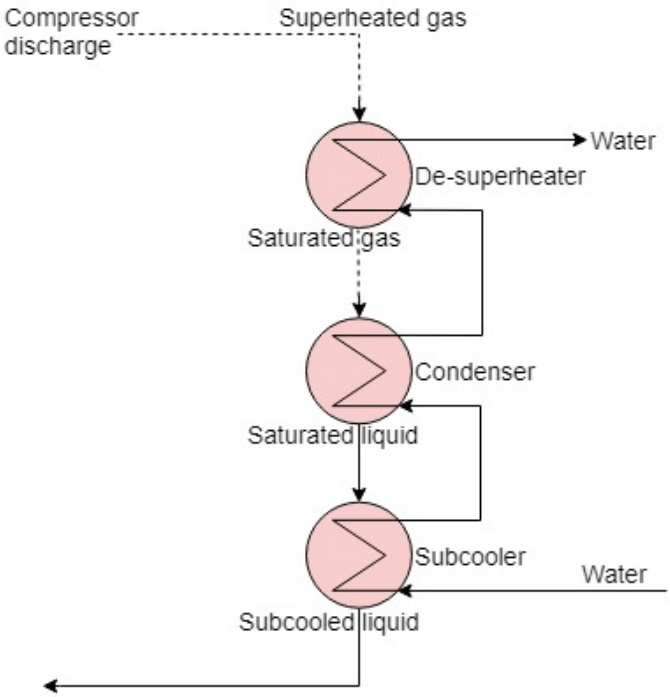

Figure 5.22: The heat pump system with 3 HEXs in series for condensing.

5.11.1. Failure Description

If the subcooling of the condenser, T_{sc}, becomes unstable this could be due to a number of reasons. Typically it is the water flow in the condenser having too high fluctuations (Fault 5.6), a defect butterfly valve controlling the flow to the condenser (Fig. 5.21) or the control of the motor controlled valve working as an expansion valve (Fault 6.2).

Unstable subcooling leads to a difficulty maintaining the de-superheating, the condensing and the

subcooling separated in individual heat exchangers. The exiting water temperature will vary which again makes the heat load varying and unstable, which is undesirable and may lead to other faults.

5.11.2. Failure Symptoms

The fault can be detected through the one symptom listed below.

- The subcooling in the refrigerant becomes very unstable. Monitored by the temperature difference between the saturated discharge temperature and the temperature of the refrigerant exiting the condenser.

There are no known examples of unstable subcooling occurring in a heat pump system, thus it is not known what qualifies as faulty unstable subcooling a fault-free unstable subcooling.

5.11.3. Failure Detection Approach

Unstable subcooling is detected in the same manner as too high fluctuations in the heat source or sink flow or temperature (Fault 5.3 and Fault 5.6). There were no known examples of unstable subcooling when using the same threshold of 2 K per minute for T_{sc}. The approach of the FDD algorithm to detect unstable subcooling is the same as in Fig. 5.9. The FDD program compares the average T_{sc} over the last minute to the average T_{sc} over the next minute with the fault threshold of 2 K.

The fault is detected in a qualitative rule based limit checking manner, where T_{sc} is compared to a predefined threshold.

5.11.4. Results

After analyzing different heat pump systems with the FDD algorithm for detecting unstable subcooling, the fault was not detected. There is a link with between the high variations in the incoming water flow to the condenser (Fault 5.6) and unstable subcooling. In Fig. 5.23 the flow to the condenser had high fluctuations, but the rate of change of $T_{cond,water,in}$ was too slow. T_{sc} remained unaffected as both $T_{dis,sat,system}$ and $T_{cond,out}$ responded directly to the change of $T_{cond,water,in}$. This illustrates why the fault is more frequent for heat pump systems with three heat exchangers in series, as Fig. 5.23 only had one HEX.

For a heat pump system with three heat exchangers in series, a drop in $T_{cond,water,in}$ would mean that the refrigerant gas going into the de-superheater would have too much heat removed. The refrigerant could start condensing in the de-superheater. This would lead to liquid being the input to the condenser, a HEX designed for gaseous refrigerant as an input. This would probably affect the heat transferring abilities of the condenser poorly, and it will ultimately lead to changes in T_{sc}. A time delay is expected as $T_{dis,sat,system}$ will change immediately after $T_{cond,water,in}$ changes while $T_{cond,out}$ will have a time delay before it changes.

In Fig. 5.23 T_{sc} is varying by more than 2 K per minute from time step 34000 when $T_{water,cond,in}$ was relatively constant, however the fault is not detected. The FDD algorithm averages T_{sc} for the 60 previous time steps, and investigates for fluctuations of more than 2 K per minute. The fluctuations in Fig. 5.23 follows a sinusoidal wave with a period of approximately 60 seconds, thus the average every 60 seconds will remain relatively constant. These fluctuations are due to the time delay between the measurements of $T_{dis,sat,system}$ and $T_{cond,out}$ and should not be detected as a faulty unstable subcooling.

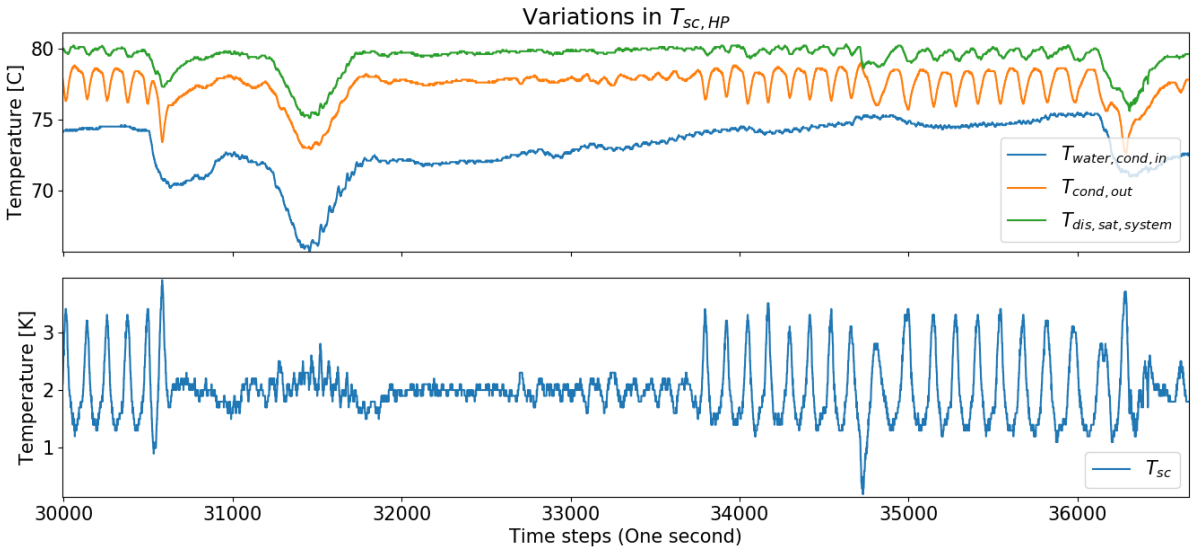

Figure 5.23: High variations in T_{sc} (bottom graph) where faulty unstable subcooling was not detected. T_{sc} is $T_{dis,sat,sys}$ (green line) minus $T_{cond,out}$ (orange line) from the top graph. It is apparent that T_{sc} is subject to a time delay, as the green and orange peaks occur at slightly different times. In addition $T_{cond,out}$ is varying at a much higher pace than $T_{dis,sat,system}$ and $T_{water,cond,in}$ has a small affect on T_{sc}.

6

Heat Pump Component Failures

The heat pump systems consist of several components prone to damage and unrelated to the compressor. The failure of these components can however lead to damage in the compressor, or unsatisfactory operation. There are five different failure modes classified as heat pump component failures. These are classified as the faults involving all components in the heat pump except the compressor. The heat pump component faults can occur for all heat pump systems and compressors. Except Fault 6.5 introduced in subsection 6.5 which can only happen in systems with the "5HP-compressor".

6.1. Defect non-return valve in the compressor discharge line

In the heat pump systems with two compressors in parallel both compressors will have a non-return valve in the discharge line as in Fig. 6.1. Whenever one compressor is operating and the other compressor is not the non-return valve in the discharge line ensures no back flow in the non-operating compressor. The fault is identified by the non-return valve leaking, introducing a back flow through the discharge in to the compressor. The fault can occur in both compressors, it is however detected slightly differently for the two compressors, the FDD program is dependent on a measurement interval of 1 second to detect the fault.

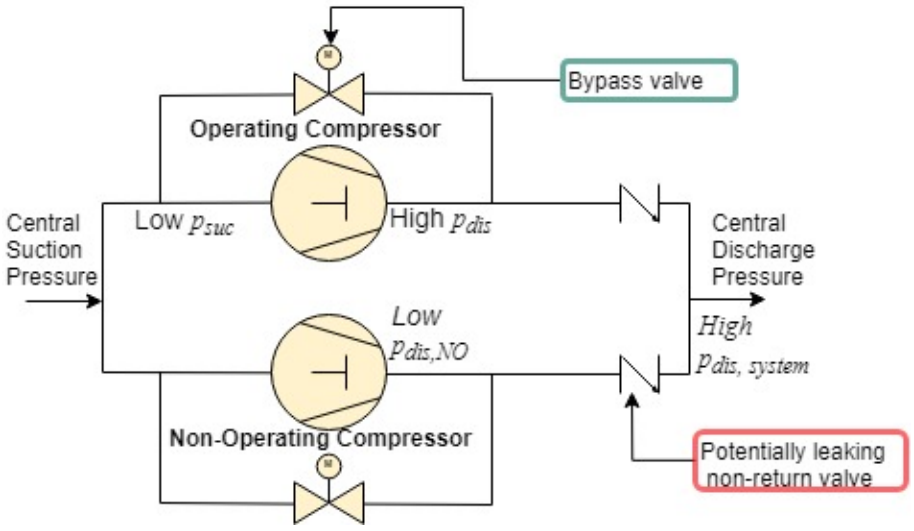

Figure 6.1: Schematic of problematic parallel setup of compressors.

6.1.1. Failure Description

If the non-return valve in Fig. 6.1 is leaking then the discharge pressure (and the saturated discharge temperature) of the non-operating compressor will increase. It will increase to that of the operating

compressor as in Fig. 6.2.

The compressors are not insulated for these high pressure conditions during standstill. The non-operating compressor discharge line will have a heat loss to the environment. The crankcase heater cannot maintain the refrigerant in a gaseous state (as it now has to maintain a higher saturation temperature than previously). The enthalpy will decrease at constant pressure, causing the refrigerant to condensate inside the compressor cylinder heads as in Fig. 6.2.

6.1.2. Failure Symptom

This failure is recognizable through the following three symptoms.

1. The discharge pressure of the non-operating compressor remains at operating conditions after shutdown for a longer period as seen in both graphs of Fig. 6.2.

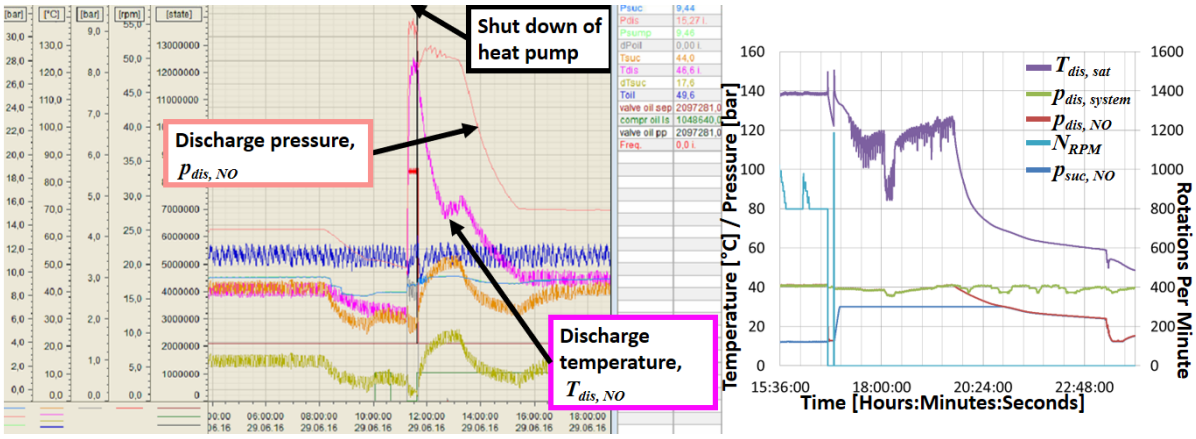

Figure 6.2: The illustration on the left side shows an example of a leaking non-return valve in a "5HP-compressor", the black vertical line represents a shut-down of one compressor. The discharge pressure (red line) remains at operating conditions up to two hours after shut-down. The discharge temperature (pink line) decreases fast until it reaches the saturation temperature where the temperature remains relatively constant for a longer time periodand the refrigerant condenses. The right hand side shows an example of a leaking non-return valve in a "5HP-compressor". After the rotational speed (light blue line), N_{RPM}, reaches zero the suction pressure (dark blue line), $p_{suc,NO}$, increases to almost twice as high. The discharge pressure (red line), $p_{dis,NO}$, remains at operating conditions for more than 2 hours.

2. A sudden temperature decrease in the discharge temperature during startup of the previously non-operating compressor due to liquid in the compressor.

3. The suction pressure in the "5HP-compressor" increases above its expected values. p_{suc} can reach higher than its imposed pressure limit (26 bar) as it did on the right side of Fig. 6.2.

6.1.3. Failure Detection Approach

The fault is detected differently for the different compressors. The "V-compressor" discharge valve never leaks backward, thus the high pressure never reaches the suction line. The "5HP-compressor" discharge valve is not protected for a back flow and will leak to the suction line which can damage the suction line.

The FDD program investigates the shutdown of the non-operating compressor to detect the fault through the pressures, the detailed approach of the FDD is explained in Fig. 6.3. The FDD approach to detect a leaking non-return valve is based on limit checks. These limit checks compare the discharge pressure and suction pressure of the operating and non-operating compressor. The dip in T_{dis} during startup only occurs in the "V-compressor", but it can occur without the fault being present. Hence the FDD program is not detecting the fault through this symptom.

All symptoms are detected through a qualitative simple-rule based reasoning looking for a specific residual between two parameters, where priori knowledge defines the residual as faulty or fault-free.

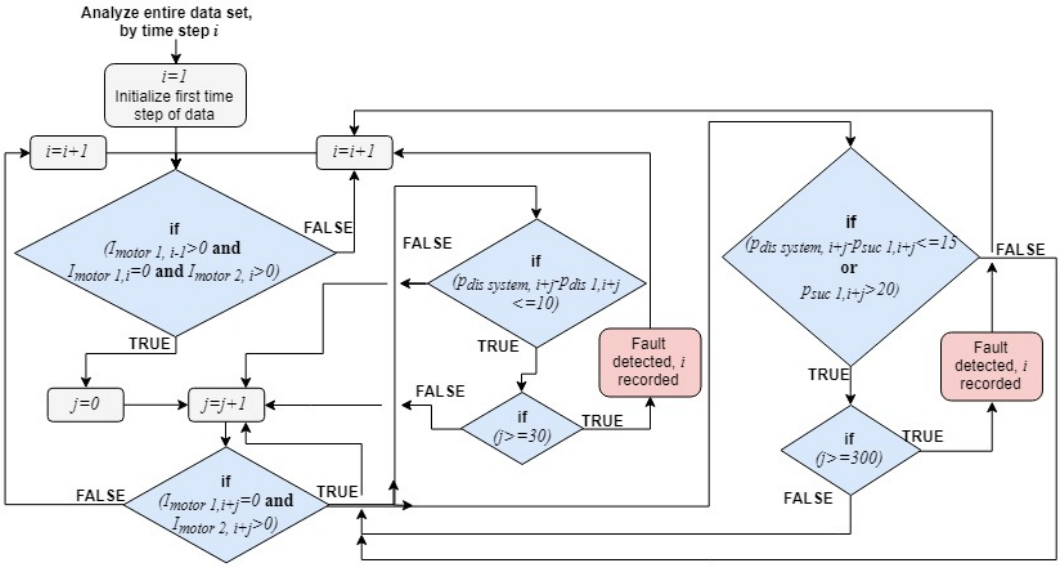

Figure 6.3: Approach of the FDD program to detect a leaking non-return valve through the presures at shutdown. The fault is detected if the pressure difference over the non-return valve is less than 10 bar 30 seconds after shutdown, ideally this should be 25 bar or more after 10 seconds. For the "5HP-compressor" the fault can also be detected through p_{suc}. If $p_{suc,NO}$ is above 20 bar or if $p_{dis,system} - p_{suc,NO}$ is below 12 bar 5 minutes after a shutdown the fault is detected. Ideally $p_{suc,NO}$ is below 15 bar and $p_{dis,system} - p_{suc,NO}$ is above 22 bar 10 seconds after the shutdown.

6.1.4. Results

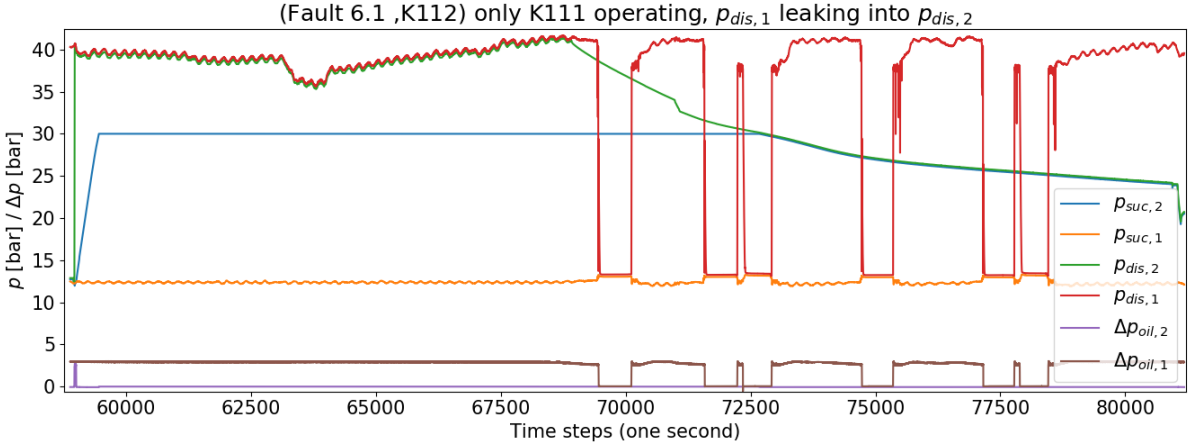

Figure 6.4: Example from a leaking non-return valve, after $\Delta p_{oil,2}$ (purple line) reaches zero $p_{suc,2}$ (blue line) increases to almost twice as high. $p_{suc,2}$ approaches the upper limit for the suction line and the system discharge pressure, $p_{dis,1}$ (red line), which is the third fault symptom. It can also be seen that the non-operating discharge pressure, $p_{dis,2}$ (green line), is equal to the operating discharge pressure $p_{dis,1}$ long after shutdown, which is the first fault symptom.

The FDD program was able to detect two examples of a leaking non-return valve, in heat pump systems with both a "5HP-compressor" and a "V-compressor". The first and third symptom are depending on investigating the shutoff of a heat pump. Thus if the fault would occur after a longer period of non-operation the program would not detect until next shutoff.

Fig. 6.4 shows a leaking non-return valve occurring in a "5HP-compressor". After the first shutdown, marked by Δp_{oil} (purple line) reaching zero, p_{suc} increases to more than twice its value original value. It reached the limits of the pressure sensor in the suction line, set at 30 bar, thus the actual pressure is probably the same as $p_{dis,system}$ (green line).

Fig. 6.5 shows a leaking non-return valve occurring in a "V-compressor" with only one compressor

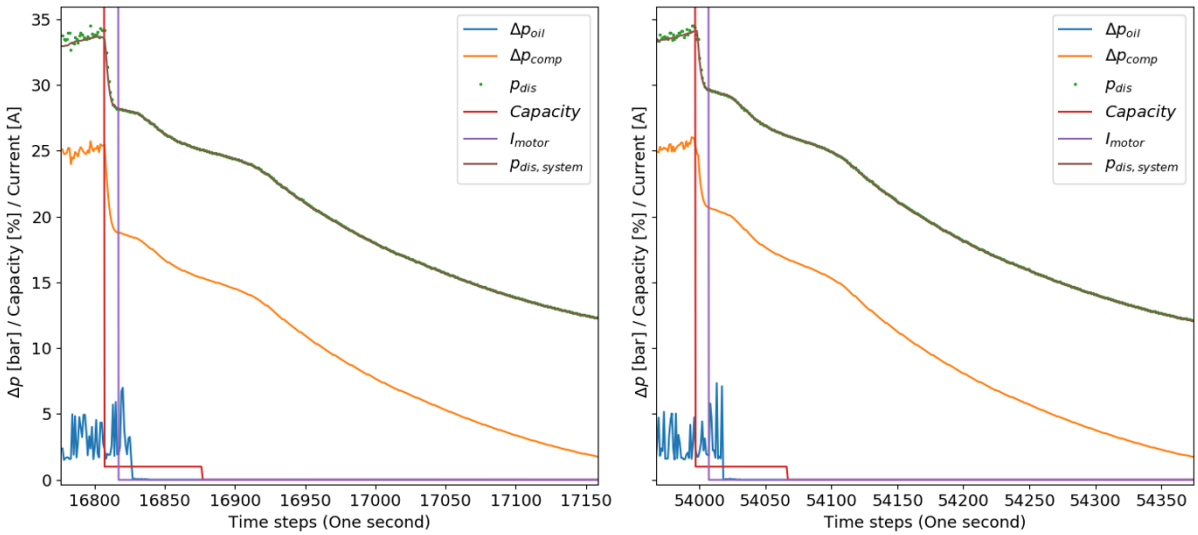

Figure 6.5: Example from a leaking non-return valve detected during two shutdowns, after $Capacity$ (red line) reaches zero p_{dis} and $p_{dis,system}$ remain equal. Ideally p_{dis} (green dots) should equal to p_{suc} (brown line) immediately after the shutdown, i.e. Δp_{comp} should go to zero immediately after a shutdown as it was seen in Fig. 4.3, instead it takes 300-400 seconds to equalize.

operating. During shutdown Δp_{comp} does not equalize immediately and p_{dis} is equal to $p_{dis,system}$ when $p_{dis,system}$ has its delayed decrease, due to the system cooling down.

In Fig. 6.5 there is a link between the previously seen closed bypass during shutdown (item 2 of Fault 4.1) and the leaking non-return valve.

The FDD program detected both faults, but upon inspection it is reason to believe that Fig. 6.5 is an example of a leaking non-return valve and not a closed bypass valve. The delayed decrease of Δp_{comp} is the known symptom of both faults, however $p_{dis,system}$ and p_{dis} remain equal after the shutdown. This would imply that there is no closed valve separating the two flows. They would have a different development should there be a closed valve between the two. Ideally p_{dis} is expected to drop down to p_{suc} immediately after shut down and Δp_{comp} would also drop to zero immediately after a shut down (illustrated in Fig. 4.3). In Fig. 6.5 $p_{dis,system}$ has the expected development after a shut down of a heat pump system with only one compressor operating.

Conclusions about link between a leaking non-return valve and a broken bypass valve

The closed bypass valve during shutdown of a compressor is linked with the leaking non-return valve through Δp_{comp} remaining too high for too long after a compressor shutdown. Their intertwined nature made it impossible to differentiate between the two in the FDD algorithm. Upon investigation there is bigger reason to believe that the example in Fig. 6.5 is an example of Fault 6.1. But there is no way of knowing for certain without visual inspection, which fault is apparent. The FDD algorithm for these two faults has a low score on the metrics 'Isolability' and 'Multiple fault identifiability' from Table 1.1.

6.2. The motor driven control valves

There are three different motor driven control valves in most heat pump systems. A thermal expansion valve, a valve controlling the heat source and a valve controlling the suction line of the compressor, the four red valves in Fig. 6.6. They have similar failure symptoms where the time rate is what differentiates them. The valves and hence also the faults can be in all heat pump systems independent of the compressor type. A measurement interval of 1 second is required to detect the fault in Fig. 6.7.

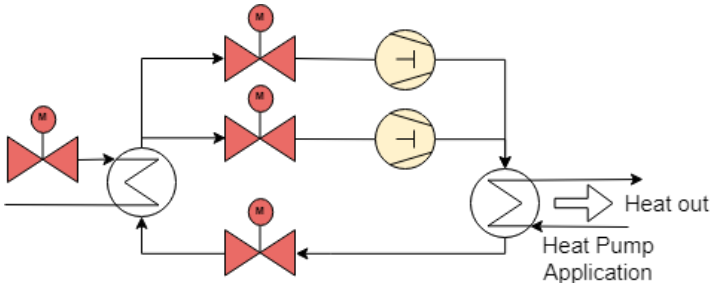

Figure 6.6: Simplified heat pump schematic, with the four different motor driven control valves in red.

6.2.1. Failure Description and Symptoms

When one of the three motor driven control valves are defect, they tend remain closed when they should instead be open. This results in a decreasing suction pressure due to having a finite and decreasing volume of gaseous refrigerant which the compressor can suck. The failure mode of the three different valves are described below.

1. The motor driven control valve in the compressor suction line remains closed, Fig. 6.7 is an example of this. The pressure in the suction line decreases rapidly until it the compressor shuts down on limit checks in the control system.

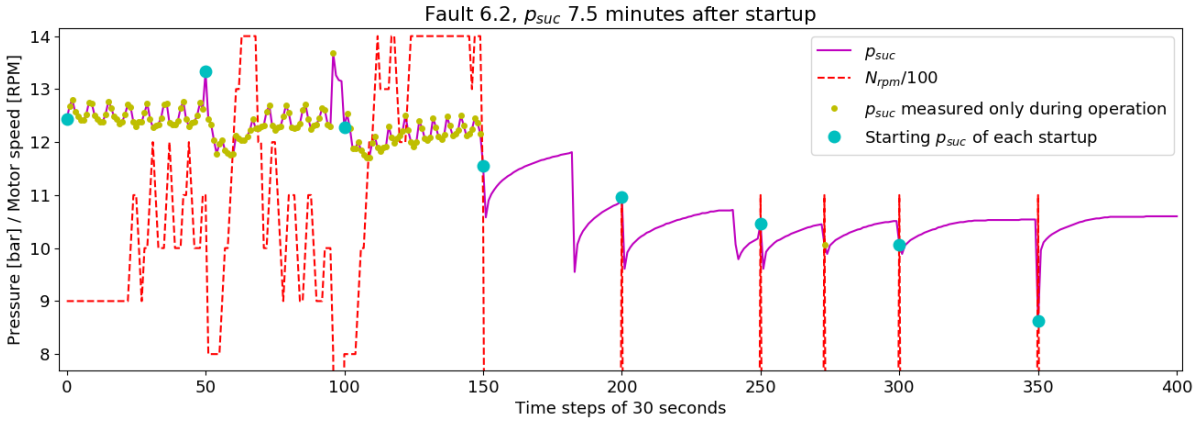

Figure 6.7: A broken motor driven control valve functioning in the suction line causes the heat pump to shutdown immedetiately after startup repeatedly. The blue dots represents each startup, after startup number 4, 5, 6 and 7 the suction pressure (purple line) decreases until the compressor shuts off, recognized by the N_{RPM} reaching zero.

2. The motor driven control valve for the heat source flow is closed resulting in a stand-still of the heat source flow. The compressor slowly extracts all gas in the evaporator and suction line, lowering the pressure in the suction line. The suction pressure is decreasing until the control system shuts down the compressor, but at a slower pace than for the suction line valve.

3. The thermal expansion motor driven control valve is closed. The same fault occurs as previously seen, but at an even slower rate.

6.2.2. Failure Detection Approach

The FDD program will detect these symptoms by isolating the startup sequences. The fault is detected if the suction pressure decreases every four seconds after startup until the motor is turned off. In addition the suction pressure at shutoff is lower than the minimum recorded discharge pressure. The FDD approach for detecting defect motor driven control valves is illustrated in Fig. 6.8.

The FDD program will output a graph with the rotational speed and the suction pressure after startup.

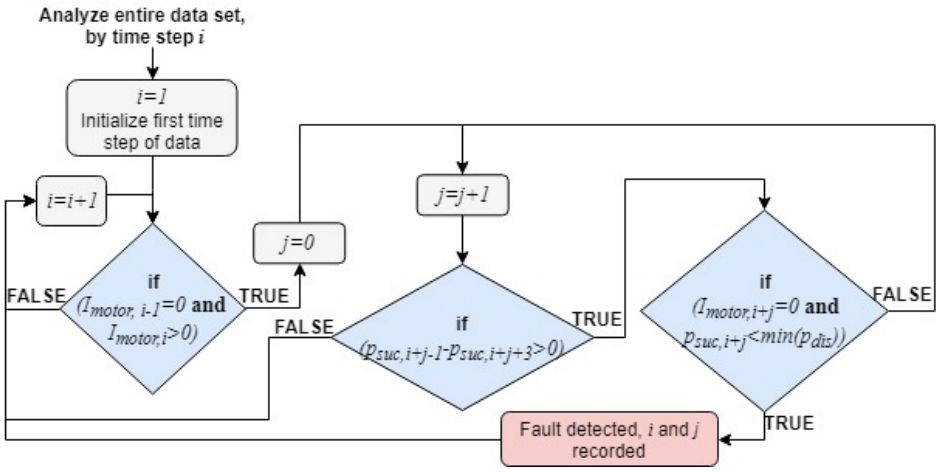

Figure 6.8: FDD approach to detect all symptoms of the defect motor driven control valves

All symptoms are detected through a qualitative simple-rule based reasoning looking for a combination of two trends, where priori knowledge defines the combination as faulty or fault-free.

6.2.3. Results

The FDD program checks the suction pressure of the compressor every four seconds to ensure that the program will detect the fault occurring at slower rates. The lowest recorded p_{dis} should be from a standstill period where the pressures are equalized. Therefore p_{suc} during the faulty shutdown should be lower than the lowest recorded p_{dis} as a fault threshold.

The example in Fig. 6.7 is the only example of this fault occurring, thus the time rate for the three different symptoms is not known. In addition the example in Fig. 6.7 has a measurement interval of 30 seconds, a measurement interval of 1 second is required to detect faulty motor driven control valves. In one time step the motor is started and in the next time step the suction pressure is too low and the motor is already turned off.

6.3. Liquid level in the evaporator

The liquid level in the evaporator is monitored and controlled by a sensor in order to ensure optimal heat transferring abilities in the HEX. A changing liquid level in the evaporator is typically a result of too sudden changes in the heat source flow or temperature (Fault 5.3). The fault can occur in all heat pump systems independent of the compressor type. However it is expected to occur more frequent in heat pump systems functioning as an add-on to refrigeration plants. The FDD program needs a measurement interval of 30 seconds to detect the fault.

6.3.1. Failure Description

The failure occurs when the transmitter or sensor of the liquid level indicator is broken, there is a refrigerant undercharge or the refrigerant is leaking. During steady state operation of the heat pump system with a steady supply of heat the liquid level should remain constant.

6.3.2. Failure Symptom

A broken liquid level indicator is detectable by the one symptom listed below. An example of this occurring in a heat pump system is illustrated in Fig. 6.9.

- The liquid level in the evaporator is changing during steady state operating conditions.

6.3.3. Failure Detection Approach

The FDD program is able to detect a broken liquid level indicator, a leaking evaporator or a refrigerant undercharge through the liquid level indicator in the evaporator. It can be detected by isolating the

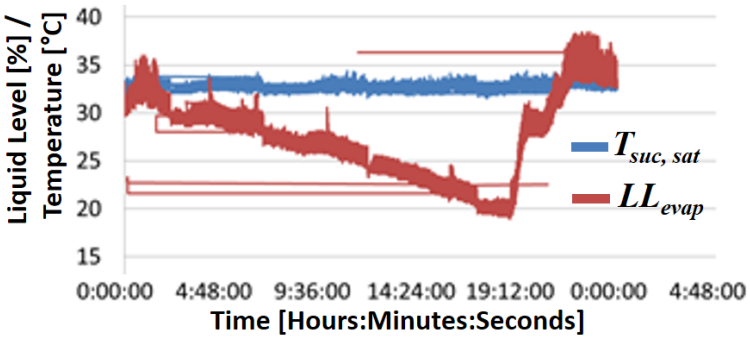

Figure 6.9: Example of a broken liquid level indicator in the evaporator, the liquid level is changing, but it does not affect the suction temperature noticeably.

periods of steady state operation of all compressors. The liquid level in the evaporator, LL_{evap}, and the system suction pressure $p_{suc,system}$ are recorded in this period.

$$y = \frac{LL_{evap}}{p_{suc,system}} \tag{6.1}$$

A linear regression model of the quotient, y, seen in equation 6.1 with respect to time is made for the previous 900 time steps (15 minutes). If the regression model gives a total change higher than 0.3 or lower than -0.3 for the quotient over the 900 seconds the fault is detected.

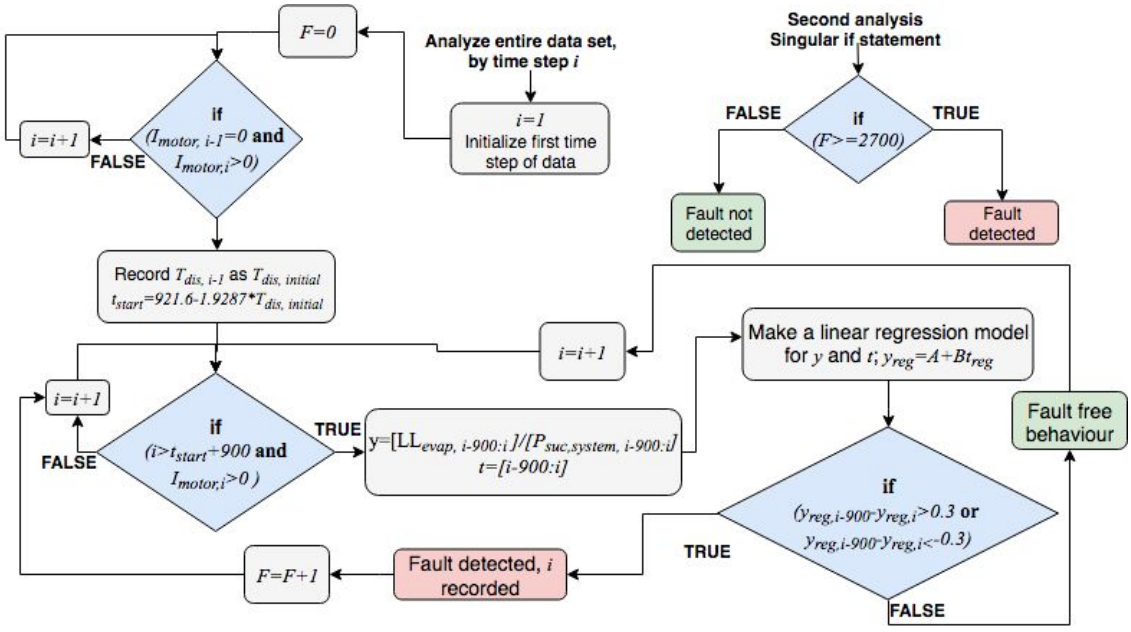

Figure 6.10: Approach to detect a faulty liquid level in the evaporator during operation occurring in a heat pump. Do note that the FDD algorithm requires two analyses, making the FDD algorithm unsuitable for on-line detection.

The fault is detected utilizing a quantitative sensitivity ratio method, where the combination of two parameters should be uniquely sensitive to this fault.

6.3.4. Results

In Fig. 6.9 the quotient between the evaporator liquid level and system suction pressure changes with approximately 0.5 over 19 hours. Thus the fault threshold might be, if anything, too low, however after validation the fault was not detected falsely in any cases. The faulty liquid level in the evaporator

was detected in one case, in Fig. 6.11, here the quotient decreases by 0.6 over 2.7 hours.

However, the problem was that the suction pressure increased by 1 bar in less than 30 seconds. This is equivalent to an increase of the saturated suction temperature of approximately 3.08 K over two minutes. This is a result of too high variations in the temperature or flow of the incoming heat source (Fault 5.3) occurring. An increase of the suction pressure decreases the amount of liquid, as more of the liquid will be evaporated to a gaseous state. The suction pressure should remain relatively constant as in Fig. 6.9, this is a shortcoming of the algorithm and it gives the FDD algorithm a low score on the "Isolability" metric from Table 1.1.

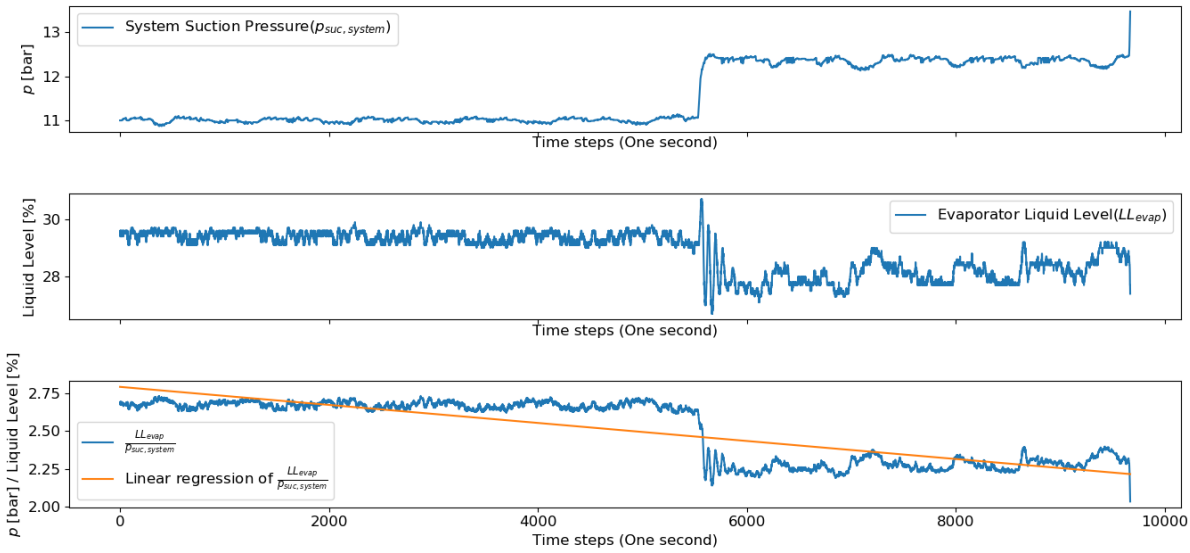

Figure 6.11: A faulty liquid level in the evaporator. The quotient is decreasing 0.579 over 2.7 hours, the fault threshold was chosen as 0.3. Hence the detected quotient decrease was almost twice as much as the fault threshold. This an example of too high fluctuations in the heat source (Fault 5.3), which again results in a faulty liquid level in the evaporator. The system suction pressure in the top graph should ideally remain constant for the entire period of operation.

6.4. Liquid refrigerant transferring away during standstill

After shutdown of the heat pump system the liquid level of the evaporator would ideally remain quite constant. For the heat pump functioning as an add-on, the liquid level is prone to changes if the refrigeration plant is operated and the heat sink or source is changing as in Fig. 6.12. The problem can however occur for all heat pump systems independent of the compressor type, a measurement interval of 1 minute is required to detect the fault.

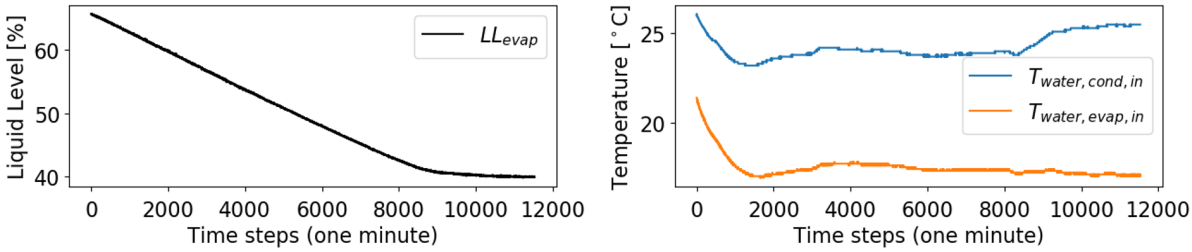

Figure 6.12: Example of changes in the evaporator liquid level (top left graph, black line) during standstill of a water cooled "5HP-compressor". Changes in both the incoming heat source and sink (top right image) affects the evaporator liquid level which is decreasing over 5 days. This leads to changes in both the discharge and suction pressure which could lead to condensation (bottom graphs).

6.4.1. Failure Description and Symptom

The problem occurs when the liquid refrigerant transfers away to the condenser from the evaporator during standstill, this is is recognizable by the symptom below.

- The liquid level in the evaporator is decreasing during standstill, while it should remain constant as observed in Fig. 6.12.

Changes in the liquid level during standstill can change the saturation points in the heat pump system, as in Fig. 6.12, which could lead to undesirable condensation in the heat pump system.

6.4.2. Failure Detection Approach

The liquid level is recorded 60 seconds after a known shutdown of all compressors until 60 seconds before the startup of one or more compressors. During this period the program makes a linear regression model of the liquid level in the evaporator every time step for the next 15 minutes. If the linearly regressed model predicts a liquid level decrease of 5 % or more during the next 15 minutes the fault is detected.

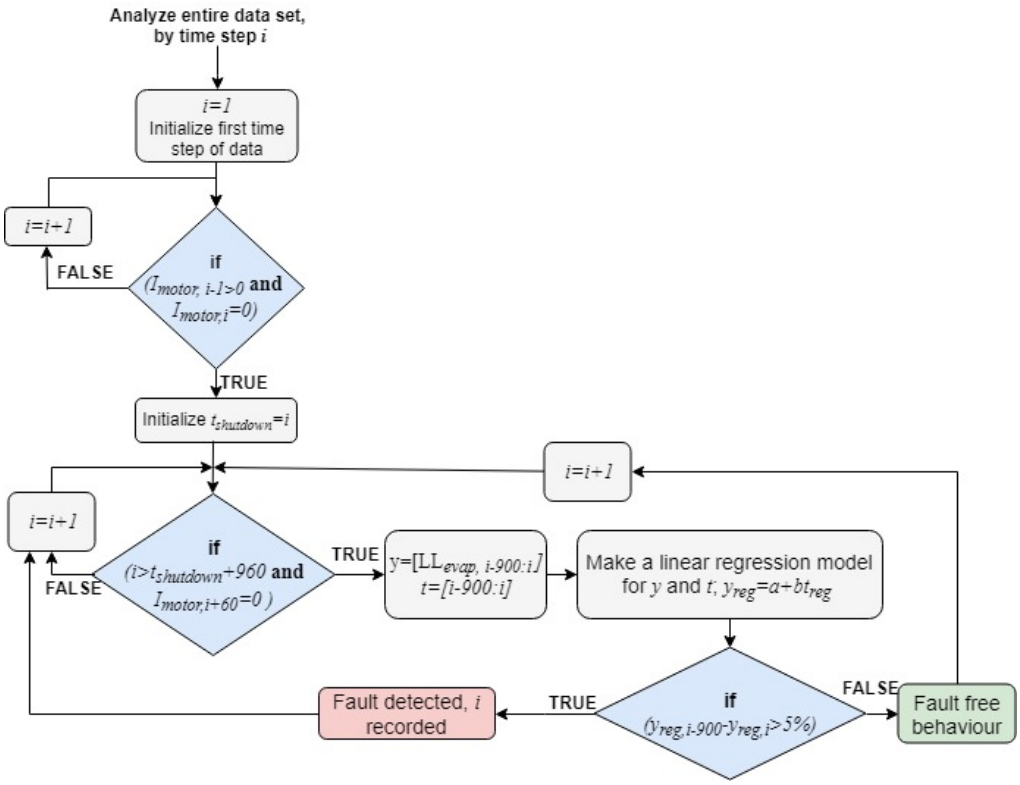

Figure 6.13: The FDD approach to detect liquid transferring away from the evaproator during standstill.

The fault is detected in a qualitative rule-based manner where the development trend of one variable is compared to the expected trend from priori knowledge.

6.4.3. Results

Liquid refrigerant transferring away during standstill was detected in Fig 6.12. It was not concluded why the liquid was transferring away. It was detected in a water cooled heat pump, the water temperatures have a slight change. However, not high enough to cause the observed change in the liquid level.

6.5. Oil pump

For the ”5HP-compressor” the oil pump circulating the oil in the system is connected on the same shaft as the compressor, i.e. its operation is dependent on the compressors. This fault is occurring for all

heat pump systems fitted with a ”5HP-compressor”. It requires a measurement interval of 1 second to be detected.

After a compressor startup the differential oil pressure should build up to operating conditions after no more than five seconds. During operation the differential oil pressure should be quite constant.

6.5.1. Failure Description

In some instances the oil pump is not able to build up sufficient differential oil pressure in the compressor. The compressor is shut down before the actual operation can commence due to the lack of Δp_{oil}. The pump could also generally not be performing as intended during operation.

6.5.2. Failure Symptom

A defect or malfunctioning oil pump is recognized through the symptom below.

- After the compressor initiated, indicated by the motor current having a non-zero value, the differential oil pressure takes more than 5 seconds to increase to its running conditions.
- The differential oil pressure steadily decreases during constant operating conditions

The first symptom is furthermore divided into two categories; where one is considered a potential fault and the other is considered an actual fault. If the time delay between the compressor startup and the increase of the differential oil pressure is between 5 and 30 seconds it is considered a potential fault. If it is more than 30 seconds or if it never increases an actual fault can be diagnosed.

6.5.3. Failure Detection Approach

The lack of Δp_{oil} can be detected by isolating the startups and recording the motor current and differential oil pressure in the first minute after the startup. If the differential oil pressure remains below the threshold of 1.2 bar, half of the normal operating differential oil pressure, after the first five seconds then the fault is detected. The FDD program furthermore detects how long it takes to build up the differential pressure, if it is less than 30 seconds it gives a warning, if it is more than 30 seconds or if it never happens the fault is detected. This is illustrated in Fig. 6.14.

The second failure symptom is detected by making a linear regression model for the differential oil pressure the last 5 minutes during the steady state operation period. If the regressed difference over the total 5 minutes is more than 0.5 bar then the fault is detected as illustrated in Fig. 6.15.

The first symptom is detected in a qualitative rule-based manner where the development trend of one variable is compared to the expected trend from priori knowledge.

The FDD analysis for the second symptom utilizes a process history based approach with a black box linear regression model to predict the expected trend in Δp_{oil}.

6.5.4. Results

There was only data available from the first symptom occurring in Fig. 6.16. Here the FDD program was able to detect the fault by detecting the increase of the motor current. However, it never detects the increase of the differential oil pressure.

The second symptom was recognized in a heat pump, and the FDD program detected the fault. Fig. 6.17 shows the result of the FDD program for a decreasing Δp_{oil}, where the fault threshold proved vital. By changing the the threshold to 0.6 bar the fault is not detected at all, while if it is changed to 0.4 bar the fault was detected over 200 times at different times. The threshold of 0.5 bar is vaguely defined and could need a clearer definition.

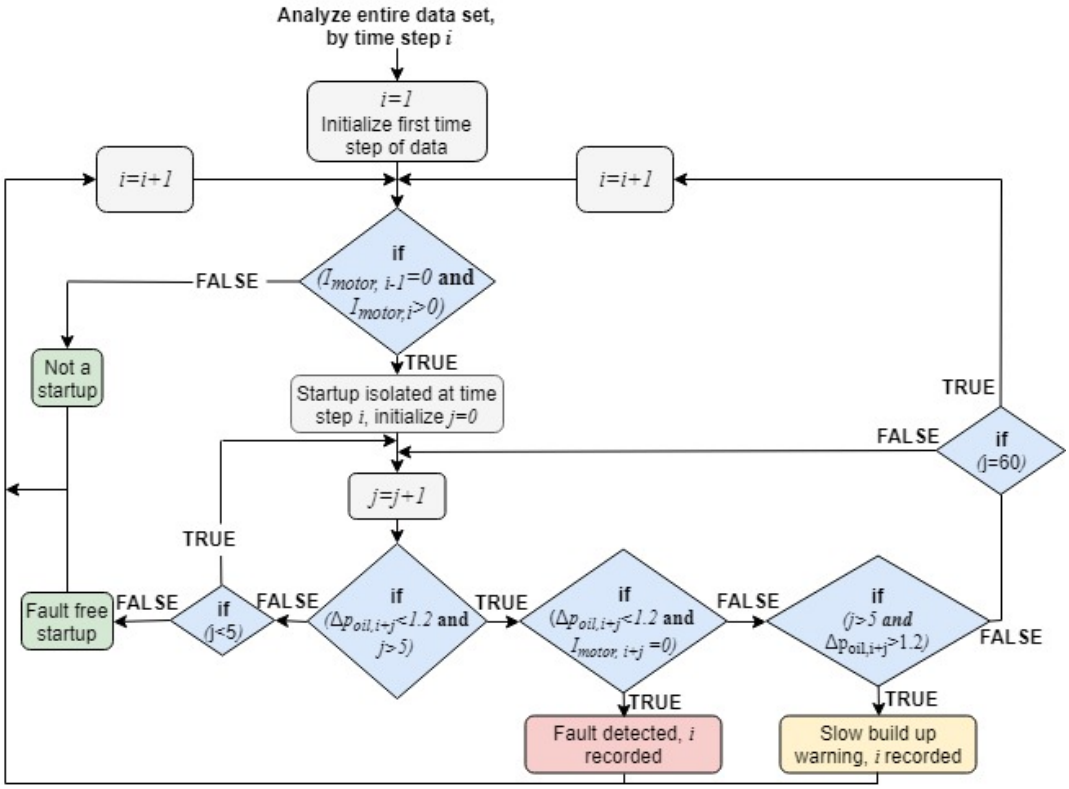

Figure 6.14: Detection approach to detect the lack of Δp_{oil} during startup of a "5HP-compressor".

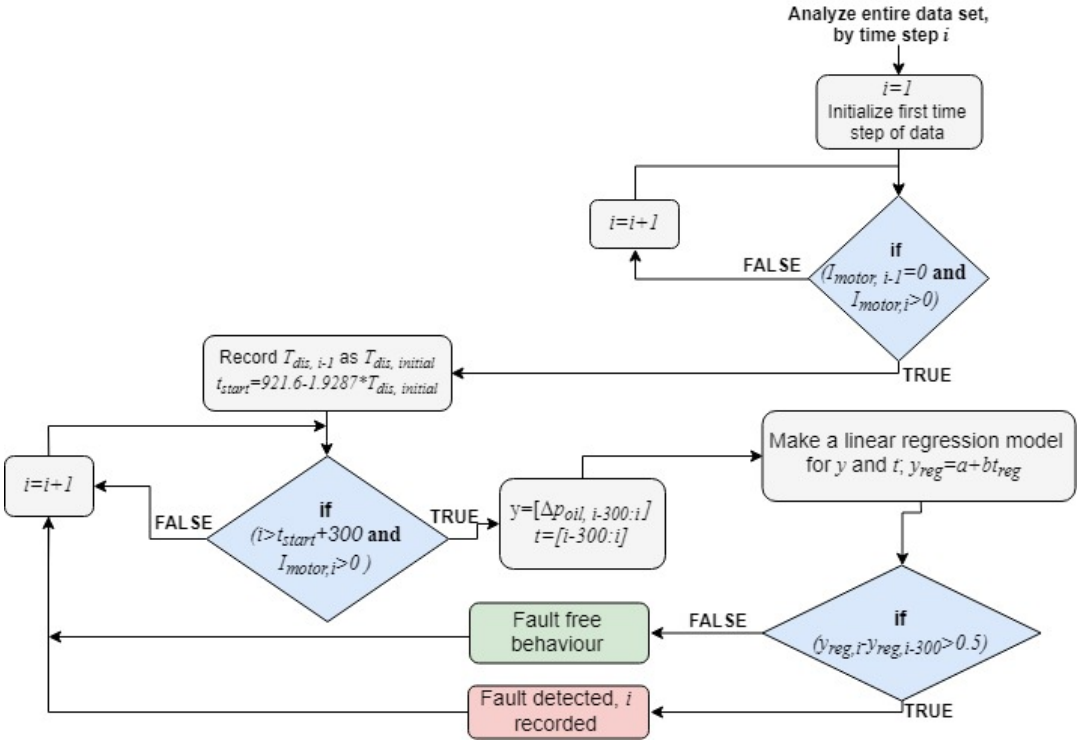

Figure 6.15: Detection approach to detect the decreasing Δp_{oil}, the algorithm makes a new linear regression every time step.

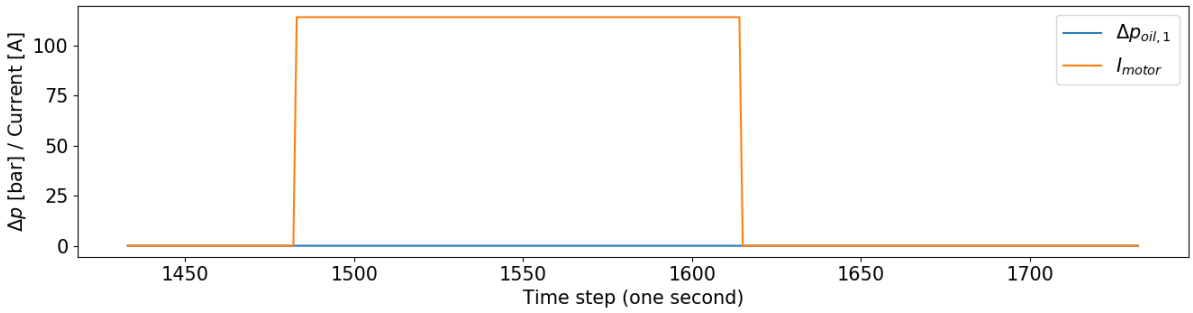

Figure 6.16: A lack of Δp_{oil} during startup causing the heat pump to shut down. The FDD program has detected the current increase, but it never detects the desired increase of the differential oil pressure.

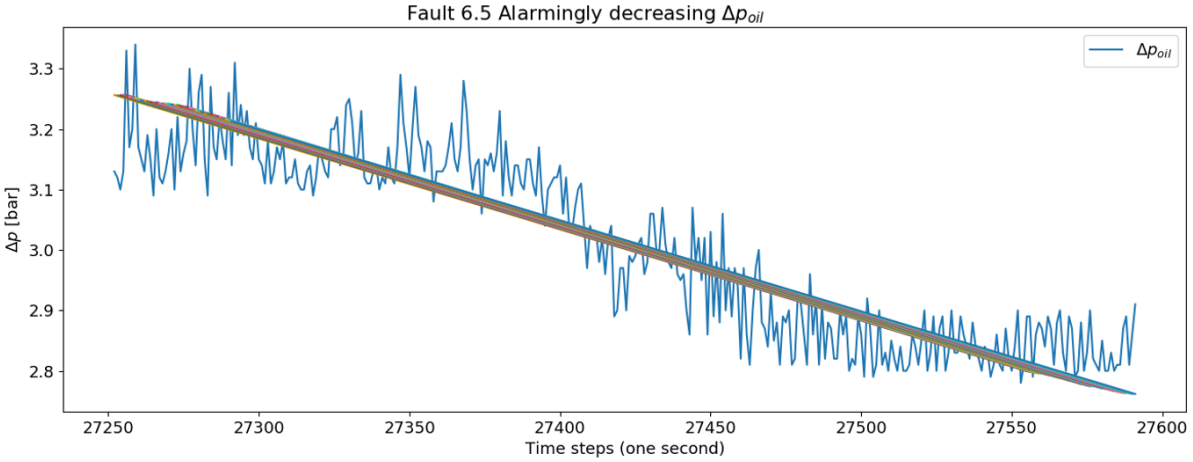

Figure 6.17: The FDD program has detected that the linear regression model has a total decrease for at least 0.5 bar over 5 minutes or 300 seconds. Every time the fault is detected, the linear regression that detected the fault is drawn in the graph. For this scenario the fault was detected 40 times, and 40 lines are drawn in the graph.

7

Discussion

In this chapter the results from the FDD program made specifically for the 23 faults in section 4, 5 and 6 will be discussed. Furthermore, The FDD programs ability to fulfill GEA Groups requirements, outlined in the beginning of the report in Table 1.1, will be discussed in this section.

7.1. The general FDD program

The goal and scope of the project was to develop a FDD program that can be implemented in the control system of the heat pumps in order to perform on-line FDD analysis of faults. The FDD algorithms were designed in a manner that ensured the program could detect the fault as it first occurs. This falls under the category ”Explanation facility” and ”Quick detection and diagnosis”. In other words, to be able to detect the fault as it is developing, to be able to say how it developed, and to report the fault before any serious damage to the plant occurs.

The FDD program utilizes a combination of a qualitative and process history based approach for all faults except Fault 6.3. A quantitative approach would prove more accurate, but for GEAs heat pump systems it would be difficult. Developing a digital physical twin of the system to compare with the actual system would prove demanding due to the complexity of the systems and was beyond the scope of this project. A qualitative approach was chosen for the faults where the fault trend was well known through extensive previous knowledge. A process history based approach was taken for the faults where the exact trends were not known. The FDD program is not able to recognize new faults as it is using a qualitative approach that mimics expert behaviour for previously seen faults. However it will be able to differentiate faulty from fault-free operation through the COP, T_{dis} and $\dot{Q}_{cond}$ in a process history based approach.

The FDD program employs a qualitative case-based reasoning system and includes a stored database of several different types of FDD algorithms and trends from previously seen faults. Based on a set of if-then-else rules the FDD program searches through the heat pump data looking for these given trends. Fault trends are constructed individually and are not necessarily qualitative. The resulting FDD algorithms can be seen for the individual faults in section 4, section 5 and section 6.

A process history based fuzzy logic approach was employed in order to detect certain faults. Here, residuals between predicted and measured variables where weighted either based on their relation to the fault or based on how often the residuals exceeded a certain threshold. However several of the variables analyzed with this fuzzy logic approach had large fluctuations on the micro time scale. To filter out the noise in the measurements, a larger threshold could be used, this would not capture all faults however. The data could also be filtered by using a running average over the 10 previous time steps for each measurement. This would however remove some of the fluctuations that are important

to detect other faults.

Most algorithms developed can be fitted into the control system for on-line FDD, however some might require more adaptation.

7.1.1. Developing / Sudden faults

It was desirable to have a FDD program that could detect and diagnose faults early, preferably the moment they occur for the first time. For some faults this proved challenging due to the very nature of the fault. Several of the previously discussed faults were so called sudden faults. Sudden faults occur without any signs or warnings and they are detectable from the moment they first occur.

Developing faults are defined when the heat pump system is being operated in an undesired manner and faults are slowly developing. These faults can often be more challenging to detect in an on-line manner as the fault threshold has a vague definition. The true difference between faulty and fault-free operation is difficult to define as there is no damage but rather a decrease of performance. Fouling and air in the condenser are typical examples of this, they will lead to a decrease of the COP and $\dot{Q}_{cond}$ over time. At some point in time they will be detected by the fault thresholds. However, at the time of detection, they could have developed over several months slowly decreasing the performance. Thus the fault threshold plays an important part to detect the developing faults and a fuzzy logic approach helped quantify this. The fault threshold is a representation of how much of a decrease of performance is tolerable for GEA.

Bearing damage

Damage to the bearings of the compressor (Fault 4.3), was detected using a combination of a process history based gray-box linear regression model and a qualitative case-based reasoning approach. In one heat pump system bearing damage was detected, and later it was seen that Δp_{oil} was too dependent on N_{RPM}. From that heat pump system, the first failure symptom arose. However, it was not certain whether bearing damage could be detected in the same way in other systems as this had only occurred once.

The FDD algorithm was tested on a heat pump system where there was a suspicion that something was wrong due to frequent starting and stopping of the compressor. In this heat pump system the FDD algorithm detected that Δp_{oil} was too dependent on N_{RPM} beyond the threshold defined. Upon inspection of the heat pump system, the bearings appeared to be slightly damaged. This is typical of a developing fault. The symptom is detected due to poor lubrication between the shaft and the compressor which ultimately leads to severe damage to the bearings if not detected. Fig. 7.1 shows the bearings which are slightly damaged. This is a confirmation that the first symptom of Fault 4.3 is a re-occurring symptom and a way to detect bearing damage. The differential oil pressure will be too dependent on N_{RPM} as the clearance between the bearing housing and shaft is too small. Rubbing occurs between the bearing and shaft walls creating an increasing flow resistance that the oil pump has to overcome. Thus the moment this fault occurs the symptom will be detectable. It is only after operating with this symptom for a longer period that the bearings will be damaged.

This also illustrates one of the issues with the FDD program, the expert knowledge is not always infallible. Other faults also had fault trends that were only seen once or twice before. Faults could occur in unforeseen ways, or the trends previously seen could be a one time occurrence.

7.1.2. Adaptability of the FDD program

One of the most important aspects of the FDD program was its ”Adaptability”, referenced in Table 1.1, which was defined as the FDD programs ability to adapt to physical changes of the heat pump system. As the heat pump systems from GEA differ in many ways due to the application and the compressor types, it was of great importance to have a FDD program that was applicable across a range of systems and compressors.

Based on design inputs specified by the compressor type and the type of heat pump system, the

Figure 7.1: Slight bearing damage detected in a compressor bearing by the FDD program. This a typical example of early stage development of Fault 4.3, bearing damage, where the heat pump system was inspected early enough to avoid any serious damage.

FDD program will run different algorithms for the different faults that require dedicated unique algorithms. This is made to fit every current system configuration, however there are two problems which should be addressed for ”Adaptability”.

Firstly, there are dedicated algorithms made for the current different setups where it is required. However future adaptations to the system have not been considered. The algorithms will probably not work directly on new systems with different setups.

Secondly, the FDD program was adapted to detect and diagnose faults in the ”V-compressor”. However there was only one working example of this compressor available. The sampled data for validation of the compressor prediction tool used for the process history based faults might not be accurate for other ”V-compressors” in the future. The ”V-compressor” was also newly developed, due to this there was a limited amount of expert knowledge available for the qualitative faults, it was mostly assumed that the faults would not differ from faults of the ”5HP-compressor”.

7.1.3. Intertwining nature of faults

Several faults and their respective symptoms are mixed. The expected link between different symptoms and faults was a good way to test the FDD algorithm for the faults that were never detected before. Air in the condenser (Fault 5.2) and its influence on $\dot{Q}_{cond}$ and the COP was investigated in detail. Some abnormalities were detected as it was expected that air in the condenser would influence the COP and $\dot{Q}_{cond}$ noticeably. However, in the example where air in the condenser was known to be an issue neither $\dot{Q}_{cond}$ nor the COP was seen to be faulty. The logical conclusion was that the inputs of the black-box model used in the compressor prediction tool calculating $\dot{Q}_{PR,cond}$ and $P_{PR,e}$ were influenced by air in the condenser. This is a possible downside of using a black-box model for the compressor prediction tool where the calculation methods are not based on physical principles.

A suggestive map was drawn in Fig. 1.5, where symptoms were mapped with the corresponding fault detections. These are the known and obvious links, other unforeseen links will also occur that are not as obvious. In the beginning in Table 1.1 it was decided that the two metrics ”Isolability” and ”Multiple fault identifiability” were not of great importance for this project. Therefore, the linking between the faults was not investigated further. It was decided that it was of greater importance to have an FDD program with ”Novelty identifiability” that could distinguish between faulty and fault-free operation.

7.2. Compressor Prediction Tool

The FDD program is linked with the compressor prediction to predict $T_{PR,dis}$, $P_{PR,e}$ and $\dot{Q}_{PR,cond}$ based on the running conditions for the process history based black-box FDD algorithms. Some faults are highly dependent on the calculation methods from the compressor prediction tool, which is a black-box model with unknown details. The black-box model has been validated for several heat pump systems with the ”5HP-compressor”. However it has not been sufficiently validated for the heat pump systems with the ”V-compressor”. Further validation is required on the compressor prediction tool with heat pump systems with a ”V-compressor”, as this type of compressor is currently being introduced.

7.3. Startup and shutdown

The startups and shutdowns of the heat pump system were seen to be specifically prone to damage and failures. In addition to this both analyzed compressors were seen to have different and very specific startup procedures. It was intended that the FDD program would have a gray-box feature extrapolation of failure trends, where the program was mainly looking to recognize faulty trends previously experienced. Startups can still be faulty in ways not seen before, this was typical for the newer ”V-compressor” where there is only data from 9 startups in total, which are all fault free.

It would benefit the FDD program to have a dynamical model that can predict how the ideal startup and shutdown should look like. By comparing the actual shutdown or startup to the predicted shutdown or startup the program can better detect faults not seen before. In this way, the program classifies shutdowns and startups as faulty or fault free rather than looking for specific trends. This is important as $T_{PR,dis}$ and $\dot{Q}_{PR,cond}$ are not accurately predicted during startup.

7.4. Faults not included in the FDD program

Several faults were not included in this FDD program due to either their simplicity, complexity, or their relevance to the desired FDD program. Some of the faults that were outside the scope of this report are listed below with a simple explanation.

- Sudden pressure changes can result in the refrigerant dissolved in the oil to boil out, rapidly changing the properties of the lubricating oil.
- The oil return system that circulates the lubrication oil can have any number of faults. It is often seen that it does not return sufficient oil, or if the operating periods are too short it not does return oil at all to the compressor.
- Both the condenser and the evaporator are prone to fouling. It was decided that this will be picked up by the two faults looking at the delivered heat and the COP (Fault 5.8 and Fault 5.9).
- If there is not sufficient liquid in the evaporator, it will change the heat transferring abilities in the evaporator, each evaporator has a minimum allowable limit.
- The control system not being operated with the correct settings. This often leads to frequent starting and stopping of the heat pump which is damaging for the lifetime expectancy of the system.

The first two faults in the list above were not included due to their complexity. The first fault in particular needs a pressure-temperature diagram for solubility of oil and the refrigerant. The first fault is also a result of other faults included in the scope of the project. The oil return system has a complicated control procedure that would have been challenging to implement in to the FDD program.

The last two faults are system specific, i.e. they depend on values that are unique for each system. They would require too much design input, and hence it would give the FDD program a low score on the ”Adaptability” metric from Table 1.1.

The fourth fault should however be picked up when there is liquid carry-over during operation, when the liquid level in the evaporator is transferring away during standstill, or when the liquid level is faulty (Fault 5.7, Fault 6.3 and Fault 6.4).

The fifth fault would depend on having extensive knowledge about how that exact control system, which differs per heat pump system, should operate to be able to detect the wrong settings.

8

Conclusions and Recommendations

There are several improvements that could be made to the FDD program before or during implementation in to the control system. Some suggestions are listed below.

- Considering sensor accuracy, it would be pragmatic to look into the contribution of sensor uncertainty to the FDD uncertainty. This would effect the fault thresholds.
- The sensor that measures the incoming heat sink temperature to the condenser should be moved to the other side of the butterfly valve controlling the ehat sink. Then the sensor would capture the problematic startup of the heat sink flow (the first symptom of Fault 5.10).
- The flow of the heat sink going into the condenser should be measured. This would improve the accuracy of several FDD analyses; the high fluctuations in the secondary flow of the evaporator and the condenser (Fault 5.3 and Fault 5.6), the low $\dot{Q}_{cond}$ (Fault 5.8) and the low COP (Fault 5.9). When a fluctuating heat sink flow is detected in the condenser (Fault 5.6), it is not directly known what caused it. It could be that the mass flow is fluctuating or the calculated mass flow is fluctuating due to variations in the temperatures used for the calculations. However, if the flow of the heat sink is measured this would not be an issue.
- The fault threshold for the decreasing differential oil pressure in the ”5HP-compressor” (Fault 6.5) of 0.5 bar over 5 minutes could be wrong. In the example, the fault was detected 40 times using 0.5 bar as the threshold. It was not detected at all using 0.6 bar, and was detected over 200 times using 0.4 bar. This should be further investigated to create a better FDD analysis. One idea would be to develop a strength relationship or a fuzzy logic approach where the total decrease of Δp_{oil} is paired with the amount of times the fault is detected.
- For the compressor prediction tool it is not known how it actually calculates $T_{PR,dis}$, $P_{PR,e}$ and $\dot{Q}_{PR,cond}$. It is a black-box model using a nonphysical approach. Another student is doing a master thesis with the topic of building his own compressor prediction tool in a quantitative manner based on physical relations for GEA. Implementing this model into the FDD program would prove advantageous as it could better extrapolate for previously unseen faults. However, it could also prove too computationally demanding for the desired on-line analysis.
- It is advisable to continually develop the FDD program as the new ”V-compressor” is being introduced and data is being logged from it. Implementing a machine learning scheme may be beneficial for the FDD program to allow it to predict the failure thresholds, the uncertainties, or simply to increase the accuracy between the predicted and measured values. The compressor prediction tool uncertainties are too large for the ”V-compressor”. There is only one heat pump system sampled. It is not known if the one system sampled is faulty, or if the compressor prediction tool cannot properly capture the values in the heat pump system.
- Some faults have no data or examples available, and the failure thresholds are quite ambiguous. A possible solution could be to simulate the faults in actual heat pumps and see how the values react for the faults that are not causing direct damage (for example Fault 6.2).

- Utilization of the qualitative case-based or rule-based reasoning to detect certain faults relies on expert knowledge. This expert knowledge is mostly based on previously seen faults, and the data trends seen in those faults. However, some of these data trends are only observed once or twice. Other trends are based on what service engineers have seen once, without an actual example of the data trend. As the FDD program is being implemented the expert knowledge should be revised, stored and included in the FDD program.
- The two faults which label the general operation as faulty or fault free through $\dot{Q}_{cond}$ and the COP (Fault 5.8 and Fault 5.9) should be changed. $\dot{Q}_{cond}$ and the COP should not be compared to values from the compressor prediction tool, but rather design conditions of the individual system. All heat pumps delivered have a promised $\dot{Q}_{cond}$ and COP during steady state operation. The compressor prediction tool inputs were affected by faults occurring, and did not pick up on a faulty $\dot{Q}_{cond}$ or COP due to this.
- For the capacity valve mechanism (Fault 4.2), another approach could be to compare the measured power to the power predicted by the compressor prediction tool for the ”V-compressor”. The compressor prediction tool can be used from the first capacity step for the ”V-compressor”, and the predictions were accurate. The power follows the same capacity steps as the current during a startup (Fig. 3.14), hence this approach could be more accurate.

As a final comment for the FDD program the implementation period will be of high importance. During the implementation there will likely be some troubleshooting and changing of FDD approaches or thresholds. Therefore, it is important to have an implementation period where the performance of the control system with the FDD program is closely monitored.

Bibliography

Andersen, S. K., Olesen, K. G., Jensen, F. V., and Jensen, F. (1989). HUGIN - a shell for building Bayesian belief universes for expert systems. *Proceedings of the Eleventh International Joint Conference on Artificial Intelligence*, pages 1080–1085.

Broenink, J. F. (1999). Introduction to Physical Systems Modelling with Bond Graphs. Lecture Notes, University of Twente.

Brownlee, J. (2016). Logistic regression for machine learning.

Chen, B. and Braun (2000). Simple Fault Detection and Diagnosis Methods for Packaged Air Conditioners . *International Refrigeration and Air Conditioning Conference*.

Delgoshaei, P., Austin, M. A., and Veronica, D. (2017). Semantic Models and Rule-based Reasoning for Fault Detection and Diagnostics: Applications in Heating, Ventilating and Air Conditioning Systems. *ICONS 2017: The Twelfth International Conference on Systems*.

Dexter, A. and Pakanen, J. (2001). Demonstrating Automated Fault Detection and Diagnosis Methods in Real Buildings. pages 56–57, Espoo, Finland. VTT Symposium: 217.

Frank, S., Heaney, M., Jin, X., Robertson, J., and Elmore, R. (2016). Hybrid Model-based and Data-driven Fault Detection and Diagnostics for Commercial Buildings. *ACEEE Summer Study on Energy Efficiency in Buildings*, (12):1–14.

Fritzson, P. (2004). *Principles of Object-Oriented Modeling and Simulation with Modelica 2.1*.

Gordon, M. and Ng, K. (2001). *Cool thermodynamics*. Cambridge International Science Publishing.

Gordon, M. J. and Ng, K. C. (1995). Predictive and diagnostic aspects of a universal thermodynamic model for chillers. *International Journal of Heat and Mass Transfer*, 38(5):807–818.

Höskuldsson, A. (1988). PLS regression Methods. *Journal of Chemometrics*, 2(August 1987):211–228.

Jha, M.-S., Dauphin-Tanguy, G., and Ould-Bouamama, B. (2017). Robust fault detection with Interval Valued Uncertainties in Bond Graph Framework. *Control Engineering Practice*, (71):61–78.

Katipamula, S. and Brambley, M. R. (2005a). Methods for Fault Detection, Diagnostics, and Prognostics for Building Systems - A Review, Part I. *HVAC&R RESEARCH*, 11(1).

Katipamula, S. and Brambley, M. R. (2005b). Methods for Fault Detection, Diagnostics, and Prognostics for Building Systems - A Review, Part II. *HVAC&R RESEARCH*, 11(2).

Kulkarni, M., Abou, S. C., and Stachowicz, M. (2009). Fault Detection in Hydraulic System Using Fuzzy Logic. *the World Congress on Engineering and Computer Science*, II:5–10.

Li, H. and Braun, J. (2002). On-Line Models for Use in Automated Fault Detection and Diagnosis for HVAC&R Equipment. *American Council for an Energy Efficient Economy*, (12).

Madsen, A. L., Lang, M., Kjærulff, U. B., and Jensen, F. (2003). The Hugin Tool for Learning Bayesian Networks. *European Conferences on Symbolic and Quantitative Approaches to Reasoning with Uncertainty (ECSQARU)*, (2003):594–605.

Mechefske, C., Mar, J. D., and Prendergast, D. (1996). Automatic machinery fault detection and diagnosis using fuzzy logic. *Proceedings of a Joint Conference, Mobile, Alabama*.

Mehranbod, N., Soroush, M., and Panjapornpon, C. (2005). A method of sensor fault detection and identification. *Journal of Process Control*, (15):321–339.

Rebouças and Leite, D. (2012). Use of Artificial Neural network To fault Detection and Diagnosis. *ABCM Symposium Series in Mechatronics*, 5:666–675.

Rossi, T. M. and Braun, J. E. (1997). A statistical, rule-based fault detection and diagnostic method for vapor compression air conditioners. *HVAC&R Research*, 3(1):19–37.

Rosvold, G. I. (2017). PV monitoring and fault detection prediction of PV soiling in Northern. Master's thesis, University of Oslo, Problemveien 7, 0315 Oslo, Norway.

Schagen, J. D., Taal, A., and Itard, L. (2016). Bayesian Belief Networks (BBN) and Expert Systems for supporting model based sensor fault detection analysis of smart building systems . *CLIMA 2016 - proceedings of the 12th REHVA World Congress*, 8.

Schein, J. and Bushby, S. (2005). A Simulation Study of a Hierarchical , Rule-Based Method for System-Level Fault Detection and Diagnostics in HVAC Systems.

Vecchio, D. (2014). Fault detection and diagnosis for brine to water heat pump systems. Master's thesis, KTH Royal Institute of Technology, Brinellvägen 8, 114 28 Stockholm, Sweden.

Venkatasubramanian, V., Rengaswamy, R., and Kavuri, S. N. (2002a). A review of process fault detection and diagnosis part II: Qualitative models and search strategies. *Computers and Chemical Engineering*, (27):313–326.

Venkatasubramanian, V., Rengaswamy, R., Kavuri, S. N., and Yin, K. (2002b). A review of process fault detection and diagnosis part I: Quantitative model-based methods. *Computers and Chemical Engineering*, (27):293–311.

Venkatasubramanian, V., Rengaswamy, R., Kavuri, S. N., and Yin, K. (2002c). A review of process fault detection and diagnosis part III: Process history based methods. *Computers and Chemical Engineering*, (27):327–346.

Villegas, T., Fuente, M. J., and Rodríguez, M. (2010). Principal Component Analysis for Fault Detection and Diagnosis. Experience with a pilot plant. *Advances in Computational Intelligence, Man-Machine Systems and Cybernetics*, pages 147–152.

Wissink, A., Shende, S., and Malloney, A. D. (2011). A Fault Detecting Diagnostic Tool for Python-driven Multi-language Scientific Code. *DoD High Performance Computing Modernization Program Users Group Conference 2011*, pages 489–498.

Zogg, D., Shafai, E., and Geering, H. (2005). Fault diagnosis for heat pumps with parameter identification and clustering. *Control Engineering Practice*, (14):1435–1444.